# Analyses of Coenzyme A Biosynthesis in the Human Enteric Parasite *Entamoeba histolytica* for Drug Development

A Dissertation Submitted to

the Graduate School of Life and Environmental Sciences,

the University of Tsukuba

In Partial Fulfillment of the Requirements

for the Degree of Doctor of Philosophy in Science

(Doctoral Program in Biological Sciences)

**Arif NURKANTO**

## Table of Contents

## Abstract

*Entamoeba histolytica* is an enteric protozoan parasite responsible for human amebiasis. According to the World Health Organization, 50 million people, especially in the tropical countries, suffer from this infection, resulting in estimated 100 thousand deaths annually. No effective vaccine has yet been developed, and only metronidazole and its derivatives are the drugs of choice for treatment. It has been demonstrated that metronidazole targets pyruvate:ferredoxin oxidoreductase, which is involved in acetyl CoA production in central energy metabolism. However, their low efficacy against asymptomatic cyst carriers, cases of treatment failure and emergence of resistance have been reported. Therefore, other rational targets need to be explored to develop new chemotherapeutics against amebiasis.

Coenzyme A (CoA), as a cofactor involved in >100 metabolic reactions, is essential to the basic biochemistry of life. Here, I investigated the CoA biosynthetic pathway of *Entamoeba histolytica*. I identified four key enzymes involved in the CoA pathway: pantothenate kinase (PanK, EC 2.7.1.33), bifunctional phosphopantothenate-cysteine ligase/decarboxylase (PPCS-PPCDC), phosphopantetheine adenylyltransferase (PPAT) and dephospho-CoA kinase (DPCK). Cytosolic enzyme PanK and DPCK, were selected for further biochemical, genetic, and phylogenetic characterization. The *E. histolytica* genome encodes single copy of PanK (EhPanK) and two DPCK isotypes (EhDPCK1 and EhDPCK2). Epigenetic gene silencing of *PanK* resulted in a significant reduction of PanK activity, intracellular CoA concentrations, and growth retardation *in vitro*, reinforcing the importance of this gene in *E. histolytica*. Similar to PanK, epigenetic gene silencing of *EhDPCK1* and *EhDPCK2* also caused significant reduction of DPCK activity, intracellular CoA concentrations, and also led to growth retardation *in vitro*. These results indicated importance of PanK, DPCK1 and DPCK2 for CoA synthesis and proliferation.

Metabolomics analysis using capillary electrophoresis-mass spectrometry showed that *PanK* gene silencing caused significant changes in metabolites such as overall increase in majority of upstream (down to pyruvate) intermediates of glycolysis and the pentose phosphate pathway, and decrease in acetyl CoA, xanthine, hypoxanthine, ATP, cyclic nucleotides, ornithine, and *S*-adenosyl-L-methionine. On the other hand, suppression of *EhDPCK* gene expression also caused decrease in the level of acetyl-CoA, and metabolites involved in amino acid, glycogen, hexosamine, nucleic acid metabolisms, chitin and polyamine biosynthesis. Phylogenetic analysis also supported the uniqueness of the amebic enzymes compared to the human counterpart. Its biochemical, evolutionary features, and physiological importance of EhPanK and EhDPCKs indicate that these enzymes represent the rational target for the development of anti-amebic agents.

Furthermore, I screened the Kitasato Natural Products Library for inhibitors of recombinant EhPanK, and identified 14 such compounds. One compound demonstrated moderate inhibition of PanK activity and cell growth at a low concentrations, as well as differential toxicity towards *E. histolytica* and human cells. Moreover, I also screened Indonesia microbial extracts against both recombinant EhPanK and EhDPCKs. Approximately 0.3 % of extracts inhibited EhPanK, 2.6% specifically inhibited EhDPCK1, 3.7% specifically inhibited EhDPCK2 and 2.2% inhibited both EhDPCK1 and EhDPCK2 from around 3,000 extracts tested.

# Chapter 1. General Introduction

## 1.1. *Entamoeba histolytica* causes amebiasis

*Entamoeba histolytica* is the protozoan agent responsible for human amebiasis, an infectious disease causing dysentery and amebic liver abscesses, responsible for 100,000 deaths annually throughout the world. It represents the third most common parasitic cause of death, after malaria and schistosomiasis (Stanley, 2003; Ali and Nozaki, 2007; Ralston and Petri, 2011). The elaborate pathogenesis of this parasite is well documented (Espinosa-Cantellano and Martínez-Palomo, 2000; Nozaki and Bhattacharya, 2015). Metronidazole has, for decades, been the most effective drug in the treatment of amebiasis despite its known side effects and low efficacy against asymptomatic cyst carriers. Moreover, resistance, virulence and host immune response to metronidazole treatment in amebiasis have been reported in some countries (Griffin, 1973; Pittman and Pittmann, 1974; Johnson, 1993; Koch et al., 1997; Ali and Nozaki, 2007). The molecular target of metronidazole has been well described as a key metabolic enzyme, pyruvate:ferredoxin oxidoreductase, which is involved in acetyl CoA production from pyruvate as part of central energy metabolism. Identification and characterization of novel drug targets unique to *E. histolytica* are therefore needed to design better therapeutics against amebiasis.

## 1.2. Coenzyme A is an important cofactor

Coenzyme A is an essential cofactor in all living organisms as an acyl group carrier and carbonyl-activating group involved in more than 100 cellular reactions (Begley et al., 2001); it is estimated to be a cofactor used in 9% of identified enzymatic reactions (Strauss, 2010). CoA biosynthesis is considered to be an essential and universal pathway of the majority of prokaryotes and eukaryotes (Leonardi et al., 2005b). In general, CoA participates in fatty acid metabolism, the tricarboxylic acid cycle and numerous other intermediary metabolic reactions (Abiko, 1975). CoA is synthesized from pantothenate (vitamin $B_5$), cysteine, and ATP

(Jackowski, 1996; Leonardi et al., 2005b). Most eukaryotes are unable to synthesize pantothenic acid and thus rely on an external supply.

CoA is synthesized from several enzymatic steps. A water-soluble vitamin $B_5$ (pantothenate acid) is used for CoA biosynthesis by serving the main precursor. First, pantothenate is phosphorylated to 4'-phosphopantothenate by pantothenate kinase. The second enzyme, phosphopantothenoylcysteine synthase and 4'-phosphopantothenoylcysteine decarboxylase, play an important role to condense 4'-phosphopantothenate and cysteine to form 4'-phosphopantetheine. 4'-Phosphopantetheine is subsequently converted to dephospho-CoA by phosphopanthetheine adenylyltransferase and phosphorylated by dephospho-CoA kinase at the 3'-OH to form CoA. This process is relatively conserved among organisms, both prokaryotic and eukaryotic.

### 1.3. Gene silencing strategy to understand the essentiality of the particular gene in *E. histolytica*

Because of the lack of the tool for the genetic manipulation in *E. histolytica*, several approaches based on RNA interference (RNAi) methods or gene silencing has been successfully developed (Morf et al., 2013; Zhang et al., 2011b). Gene silencing is the regulation of gene expression in the cell to prevent the expression of a specific gene. The silencing process is started by transfecting the truncated-nucleotides that constructed in a specific plasmid containing a drug resistance gene, such as geneticin, into trophozoites of *E. histolytica*. After drug selection towards the transfected-cell line, the level of silencing of the certain target gene could be evaluated. Other important parameters such as growth kinetics, mRNA level, corresponding enzymes activity and metabolites disturbance also could be investigated from gene-silenced strains. Based on this strategy, I can evaluate the essentiality of the particular gene in *E. histolytica* parasite indicated by cell survival or growth retardation and physiological changes.

### 1.4. Metabolomics analyses reveal the metabolites disturbance during gene silencing

To observe the effect of gene silencing throughout cellular metabolites or pathway, I performed the metabolomics analyses. Metabolomics analyses are described as a comprehensive assessment of endogenous metabolites and attempts to systematically identify and quantify metabolites from a biological sample (Zhang et al., 2012). This analyses is also important and integrated part of "multi-omics" analysis (i.e. proteomics, transcriptomics and metagenomics). Metabolites are the end product of the cellular reaction and the snapshot of instantaneously of the cell physiology. Therefore, this method provides a better understanding of cellular biology. Many advantages will be obtained due to metabolomics analyses, such as sensitive and specific and for functional genomic has benefit to detect phenotypic caused by genetic manipulation, gene deletion or silencing. Moreover, these analyses are also used to predict the functional mechanism of unknown genes.

### 1.5. Enzymatic-based screening for rapid discovery of anti-amebic agent

Another strategy to rapidly discover some anti-amebic agents, instead of conventional cell-based screening, is enzymatic-based screening. Enzymes continue to be a major drug target are one of the best choices for identifying initial active chemical compounds (Williams and Scott, 2009). Some criteria to propose enzymes as a novel target should be fulfilled, such as enzymes must essential in this parasite, no similarity or low homology compared to the human ortholog, enzyme stability and reproducible in the assay system (Acker and Auld, 2014). Some approaches to developing, validating, and troubleshooting assays system are also an important factor for the enzymatic-based screening. In this study, I proposed and developed the enzymatic screening system for pantothenate kinase and dephospho-CoA kinase in *E. histolytica* as targets to discover potential specific inhibitors.

### 1.6. Research objectives

The objectives of this research are to search a potential novel drug target from CoA pathway. Since no publication related to CoA pathway and its importance in *E. histolytica*, I also did analyze, confirm and characterize enzymes involved in CoA biosynthesis and evaluate their essentiality to this parasite. The second objective is to characterize biochemically the selected essential enzymes in CoA pathway. The third objective is to find potential inhibitors of essential enzymes. In this study, I investigated PanK and DPCK from *E. histolytica*, the first and the last enzyme involved in CoA pathway, respectively. In order to understand their essentiality, I used epigenetic gene silencing strategy and observed the disturbance in genetic and phenotypic level such as mRNA expressions, enzyme activities, CoA concentrations and growth kinetics. To expand my understanding of the independent role of PanK and DPCK, I also did metabolomics analyses of these gene silencing strain. Further investigation was the biochemical characterization of these recombinant PanK DPCK1 and DPCK2. Using these enzymes, I developed assay system and screened compound library and microbial extracts to find potential inhibitors against *E. histolytica*.

In this report, I presented my result study of Entamoeba PanK and DPCKs into two separated main Chapters. The first Chapter was "Characterization and validation of *Entamoeba histolytica* pantothenate kinase as a novel anti-amebic drug target". Another Chapter was "Genetic, biochemical, and metabolomic analyses of DPCK involved in coenzyme A biosynthesis in the human enteric parasite *Entamoeba histolytica*". I also included 27 figures and 12 tables related to this study that distributed into two Chapters above.

## Chapter 2. Characterization and validation of *Entamoeba histolytica* pantothenate kinase as a novel anti-amebic drug target

### 2.1. Abstract

Coenzyme A (CoA), as a cofactor involved in >100 metabolic reactions, is essential to the basic biochemistry of life. Here, I investigated the CoA biosynthetic pathway of *Entamoeba histolytica* (*E. histolytica*), an enteric protozoan parasite responsible for human amebiasis. I identified four key enzymes involved in the CoA pathway: pantothenate kinase (PanK, EC 2.7.1.33), bifunctional phosphopantothenate-cysteine ligase/decarboxylase (PPCS-PPCDC), phosphopantetheine adenylyltransferase (PPAT) and dephospho-CoA kinase (DPCK). Cytosolic enzyme PanK, was selected for further biochemical, genetic, and phylogenetic characterization. Since *E. histolytica* PanK (EhPanK) is physiologically important and sufficiently divergent from its human orthologs, this enzyme represents an attractive target for development of novel anti-amebic chemotherapies. Epigenetic gene silencing of *PanK* resulted in a significant reduction of PanK activity, intracellular CoA concentrations, and growth retardation *in vitro*, reinforcing the importance of this gene in *E. histolytica*. Furthermore, I screened the Kitasato Natural Products Library for inhibitors of recombinant EhPanK, and identified 14 such compounds. Approximately 4.2% from 3,000 microbial extracts also inhibited EhPanK. One compound demonstrated moderate inhibition of PanK activity and cell growth at a low concentrations, as well as differential toxicity towards *E. histolytica* and human cells.

### 2.2. Introduction

CoA is important in all living organism including a human parasite, *Entamoeba histolytica.* As a cofactor, it is generated from several steps of enzymatic reaction initiated by pantothenate (Vitamin $B_5$) as a precursor. Some organisms are able to *de novo* synthesize pantothenate, but some other organism, mostly eukaryote, lack ability to synthesize it and rely

on the external uptake. *Entamoeba histolytica* is one of eukaryotes that provide intracellular pantothenate from host or culture medium. Four genes encoding sequential pathway enzymes in this parasite were identified from amoebadb database (AmoebaDB, http://amoebadb.org/amoeba/): pantothenate kinase (EC 2.7.1.33, PanK), bifunctional phosphopantothenate-cysteine ligase/decarboxylase (EC 6.3.2.5/EC 4.1.1.36), phosphopantetheine adenylyltransferase (EC 2.7.7.3), and dephospho CoA kinase (EC 2.7.1.24). However, all of these genes are annotated as putative and no evidence for it's *in vitro* expression.

Pantothenate kinase (PanK), the first enzyme in CoA biosynthesis, is an important enzyme for phosphorylating of pantothenate to 4'-phosphopantothenate. There has been reported that PanK is essential to *Plasmodium berghei* (Srivastava et al., 2016), *Mycobacterium tuberculosis* (Awasthy et al., 2010) and *Arabidopsis thaliana* (Tilton et al., 2006). Moreover, specific inhibitors of PanK in other organism, such as *P. falciparum* (Chiu et al., 2017; Macuamule et al., 2015) and *M. tuberculosis* (Reddy et al., 2014) have also been discovered. However, the essentiality of PanK in *E. histolytica* is needed to be investigated. Therefore, in this report, I showed a comprehensive experiment to evaluate the essentiality of PanK in *E. histolytica* using epigenetic gene silencing strategy.

Here, I investigate the CoA biosynthetic pathway of *E. histoltyica* and further characterized one of these enzymes, pantothenate kinase (PanK, EC 2.7.1.33), with biochemical and reverse genetic approaches. Metabolite changes because of PanK gene silencing, especially related to CoA pathway were also investigated using these analyses. Moreover, I identified *E. histolytica* PanK inhibitors by screening the Kitasato Natural Products Library and microbial extracts against EhPanK recombinant enzyme. Taken together, I demonstrate that the CoA biosynthetic pathway, in general, and PanK, specifically, represents a rational and novel drug target against amebiasis.

## 2.3. Materials and methods

### 2.3.1. Organisms, cultivation, and chemicals

Trophozoites of *E. histolytica* clonal strains HM-1: IMSS cl 6 and G3 (Bracha et al., 2006) were maintained axenically in Diamond's BI-S-33 medium at 35.5$^{o}$C as described previously (Diamond et al., 1978). Trophozoites were continuously maintained in mid-log phase after inoculation of one-thirtieth to one-twelfth of the total culture volume. *Escherichia coli* BL21 (DE3) strain was obtained from Invitrogen (Carlsbad, CA, USA). Magnesium-free ATP was procured from DiscoverX (Fremont, CA, USA). $Ni^{2+}$-NTA agarose was procured from Novagen (Darmstadt, Germany). Lipofectamine and geneticin (G418) were procured from Invitrogen. Chemicals to evaluate metals in PanK activity assay were procured from Wako (Tokyo, Japan). All other chemicals of analytical grade were procured from Sigma-Aldrich (Tokyo, Japan) unless otherwise stated.

### 2.3.2. Production of PanK gene-silenced strain

In order to construct a plasmid for epigenetic gene silencing of *E. histolytica* (Bracha et al., 2006; Zhang et al., 2011a) *PanK* (*EhPanK*), a fragment corresponding to a 430 bp 5' open reading frame of *EhPanK* gene was amplified by PCR from cDNA using the following primer set (sense primer, 5'-CAG**AGGCCT**ATGTCTCAACCATCCCATTCT-3' and antisense primer, 5'-AAT**GAGCTC**TCTGAAGATTACCAATCCCATAAA-3'). These oligonucleotides contained StuI and SacI restriction sites (shown in bold). The amplified product was digested with StuI and SacI, and ligated into the StuI and SacI double digested psAP2-Gunma construct (Husain et al., 2011) to synthesize a *EhPanK* gene silencing plasmid. The G3 strain trophozoites were transformed with empty vector as a control and the silencing plasmid was transfected by liposome-mediated transfection as previously described (Nozaki et al., 1999). Transformants were initially selected in the presence of 1 μg/mL geneticin gradually increased to 10 μg/mL.

### 2.3.3. Reverse transcriptase PCR

RNA was extracted from approximately 1 x $10^6$ trophozoites of *EhPanK* gene silenced (PanK gs) and control transformant strains using TRIzol reagent (Ambion, Life Technologies) as previously described (Chomczynski and Mackey, 1995). DNase treatment was performed using DNase I (Invitrogen) to exclude genomic DNA. RNA quantity was determined by measuring the absorbance at 260 nm with a NanoDrop ND-1000 UV-Vis spectrophotometer (NanoDrop Technologies, Wilmington, DE, USA). Approximately one µg total RNA was used for cDNA synthesis using First-Stand cDNA Synthesis (Superscript® III, Invitrogen) with reverse transcriptase and oligo (dT) primers according to manufacturer's instructions. The cDNA product was diluted 10-fold and PCR reactions were carried out in 50 µL, using the primer pair (Sense primer, 5'-ATGTCTCAACCATCCCATTC-3' and antisense primer, 5'-TTACATTAGTTCTTCTTCATACTC-3'). The PCR conditions were: 98°C, 10 sec; 55°C, 1 min; and 72°C, 1 min; 20-25 cycles. The PCR products obtained were resolved by agarose gel electrophoresis.

### 2.3.4. Quantitative real time (qRT) PCR

Relative levels of steady state mRNA of the following genes were measured using qRT-PCR: *PanK* (EHI_183060), bifunctional phosphopantothenate-cysteine ligase/decarboxylase (*PPCS-PPCDC*, EHI_164490), phosphopantetheine adenylyltransferase (*PPAT*, EHI_006680), dephospho CoA kinase 1 and 2 (*DPCK1*, EHI_040840; and *DPCK2*, EHI_155780), and RNA polymerase II gene (EHI_056690) as a control. Each 20 µL reaction contained 10 µL 2X Fast SYBR Green Master Mix (Applied Biosystems, Foster City, CA, USA), 0.6 µL each of 10 µM sense and antisense primers, 5 µL 10x diluted cDNA, and nuclease free water. PCR was performed using the StepOne Plus Real-Time PCR System (Applied Biosystems, Foster City, CA, USA) with the following cycling conditions: enzyme activation at 95°C for 20 sec, followed by 40 cycles of denaturation at 95°C for 3 sec and annealing-extension at 60°C for 30 sec. All reactions were carried out in triplicate, including cDNA-minus controls. The amount of the

steady state mRNA of each target gene was determined by the ΔCt method with RNA polymerase II as a reference gene (Livak and Schmittgen, 2001). The mRNA expression level of each gene in the transformant was expressed relative to that in the control transfected with psAP2.

### 2.3.5. Production of whole lysates from *E. histolytica* trophozoites

Approximately 1 x $10^6$ trophozoites were harvested 48 hours after initiation of culture, and washed with 2% glucose in 1X phosphate buffer saline (PBS) three times. Cells were counted and resuspended in 500 µL homogenization buffer (50 mM Tris-HCl, pH 7.5, 250 mM sucrose, 50 mM NaCl) supplemented with 1 mM phenylmethyl sulfonyl fluoride (PMSF) and 0.5 mg/mL E-64 (Peptide Institute, Osaka, Japan). Cells were disrupted mechanically by a Dounce homogenizer and kept on ice for 30 min with intermittent vortexing followed by centrifugation at 500 x g for 30 min at 4°C for removing the insoluble cellular debris. The supernatant, representing total cell lysate, was carefully collected. Protein concentrations were spectrophotometrically determined by the Bradford method using bovine serum albumin as a standard as previously described (Bradford, 1976).

### 2.3.6. Enzyme assays and quantitation of CoA in cell lysates

PanK and DPCK activities in the cell lysate were measured with coupled assays using ADP Hunter™ Plus Assay kit (DiscoverX, US) according to the manufacturer's instructions. Briefly, fluorescence intensities were continuously measured to estimate the formation of resorufin at 37°C by excitation at 530 nm and emission at 590 nm in a 25 µL reaction mixture [10 mM $MgCl_2$, 15 mM HEPES, 20 mM NaCl, 1 mM EGTA, 0.02% tween 20, 0.1 mg/mL β-globulin, 2 mM pantothenate or 2 mM dephospho CoA for PanK or DPCK, respectively, 0.1 mM ATP, 2 µL of cell lysate (~5 µg protein)]. Kinetic data were estimated by curve fitting with the Michaelis–Menten equation using GraphPad Prism (GraphPad Software Inc., San Diego, USA). This experiment was repeated three times in triplicate with proteins isolated from two

independent extractions, and kinetic values are presented as the means ± S.E. for three independent kinetic assays.

Concentrations of CoA in the cell lysate were measured using the CoA assay kit (BioVision, CA, USA) according to manufacturer's instructions. CoA at 0.05–1 nmole was used to produce a standard curve to determine the amounts of CoA in lysates. Experiment were conducted in triplicate, and repeated three times on three different days.

### 2.3.7. Monitoring of growth kinetics

Trophozoite cultures were continuously maintained in mid-log phase as described previously, and placed on ice for 5 min to detach cells from the glass surface. Cells were collected by centrifugation at 500 ×g for 5 min at room temperature. After discarding the spent medium, the pellet was re-suspended in 1 mL of BI-S-33 medium. Cell densities were estimated on a haemocytometer. Approximately 10,000 trophozoites were inoculated in 6 mL fresh BI-S-33 medium. Cultures were examined every 24 hour for 5 days.

### 2.3.8. Genome-wide survey of enzymes involved in CoA biosynthesis in the *E. histolytica* genome

Putative genes encoding PanK, PPCS-PPCDC, PPAT, and DPCK were identified in the genome of HM-1:IMSS in the *E. histolytica* genome database (AmoebaDB, http://amoebadb.org/amoeba/) using the blastp online search tool (protein-protein BLAST). Human or bacterial orthologs (Human PanK1α/ NP_683878.1, *E. coli* bifunctional CoaBC/ WP_089667520.1, Human bifunctional COASY/ AAL50813.1) retrieved from non-redundant protein sequences (nr) database of National Center for Biotechnology Information (NCBI, http://www.ncbi.nlm.nih.gov/) were used as query sequences. Pathway analysis was conducted using Kyoto Encyclopedia of Genes and Genomes database (KEGG, https://www.genome.jp/kegg). The steady state mRNA level of each gene in the trophozoite stage was examined using the previous array data as an independent experiment in both HM1:

IMSS cl6 (Penuliar et al., 2012, 2015) and G3 strains (Nakada-Tsukui et al., 2012; Furukawa et al., 2012, 2013). Then using *Entamoeba invadens* orthologs, I compared the mRNA expression levels of these genes during various timepoints during the encystation stage (De Cádiz et al., 2013).

### 2.3.9. Phylogenetic analysis of PanK

Putative orthologs of PanK from a variety of organisms were retrieved by blastp search of non-redundant protein sequences (nr) database of National Center for Biotechnology Information (NCBI, http://www.ncbi.nlm.nih.gov/) using the EhPanK sequence (XP_001913460) as a query. To comprehensively retrieve all orthologs from representative organisms in variety of major taxa, I carried out blastp search against each taxonomic group as shown in Table S1. In each blastp analysis, a list of selected sequences was made with an E-value less than $1 \times 10^{-10}$ in pairwise alignments with EhPanK. Based on the lists for all taxonomic groups in Table S1, I selected 81 sequences as a final data set. The Muscle program (Edgar, 2004) in SeaView software package version 4.6.1 (Gouy et al., 2010) was used for sequence alignment. Then 145 unambiguously aligned positions were selected by manual inspection and used for phylogenetic analyses.

The phylogenic data matrices were subjected to analysis with the IQTREE program (Nguyen et al., 2015) to select appropriate models for amino acid sequence evolution. The LG + Γ4 model was found to be the best for analysis. Maximum likelihood (ML) analysis implemented in the RAxML program version 7.2.6 (Stamatakis, 2006) was used to infer the ML tree by applying LG + Γ4 model. In bootstrap analysis, heuristic tree search was performed with a rapid bootstrap algorithm option (-f) for 100 bootstrap replicates. Bootstrap proportion (BP) values greater than 50 were indicated on the corresponding internal branches of the ML tree drawn with FigTree program Version 1.4.2 (http://tree.bio.ed.ac.uk/software/figtree/).

### 2.3.10. Production of *E. histolytica* transformant line to express Myc-tagged PanK

The *EhPanK* gene was amplified from cDNA using Ex Taq DNA polymerase (Takara) using the following primer set (sense primer, 5'- GC**CCCGGG**ATGTCTCAACCATCCCATTC -3' and antisense, 5'- GC**CTCGAG** TTACATTAGTTCTTCTTCATACTC-3'), restriction sites are indicated in bold. An amplified fragment was ligated into SmaI and XhoI double digested pEhEx-Myc expression vector (Nakada-Tsukui et al., 2012) to produce pEhExMyc-PanK. The plasmid was introduced into trophozoites of *E. histolytica* HM-1:IMSS cl6 (Diamond et al., 1978) by liposome mediated transfection (Nozaki et al., 1999). Transformants were selected and maintained as described previously.

### 2.3.11. Cell fractionation and immunoblot analysis

Trophozoites of the amoeba transformant expressing Myc-EhPanK and the mock transformant, transfected with pEhEx-Myc, were washed three times with PBS containing 2% glucose. After resuspension in homogenization buffer (50 mM Tris-HCl, pH 7.5, 250 mM sucrose, 50 mM NaCl and 0.5 mg/mL E-64 protease inhibitor), cells were disrupted mechanically by a Dounce homogenizer on ice, centrifuged at 500 x g for 5 min, and the supernatant was collected to remove unbroken cells. The supernatant fraction was centrifuged at 5,000 x g for 10 min to isolate pellet and supernatant fractions. The 5,000 x g supernatant fraction was further centrifuged at 100,000 x g for 60 min to produce a 100,000 x g supernatant and pellet fractions. The pellets at each step were further washed twice with homogenization buffer and re-centrifuged at 100,000 x g for 10 min to minimize carryover. Immunoblot analysis was performed using the fractions and anti-Myc mouse monoclonal antibody. Anti-CPBF1 (cysteine protease binding family protein 1) and anti-CS1 (cysteine synthase 1) rabbit antisera were used as organelle membrane and cytosolic markers, respectively.

### 2.3.12. Production of EhPanK recombinant protein

Plasmid was constructed as previously described (Sambrook and Russell, 2001). DNA fragment was amplified from *E. histolytica* cDNA. Primers used were sense, 5'-GCCG**GGATCC**ATGTCTCAACCATCCCATTC -3' and antisense, 5'- GCCG **GTCGAC**TTACATTAGTTCTTCTTCATACTC-3'. Bold letters indicate BamHI and SalI restriction sites. PCR was performed with primeSTAR HS DNA polymerase (Takara) and the following parameters: initial incubation at 98ºC for 30 sec; followed by the 30 cycles of denaturation at 98ºC for 10 sec; annealing at 55ºC for 30 sec; and elongation at 72ºC for 1 min; and a final extension at 72ºC for 7 min. The PCR fragment was digested with BamHI and SalI, purified with Wizard® SV gel and PCR clean up system (Promega). The fragment was cloned into BamHI and SalI double digested pCOLD1™ histidine-tag vector (Takara) to finally produce pCOLD1-EhPanK. The nucleotide sequence of the engineered plasmid was verified by sequencing.

pCOLD1-EhPanK was introduced into *E. coli* BL21(DE3) cells via heat shock at 42ºC for 1 min. *E. coli* BL21 (DE3) harboring pCOLD1-EhPanK was grown at 37ºC in 100 mL of Luria Bertani medium (Invitrogen) in the presence of 100 µg/mL ampicillin (Nacalai Tesque). The overnight culture was used to inoculate 500 mL of fresh medium, and the culture was further continued at 37ºC with shaking at 180 rpm. When $A_{600}$ absorbance reached 0.8, then 0.5 mM isopropyl β-D-thio galactopyranoside (IPTG) was added, and cultivation was continued for another 24 h at 15ºC. *E. coli* cells from the induced culture were harvested by centrifugation at 5,000 x g for 20 min at 4ºC. The cell pellet was washed with PBS, pH 7.4, re-suspended in 20 mL of the lysis buffer (50 mM Tris HCl, pH 8.0, 300 mM NaCl, and 10 mM imidazole) containing 0.1% Triton x 100 (v/v), 100 µg/mL lysozyme, and 1 mM PMSF, and incubated at room temperature for 30 min. Then the mixture was sonicated on ice and centrifuged at 25,000 x g for 15 min at 4ºC. The supernatant was mixed with 1.2 mL of 50% $Ni^{2+}$-NTA His-bind slurry, incubated for 1 hour at 4ºC with mild shaking. The recombinant enzyme-bound resin in a

column was washed three times with buffer A (50 mM Tris-HCl, pH 8.0, 300 mM NaCl, and 0.1% Triton X-100, v/v) containing 10-50 mM of imidazole. Bound protein was eluted with buffer A containing 100-300 mM imidazole. After the integrity and the purity of recombinant protein were confirmed with 12% SDS-PAGE analysis, followed by Coomassie Brilliant Blue staining, the sample was dialyzed against a 300-fold volume of 50 mM Tris-HCl, 150 mM NaCl, pH 8.0 containing 10% glycerol (v/v) and the Complete Mini protease inhibitor cocktail (Roche, Mannheim, Germany) for 18 hours at 4$^{o}$C. Pure enzyme was stored at -80$^{o}$C with 20% glycerol in small aliquots until use.

### 2.3.13. Metabolome analysis of of PanK gene silencing strain

Intracellular metabolites were extracted according to previously (Jeelani et al., 2012) with some modifications. In brief, the 1 x $10^7$ *E. histolytica* DPCK1 and DPCK2 gene silencing cells were harvested after 72 h cultivation in BIS medium. Cells were centrifuged 3,000 rpm for 5 min and washed twice with 5% mannitol. To quench metabolic activity, the cells were immediately extracted with a solvent composed of cold methanol, distillated water, chloroform (methanol: water: chloroform = 2:1:2 (v/v/v)). Internal standards, 200 µM of 2- (*N*-morpholino) ethanesulfonic acid and methionine sulfone were added to every sample to ensure that experimental artifacts such as ion suppression did not lead to misinterpretation of metabolite levels. After 30 second sonication, vortex and centrifugation at 15,000 g at 4 $^{o}$C for 15 min, supernatant were filtered through 5-kDa cutoff filter then re-centrifuged max speed at 4 $^{o}$C for 2 h. The filtrates were dried and preserved at 28 $^{o}$C until capillary electrophoresis-mass spectrometry (CE-MS) analysis (Kimball and Rabinowitz, 2006).

CE-MS was performed using an Agilent CE Capillary Electrophoresis System equipped with an air pressure pump, an Agilent 1100 series MSD mass spectrometer and an Agilent 1100 series isocratic high performance liquid chromatography pump, a G1603A Agilent CE-MS adapter kit, and a G1607A Agilent CE-MS sprayer kit (Agilent Technologies). System control,

data acquisition, and MSD data evaluation were performed using G2201AA Agilent ChemStation software for CE-MSD. Anionic and cationic metabolites were analyzed.

Anionic were coated in SMILE (+) capillary 50-µm inner diameter x 100-cm total length obtained from Nacalai Tesque (Kyoto, Japan). The electrolyte was 50 mM ammonium acetate solution (pH 8.5). Sample solution (~30 nL) was injected at 50 mbar for 30 s and a negative voltage of 30 kV. The capillary voltage was set at 3.5 kV for ESI-MS in the negative ion mode. Deprotonated [M-H] ions were monitored for anionic metabolites of interest (Soga et al., 2002).

Cationic nucleotides compounds were carried out on a gas chromatograph capillary, polydimethylsiloxane (DB-1) (50-µm inner diameter x 100-cm total length) (Agilent Technologies). CE separation was using 50 mM ammonium acetate, pH 7.5 as the electrolyte. Sample solution (~3 nL) was injected at 50 mbar for 3 s, and a positive voltage of 30 kV was applied. All other conditions were the same as in the anionic metabolite analysis. The energy charge was calculated as an index of contents of high energy phosphatebonds. Energy charge is defined as one-half the number of anhydride-bound phosphates per adenylate, using the values for ATP, ADP and AMP, as the following:

EC = (ATP + 1⁄2ADP)/(AMP +ADP +ATP).

For each experimental condition, three (control) and five (PanK gene silencing strain) independent biological replicates were made and for each biological replicate, two technical replicates were made. All data are shown as means ± S.D. for the indicated number of experiments. Statistical comparisons were made by Student's t test.

### 2.3.14. Screening of natural compounds for EhPanK inhibitors

I screened 244 compounds from the Kitasato Natural Products Library for inhibition of *Eh*PanK activity and also 3,000 microbial extracts. Initially, each compound and extract was dissolved in 50% DMSO and water at a final concentration of 1 mg/mL. Enzymatic reactions were carried out on a black 384-well microtiter plate with a 20 µL reaction mixture composed of 19 µl enzyme mix (100 µM pantothenate, 100 µM ATP, 50 ng of EhPanK recombinant enzyme

in kinase buffer (see above) and 1 µl of the individual compounds (final concentration 50 µg/mL or 25-200 µM) and extract at 37ºC for 2 hours. After the kinase reaction, ADP was measured using ADP Hunter$^{TM}$ Plus kinase assay kit as described previously. Inhibition values were measured in triplicate.

Compounds that showed more than 50% inhibition at <400 µM and extracts that showed more than 90% inhibition were re-tested to confirm that they did not inhibit the enzyme in the coupled assay (pyruvate kinase and pyruvate oxidase) in ADP Hunter$^{TM}$ Plus kinase assay kit. Inhibition of the enzymes used in the coupled assay was examined in the reaction mixture (10 mM $MgCl_2$, 15 mM HEPES, 20 mM NaCl, 1 mM EGTA, 0.02% tween 20, 0.1 mg/mL β-globulin, 60 µM pantothenate, 50 µM ATP, 10-50 µM ADP, and 25-200 µM of selected active compounds). No significant change was observed in a range of ADP and inhibitor concentrations, suggesting no inhibition of coupled enzymes by the EhPanK inhibitors. Compounds that did not inhibit enzymes used in the coupled assay were selected as hits for further evaluation, including: dose response, determination of concentration needed for 50% inhibition ($IC_{50}$) of PanK activity as well as both *E. histolytica* and human cell growth. Extracts that did not inhibit couple enzymes were re-tested for its stability in various pH (2.7 and 9) and pre-heated 60 ºC for 60 min. Stable extract were selected and reproduced in larger scale culture (5 liter). Culture then filtered, mycelium obtained were extracted using methanol and dried by rotary evaporator. Extracts purification were conducted using open column silica $F_{60}$.

### 2.3.15. Measurement of Anti-Amebic Activity of EhPanK inhibitor compounds

Approximately $1 \times 10^4$ trophozoites of *E. histolytica* clonal strain HM-1:IMSS cl6 in 200 µl of BI-S-33 medium were dispensed into each well of a 96-well plate and incubated at 35.5ºC for 2 h. Medium was then removed and replaced with 200 µl of BI-S-33 medium that contained various concentrations of each compound. The final concentrations of test compounds are: 50 to 600 µM for cephaloridine, hygromycin A, erythromycin A, and fluorescamine; 5 to 200 µM for kasugamycin, gardimycin, rosamycin, streptomycin, tirandamycin A, neomycin, and teicoplanin;

0.1 to 10 μM for *O*-methylnanaomycin A, echinomycin, and trichostatin. The plate was incubated under anaerobic conditions at 35.5ºC for 48 h. After the medium was removed, 100 μl of pre-warmed Opti-MEM I (Life Technologies, Grand Islands, NY, USA) containing one tenth volume of WST-1 (Roche, Mannheim, Germany) was added. The viability of trophozoites was estimated by measuring absorbance at 450 nm by SpectraMax® Paradigm® (Molecular Devices, CA, USA). Metronidazole was used as positive control at final concentrations of 0.1 to 10 μM and 0.5% DMSO as negative control. Each assay was performed in triplicate. $IC_{50}$ values were calculated by least squares curve fitting of the dose inhibition curves using GraphPad Prism (GraphPad Software Inc., San Diego, USA).

### 2.3.16. Evaluation of Cytotoxicity against MRC-5 Cells

Human fibroblast cells, MRC-5, were cultured on 96-well flat bottom plates at a density of $1.5 \times 10^4$ cells/well with 100 μl of MEM medium (Life Technologie) containing 10% fetal bovine serum (Hana-nesco Bio, Tokyo, Japan) and 1% penicillin streptomycin (Life Technologies). Cells were incubated at 37ºC with 5% $CO_2$ for 48 h. Approximately 100 μl of MEM medium containing 5 μl of each compound dissolved in 50% DMSO in water were added to each well. After the plates were incubated for 48 h, approximately 10 μl of WST-8 (Dojindo, Kumamoto, Japan) was added to each well and the plate was incubated at 37ºC with 5% $CO_2$ for 2 h. The absorbance was measured at 450 nm by spectrophotometer (SH-9000Lab, Corona Electric, Ibaraki, Japan). Growth of MRC-5 cells was measured in duplicate. Staurosporine (Kitasato Natural Products Library) was used as a positive (cytotoxic) control in a concentration range of 0.5 pM to 0.1 nM. $IC_{50}$ values were calculated as described previously.

## 2.4. Results

### 2.4.1. Identification of four enzymes involved in CoA biosynthesis in *E. histolytica*

I identified all putative genes involved in CoA biosynthesis in the reference genome of *E. histolytica*: HM-1:IMSS (Fig. 1). Corresponding to PanK, I detected a single putative *PanK* gene in each strain (e.g., EHI_183060 in HM-1:IMSS and EHI7A_012650 in HM-1:IMSS-A) in Amoeba Genomics Resources database, AmoebaDB (http://amoebadb.org). The nucleotide sequences of the genes in different strains are 100% identical. Therefore, *E. histolytica* seems to have only one *PanK* gene.

The previous transcriptome data verified that all four genes are expressed at low to moderate levels (Fig. 2A). The level of mRNA expression relative to RNA polymerase for PanK, PPCS-PPCDC, PPAT, DPCK1, and DPCK2 in trophozoites of the *E. histolytica* clonal strain HM1: IMSS cl6 (Penuliar et al., 2015, 2012) and G3 ( Nakada-Tsukui et al., 2012; Furukawa et al., 2012, 2013) strain were 1.2-1.8, 0.5-0.6, 0.3-0.4, 0.04-0.05 and 0.3-0.4, respectively. In Chapter 2, I described biochemical and genetic characterization of PanK. The previous transcriptomic analysis of *E. invadens* (De Cádiz et al., 2013), as a model for encystation (Donaldson et al., 1975; Kojimoto et al., 2001; Stanley, 2003; Chia et al., 2009), showed that genes encoding these four enzymes were expressed during encystation, but the expression profiles of individual enzymes largely differed (Fig. 2B). The expression profiles of PPCS-PPCDC and DPCK1 were quite peculiar with expression peaking at certain time points (2 h and 24 h, respectively); this subject was, however, not investigated as part of this study.

### 2.4.2. Features of *EhPanK* and its encoded protein

The 1,219-bp *E. histolytica PanK* gene contains two small introns, and is predicted to encode a 403 a.a. polypeptide with a molecular mass of 45.2 kDa and a p*I* value of 5.2. EhPanK showed 99, 96, 83, and 70% sequence identity to PanK from *E. nuttalli*, *E. dispar*, *E. moshkovskii*, and *E. invadens*, respectively. In general, PanK is classified into three groups, type

I through III, as determined by primary sequence analysis and kinetic properties (Song and Jackowski, 1993; Rock et al., 2002; Yang et al., 2006). *E. histolytica* PanK is classified as PanK type II, and shows a low level (~ 35%) of positional identity to the *A. thaliana* and human orthologs, both of which also belong to type II (Fig. 3 and 4). When compared to human PanK, *Entamoeba* PanK shows highest similarity to human PanK4 (35%), whereas similarity to other human PanK isotypes (PanK1α, PanK1β, PanK2, and PanK3) is ~32%. All amino acid residues were inferred to be involved in pantothenate and ATP catalysis and substrate binding include the typical ATP-binding motif have been reported in human PanK1 and PanK3 (Bum et al., 2007). Some conserved glycine residues in the ATP binding motif ($Gly^{19}$ and $Gly^{321}$ in human PanK3; $Gly^{59}$ and $Gly^{351}$ in *E. histolytica*) are indispensable for activity. Mutations of this amino acid have been demonstrated to abolish enzymatic activity because ATP is no longer able to properly bind (Bum et al., 2007). Furthermore, it is understood that phosphorylation is proceeded by an ordered sequential mechanism, with ATP binding preceding pantothenate binding (Leonardi et al., 2005a).

### 2.4.3. Phylogenetic analysis of EhPanK

I determined the phylogenetic relationship between 81 putative PanK orthologs collected from bacteria and eukaryotes (Fig. 4). The majority of eukaryotes possess the *PanK* gene. Mammals (Opisthokonta) and land plants (Viridiplantae) apparently possess twice or more two genes. For instance, four *PanK* genes were identified from *Homo sapiens*, PanK1α and PanK1β (Rock et al., 2002), PanK2 (annotated as a mitochondrial precursor protein) (Hörtnagel et al., 2003; Kotzbauer et al., 2005), and PanK3 (Zhang et al., 2005). Archaea and most bacterial groups do not possess *PanK* homologs that show similarity to *Eh*PanK with the E-value less than $10^{-10}$. *PanK* homologs were identified, however in firmicutes, specifically *Bacilli*. During sequence alignment, only the 'fumble' domain (PFAM:PFO03630) could be aligned among all 81 sequences, although insertions and deletions were needed for proper alignment due to a high degree of divergence. PanKs from Euglenozoa have an ~1,000-a.a. long N-terminal extension,

which contains an exonuclease-endonuclease-phosphatase (EEP) domain in the 300 a.a.-long N-terminal region and a 550 a.a.-long adenylate forming (AF) domain. Some of PanK from *Viridiplantae* have a 300 a.a.-long C-terminal extension, annotated as DUF89 (Domain of Unknown Function 89) (Huang et al., 2016). PanK from other organisms including the genus *Entamoeba* basically contain only a 'fumble' domain; neither the EEP/AF nor DUF89 domain is present in PanK from other organisms except that some possess an N-terminal extension that appears to be an organelle targeting sequence.

Based on 145 aligned positions from the 'fumble' domain, an optimal ML tree was created with bootstrap proportion (BP) support values (Fig. 4). Eukaryotes and firmicutes were separated clearly with a 100% BP support value. The Eukaryota clade had monophylies of several taxonomic groups reconstructed, but BP values were generally low except for those of Viridiplantae monophyly (88%) and Haptophyceae monophyly (97%). Four *Entamoeb*a species are monophyletic with 100% BP support, and the *Entamoeba* clade shares a sister group position to the clade of Euglenozoa. However, since BP support values for deep branching patterns were very low, monophly of Amoebozoa including the *Entamoeba* clade cannot be ruled out. Although this analysis could not precisely infer the phylogenetic position of the *Entamoeba* PanK, it is apparently of a eukaryotic origin.

### 2.4.4. Expression and purification of recombinant PanK

A soluble EhPanK recombinant protein with a 2.6 kDa histidine tag at the amino terminus was successfully produced using the pCOLD I *E. coli* expression system and purified to homogeneity (>95% as evaluated with Coommassie Brilliant Blue stained SDS-PAGE gel) (Fig. 5, Table 1). Immunoblot analysis of the purified recombinant protein using His-Tag antibody confirmed the absence of truncation (Fig. 5B). The molecular mass of the purified protein under reducing conditions was consistent with the predicted molecular mass 45.2 kDa excluding the histidine tag. The specific activity of the purified enzyme was estimated to be 1.5 μmole/min/mg when assayed under the standard conditions described in the "Materials and

methods" section. EhPanK is robust and catalytically active in broad pH range with maximum activity obtained at pH 6 and 37ºC (Fig. 6A).

### 2.4.5. Kinetic properties and phosphoryl donor specificities of EhPanK, and effects of metal ions on EhPanK

Table 2 summarizes the apparent $K_m$, $V_{max}$, and $K_{cat}$ values for EhPanK using pantothenate and ATP as substrates. EhPanK exhibited hyperbolic saturation kinetics when assayed over the substrate range of 4-256 μM for pantothenate in the presence of 25-100 μM ATP (Fig. 6B) and 1-100 μM ATP in the presence of 8-128 μM pantothenate (Fig. 6C). The apparent $K_m$ value for pantothenate at saturating ATP concentrations was 53.2 ± 7.1 μM, and the $K_m$ value for ATP at saturating pantothenate concentrations was 41.4 ± 3.9 μM.

EhPanK utilized various nucleoside triphosphates, ATP, CTP, GTP, UTP, dATP, and polyphosphates, as well as deoxynucleotides as phosphoryl donors, with ATP being the best phosphate donor (Table 3). EhPanK showed an absolute requirement for a free bivalent metal cofactors, with $Mg^{2+}$ as the preferred cation (Table 4).

### 2.4.6. Regulation of EhPanK by CoA, acetyl CoA and malonyl CoA

PanK from other organisms was reported to be negatively regulated by allosteric inhibition with CoA, acetyl CoA, and malonyl CoA (Calder et al., 1999; Takagi et al., 2010; Vallari et al., 1987). Similarly, EhPanK was also inhibited by CoA and its derivatives, although relatively higher concentrations were needed for inhibition compared with PanK from other organisms (Brand and Strauss, 2005; Calder et al., 1999) (Fig. 7). Double-reciprocal plots revealed the mechanisms of inhibition by CoA and malonyl CoA are competitive with ATP, while inhibition by CoA and malonyl CoA are uncompetitive or non-competitive with pantothenate, respectively. The mechanisms of inhibition by acetyl CoA were not clear, but seemed to be the mixed type with respect to ATP and pantothenate (Fig. 8).

### 2.4.7. Cellular localization of EhPanK

To examine the localization of EhPanK, I performed fractionation and immunoblot analysis of PanK using *E. histolytica* transformant-expressing Myc-tagged EhPanK. I demonstrated that EhPanK is exclusively present in the 100,000 x g supernatant fraction corresponding the cytosol (Fig. 9).

### 2.4.8. Effects of *EhPanK* gene silencing on growth, cellular CoA levels, and gene expression of the CoA biosynthetic pathway

To investigate the physiological importance and essentiality of PanK in *E. histolytica*, I created and examined an *E. histolytica* strain where *EhPanK* was silenced by antisense small RNA-mediated transcriptional gene silencing (Mirelman et al., 2008); *EhPanK* gene expression was successfully silenced (Fig. 10A). The level of silencing was estimated to be approximately 85% by qRT-PCR measurement. Interestingly, the steady-state transcript of the genes encoding other enzymes involved in CoA bioshynthesis were up-regulated 1.2 ± 0.03, 2.1 ± 0.2, 3 ± 0.1, and 5.2 ± 1.0-fold for *PPCS-PPCDC*, *PPAT*, *DPCK1*, and *DPCK2*, respectively (Fig. 10B).

In order to determine whether the protein level also increased, I measured PanK and DPCK activity in cell lysates. PanK activity decreased by approximately 81% in the *EhPanK*-silenced strain compared to the control. In contrast, DPCK activity increased 2.1 fold (Fig. 10C). CoA concentration decreased by approximately 40% in *EhPanK*-silenced strain compared to the control (Fig. 10D). Growth kinetic analysis also showed that in *EhPanK*-silenced strain showed remarkable growth retardation as the cell density of *EhPanK*-silenced strain decreased to approximately 30-52% of the control at 48-96 h, respectively (Fig 10E). Independent growth kinetic observation also showed dramatically retardation between 48-96 h incubation (Fig. 11).

### 2.4.9. Metabolomic analysis of EhPanK gene silencing

In order to understand the metabolic consequence of disturbance of CoA biosynthesis caused by repression of *EhPanK* gene expression in *E. histolytica* trophozoites, metabolomic

analysis was also performed using CE-MS. I detected and quantitated >120 metabolites, and identified 13 metabolites that significantly differed between *EhPanK* gene silenced and control transformants ($p<0.05$). I investigated the following metabolic pathways and specific metabolites in detail: carbon metabolism, nucleic acids, acetyl CoA, and related metabolites including citric acid, ornithine, and polyamines. I also checked fatty acid metabolism, CoA-associated metabolism such as malonyl CoA, *n*-propionyl CoA and methylmalonyl CoA, but there was apparently no significant change. The total amount of the glycolytic intermediates (represented by "Σ glycolysis") and pentose phosphate pathway metabolites ("Σ PPP") (Fig. 12) increased 1.4 and 1.9-fold, respectively. Most of individual intermediate metabolites in glycolysis were increased (Fig. 12). Similarly, individual metabolites in the PPP were generally increased, while increase in D-sedoheptulose 7-phosphate being significant. Nineteen out of thirty nucleic acids examined were depleted, among which hypoxanthine, xanthine, cAMP, cGMP, and cCTP were significant decreased (Fig. 13A).

As described above, *PanK* gene silencing reduced the CoA level by 40%. Accordingly, acetyl CoA was also suppressed, while other CoA conjugates remained unchanged. In addition, I found decrease in citrate, ornithine (also spermidine), and *S*-adenosyl-L-methionine (Fig. 13B). Ornithine and *S*-adenosyl-L-methionine are important intermediate metabolites for polyamine biosynthesis such as putrescine, spermidine, and spermine (Jeelani et al., 2012).

### 2.4.10. Identification of EhPanK inhibitors from Kitasato Natural Products Library and microbial extracts

Based on the significant biological role of EhPanK, inhibitors of this enzyme should be considered to possess properties needed for novel anti-amoebic agents. Therefore, I conducted enzyme-based screening of the Kitasato Natural Products Library composed of 244 structurally elucidated compounds using recombinant EhPanK to identify potential PanK inhibitors. I identified 14 compounds (Fig. 14) that demonstrated an $IC_{50}$ value of <400 μM (Table 5, Fig. 15). Among these compounds, Teicoplanin had the best inhibitory activity against EhPanK with

an $IC_{50}$ value of 26.3 ± 2.6 μM. All EhPanK inhibitors also inhibited *E. histolytica* trophozoites although the $IC_{50}$ values of most of the identified EhPanK inhibitors were high. Six compounds, *O*-methylnanaomycin A, Echinomycin, Tirandamycin A, Neomycin, Trichostatin, and Teicoplanin, showed the $IC_{50}$ values of <20μM against *E. histolytica* trophozoites, but the $IC_{50}$ values of *O*-methylnanaomycin A, Echinomycin, Tirandamycin A, Neomycin, and Trichostatin against *E. histolytica* trophozoites were lower than their $IC_{50}$ values against EhPanK activity, suggesting that the target of these compounds for growth inhibition are unlikely to be through PanK inhibition. In contrast, Teicoplanin demonstrated comparable $IC_{50}$ values against PanK activity and *E. histolytica* growth (Table 6).

Beside compound library, I also screened 3,000 microbial extracts against EhPanK. There estimated 4.2 % from total extract inhibited EhPanK (Table 7). Approximately 0.3% (9 extracts) from total extract could inhibit more than 90% EhPanK, then I categorized as hit extracts to be purified. Since compound purification from hit extracts still in progress, I excluded them (purification results) from this report.

## 2.5. Discussion

### 2.5.1. Identification of CoA biosynthesis as rational drug target

CoA is an essential and ubiquitous cofactor functioning as an acyl carrier as well as a carbonyl activating group for many metabolic reactions. In the present study, I identified four enzymes that are involved in CoA synthesis in *E. histolytica* (Fig. 1), and characterized the first rate-limiting enzyme in this process, PanK. I have provided evidence for the pivotal role of this enzyme in cell proliferation by gene silencing.

Since all genes involved in CoA biosynthesis are transcribed in all amoeba life cycle stages, this pathway is good target not only for killing the pathogenic trophozoites, but inhibiting stage conversion and thus amoeba transmission. The mechanism coordinating gene expression regulation among the five genes involved in *E. histolytica* CoA biosynthesis remains elusive.

However, based on the previous transcriptomic analysis of *E. invadens*, a related reptilian amoeba species that also causes an invasive disease and has been used as a model system for *E. histolytica* (Donaldson et al., 1975; Kojimoto et al., 2001; Chia et al., 2009) during encystation (De Cádiz et al., 2013), I found that PanK is transcribed in both trophozoite and encystation life cycle stages at comparable levels, suggesting that PanK is required in both stages.

A *EhPanK* gene-silenced strain was successfully established, after producing a strain in which *EhPanK* gene expression was ~85% repressed. Four failed attempts to create of such a cell line (data not shown) suggest the essentiality of this gene. The low levels of EhPanK in my experiment can keep the cells viable, consistent to previous publication in *Mycobacterium tuberculosis* PanK (Reddy et al., 2014). Interestingly, *EhPanK* gene silencing resulted in the simultaneous transcriptional up-regulation of genes for downstream CoA pathway enzymes. Remarkably, such genes, DPCK1 and DPCK2, were up-regulated 3- and 5-fold, respectively. This observation is similar to that in experimentation with *Plasmodium yoelii*, where other genes in the CoA biosynthetic pathway were up-regulated when *PanK2* gene was knocked out (Hart et al., 2016). Despite the apparent compensatory upregulation of downstream enzyme genes, CoA concentration was significantly reduced, which is most likely a direct cause of decreased ATP generation and retarded growth.

In order to validate EhPanK as drug target, there should be notable biochemical, structural, and genetic differences in their human homologs. Such characteristics should, in theory, minimize toxic side effects of pharmacological inhibition of human enzymes via amebiasis chemotherapy. *E. histolytica* has one PanK enzyme whereas *Homo sapiens* has five PanK isoforms encoded by four genes. EhPanK is most closely related to human PanK4 with 35% amino acid identity, but phylogenetic analyses suggests a distant relationship between EhPanK and its human counterparts.

While PanK is indispensable for optimal growth of *E. histolytica* trophozoites, but in some eukaryotes, including human, PanK was shown non-essential. It has been demonstrated

that human cells have the ability to hydrolyze exogenous CoA to 4′-phosphopantetheine by ectonucleotide pyrophosphatase, and then incorporate 4′-phosphopantetheine and enzymatically convert it back to CoA by the bifunctional enzyme CoA synthase (Srinivasan et al., 2015). In *Plasmodium*, it was reported that PanK is nonessential in blood stage parasite development, but essential in the hepatic stage, as well as oocyst and sporozoite formation in the mosquito (Hart et al., 2016; Srivastava et al., 2016). In *M. tuberculosis*, CoaA was proven to be an essential enzyme (Awasthy et al., 2010), but was also shown in *in vitro* and *in vivo* studies to be a suboptimal target for antimycobacterial drug development because expression of *CoaA* gene needs to be repressed to obtain sufficient cidal effects by inhibitors (Reddy et al., 2014). On the other hand, CoaBC, a bifunctional enzyme in the CoA biosynthesis, has proven to be essential, but its suitability as drug target needs to be chemically validated in future (Evans et al., 2016). Inhibition of PanK in human cells may be tolerated, which also supports the premise that PanK is a reasonable chemotherapeutic target against pathogens for humans.

### 2.5.2. Metabolic disturbance caused by PanK repression

Gene silencing of *EhPanK* led to increase in the total glycolysis intermediates and PPP metabolites. Decrease in CoA and acetyl CoA concentrations likely caused the accumulation of upstream metabolites in glycolysis and PPP. Depletion of CoA and acetyl CoA probably led to oxidative stress, as suggested by my previous metabolomics experiment showing that the intermediates in the non-oxidative branch of PPP also increased upon oxidative stress (Husain et al., 2012). PPP is required in general for NADPH synthesis and fatty acid synthesis, nucleic acid synthesis, and cell survival (Patra and Hay, 2014; Tsouko et al., 2014). PPP activity is increased in cancer cells and also in response to oxidative stress (Przybytkowski and Averill-Bates, 1996). Thus, it is plausible that glycolysis also increases in *E. histolytica* to respond to the decrease of CoA and acetyl/acyl CoA, although underlying mechanisms remain to be elucidated. It has shown that PPP is not functional in *E. histolytica*, since this organism lacks glucose 6-phosphate dehydrogenase (G6PDH) and transaldolases (Loftus et al., 2005). It possesses an alternative

hexose-pentose interconversion pathway that does not require transaldolases, but depends on three enzymes: phosphofructokinase, transketolase, and aldolase (Susskind et al., 1982). *Entamoeba histolytica* generates NADPH via other alternative pathways, by which NADPH is produced from NADH by NAD kinase (Jeelani et al., 2013), or NADPH and $NAD^+$ are produced from NADH and $NADP^+$ by pyridine nucleotide trans-hydrogenase using electrochemical proton gradient (Yousuf et al., 2010).

Some cyclic nucleoside monophosphates (cAMP, cGMP and cCMP) were significantly decreased by *EhPanK* gene silencing. They participate in many physiological responses (Bridges et al., 2005) such as protein-kinase cascades, down-regulation of drug responsiveness, and transmembrane signal transduction (Beavo and Brunton, 2002). They bind to protein kinase A, an enzyme family that plays an important role in glycogen, lipid, and sugar metabolism. Other nucleic acids including some purines, hypoxanthine and xanthine, were also significantly reduced by *EhPanK* gene silencing. These metabolites are involved in purine salvage pathway. In *Plasmodium falciparum*, enzymes in purine metabolic pathways are considered to be a promising novel drug target (Cassera et al., 2011).

My metabolomics analysis also uncovered that suppression of *PanK* caused disturbance in polyamine metabolism, in particular decrease in ornithine, spermidine, and spermine, and increase in *S*-adenosyl-L-methionine. Polyamines have important functions in cell growth, biosynthesis of informing molecules, cell membrane stabilization, adaptation of the cell to ionic, osmotic, thermal and pH stress (Slocum et al., 1984; Tabor and Tabor, 1985). Ornithine is synthesized from acetyl CoA by several steps involving acetyl-, amino-transfer and (de)phosphorylation. It has been reported that ornithine is the essential precursor for polyamine synthesis in other parasites such as *Leishmania* (Roberts et al., 2016) and *Trypanosoma* (Taylor et al., 2008). Ornithine decarboxylase (ODC), a rate-limiting enzyme for polyamine biosynthesis, has been extensively studied as a drug target against parasitic infections and cancers (Bacchi and McCann, 1987; McCann et al., 1987; McCann and Pegg, 1992; Müller et

al., 2001). Polyamines are required in nucleic acid packaging and other function such as DNA replication, apoptosis, transcription, and translation (Ruan et al., 1994). Beside polyamines, citrate was also decreased together with upstream metabolites, CoA and acetyl CoA. Since *E. histolytica* lacks the entire tricarboxylic cycle including citrate synthase that converts acetyl CoA to citrate, and also electron transport chain and oxidative phosphorylation (McLaughlin and Aley, 1985; Reeves, 1985), the role of citrate is also poorly understood.

### 2.5.3. Hit discovery of EhPanK inhibitors

Historically, natural products, especially secondary metabolites, have provided various drugs against human diseases (Newman and Cragg, 2012). Several natural compounds from fungi and actinomycetes that inhibit cysteine synthase, an enzyme absent in humans and involved in *de novo* biosynthesis of L-cysteine have been discovered (Mori et al., 2015). In this study, I identified 14 inhibitors of EhPanK; half of the inhibitors have sugar moieties, and some of them are aminoglycosides.

Teicoplanin showed moderate inhibitory activity with $IC_{50}$ 26.3 ± 2.6 μM and inhibition of *E. histolytica* trophozoite growth ($IC_{50}$ 15.1 ± 2.3 μM). Although Teicoplanin also demonstrated cytotoxicity to MRC-5 cells, preference towards *E. histolytica* cells was identified. Teicoplanin is a mixture of glycopeptide antibiotics used against Gram positive bacteria including methicillin-resistant *Staphylococcus aureu*s, with a mechanism of action inhibiting bacterial cell wall synthesis. Teicoplanin consists of the glycopeptide core, two carbohydrates (mannose and *N*-acetylglucosamine), and a side chain. The components of teicoplanin are classified by their side chain length and conformation; the major components are $A_2$-1 through $A_2$-5.

## 2.6. Figures and Tables

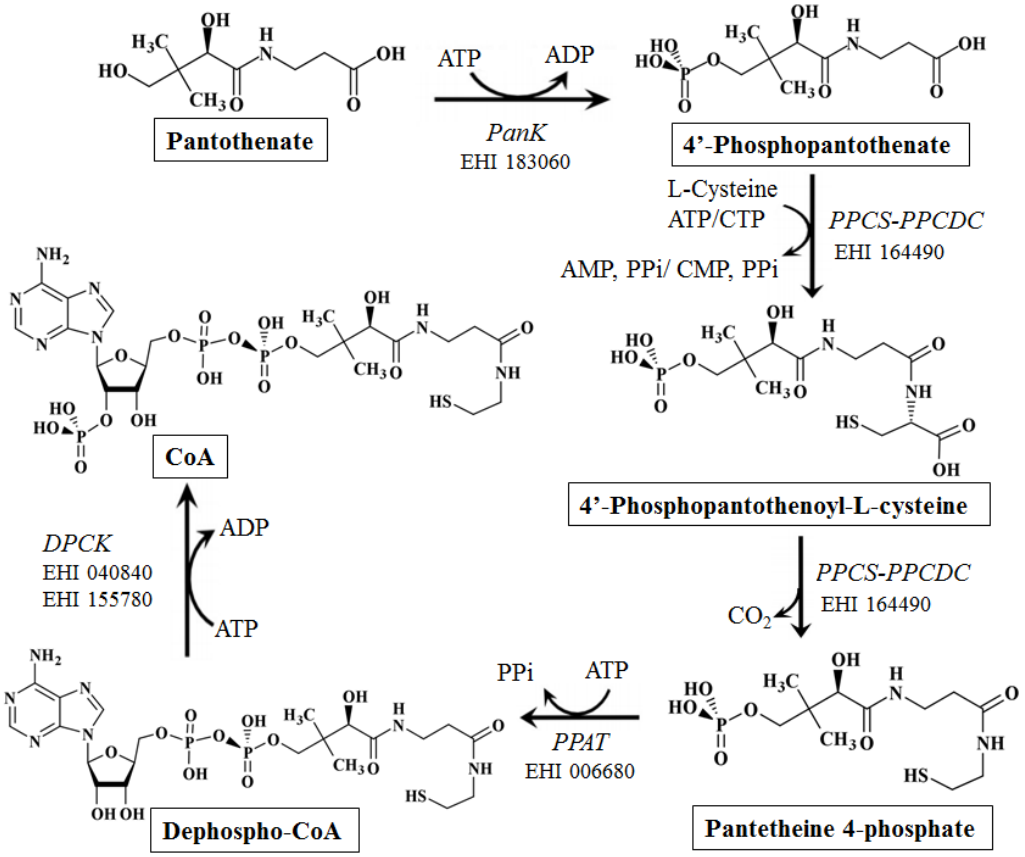


**Fig. 1.** Coenzyme A biosynthetic pathway in *E. histolytica*. ID numbers of individual enzymes in AmoebaDB are also shown. PanK, pantothenate kinase; PPCS-PPCDC, bifunctional phosphopantothenoylcysteine synthetase and phosphopantothenoylcysteine decarboxylase; PPAT, phosphopantetheine adenylyltransferase; and DPCK, dephospho-CoA kinase.

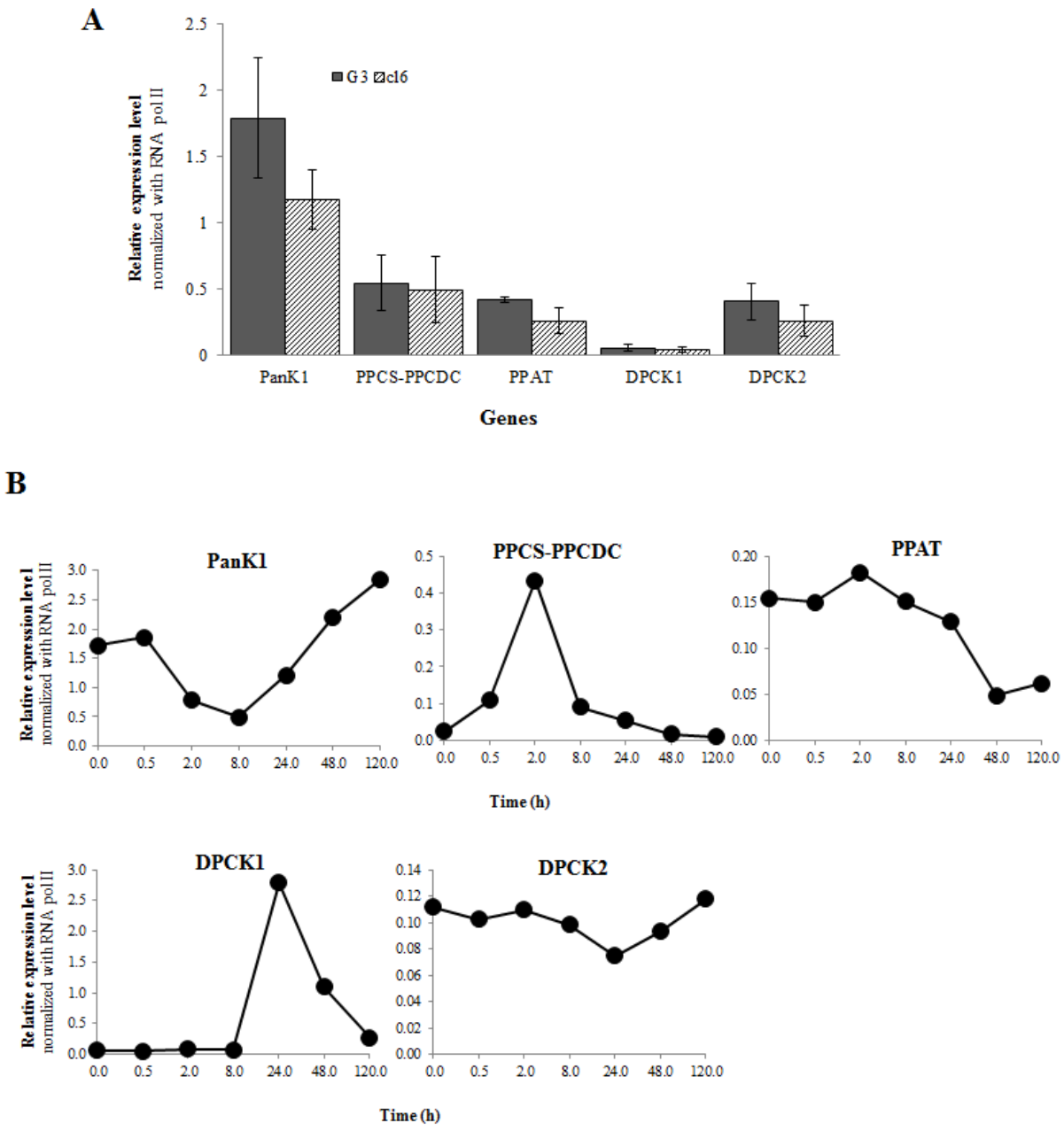


**Fig. 2.** Relative mRNA expression level of all enzymes in CoA biosynthesis. A) Relative levels in trophozoites of the *E. histolytica* HM1: IMSS cl6 (Penuliar et al., 2012, 2015) and G3 (Furukawa et al., 2013, 2012; Nakada-Tsukui et al., 2012) strain from array data. B) Relative levels in *E. invadens* encystation stage. Data was generated from previous publication (De Cádiz et al., 2013).

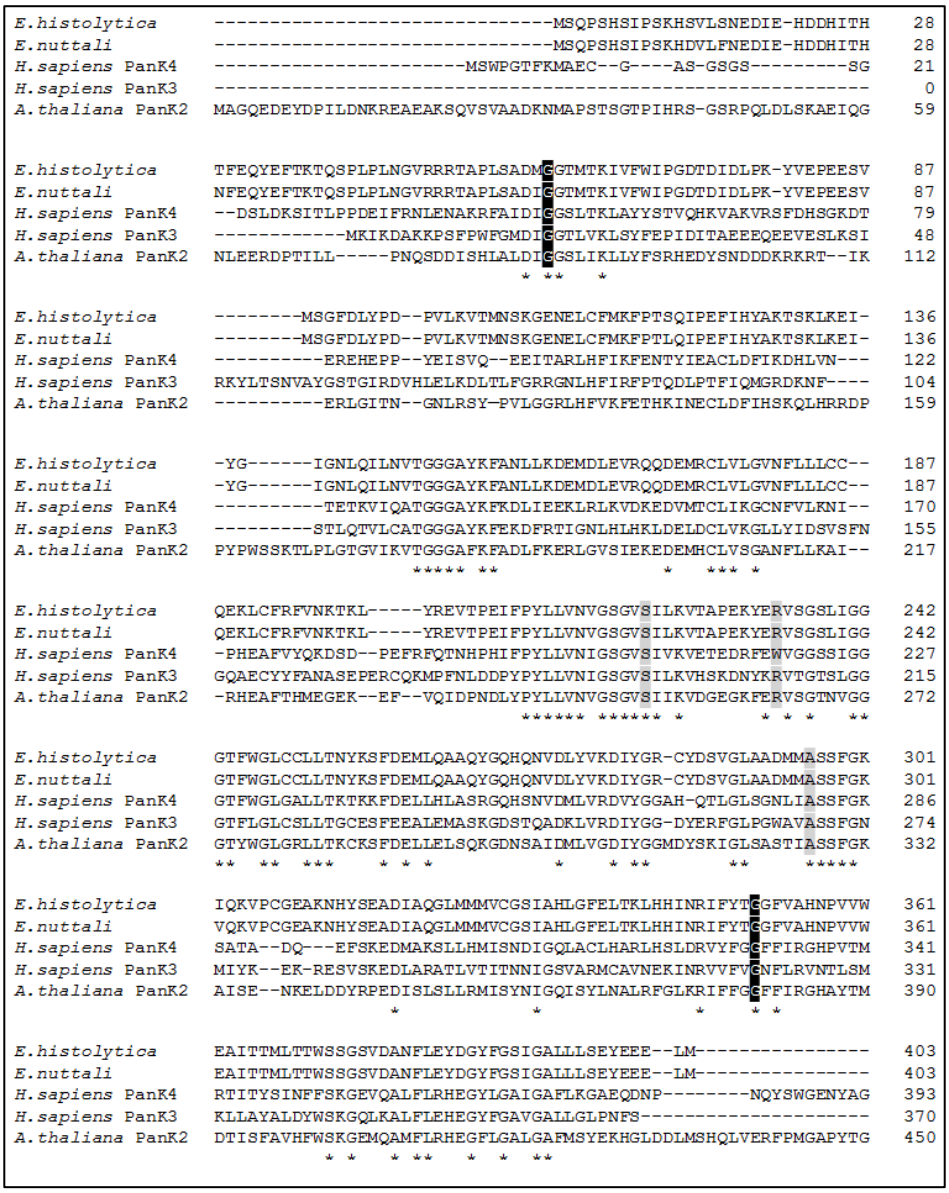


**Fig. 3.** Alignment of PanK protein sequences from *E. histolytica* and other organisms. The sequences were aligned using Muscle program (Edgar, 2004) in SeaView package version 4.6.1 (Gouy et al., 2010). The species names and the NCBI accession numbers are as follows: *E. histolytica* (XP_001913460); *Entamoeba nuttali* (XP_008855986); *Homo sapiens* PanK4 (NP_060686); *Homo sapiens* PanK3 (NP_078870); *Arabidopsis thaliana* (NP_001031768). Identical residues are denoted by asterisks (*). The glycine residue in the ATP binding sites are shown in white letter on with a black background. Serine, arginine, and alanine residues highlighted with black letters on a grey background indicate residues implicated for pantothenate binding sites.

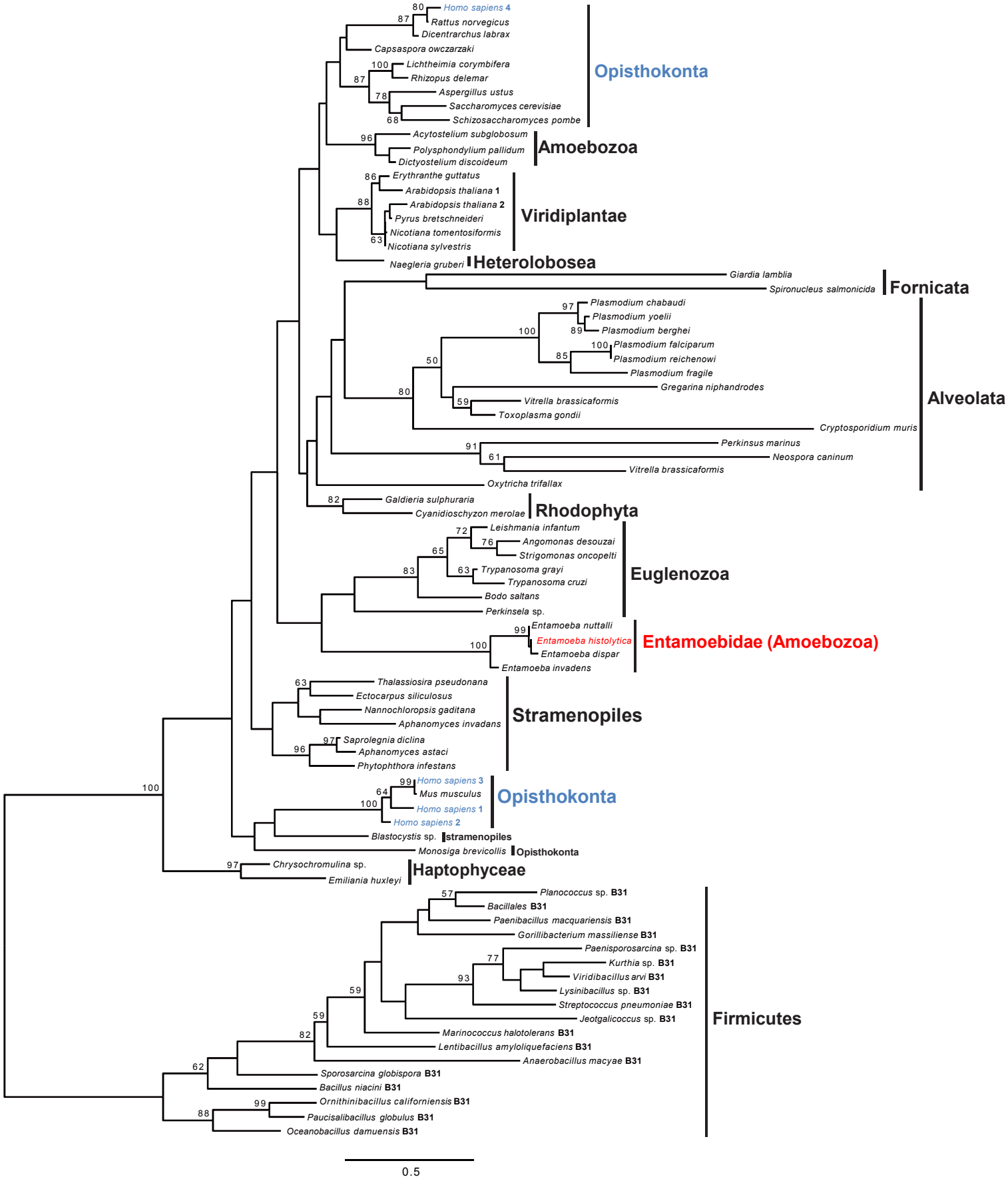


**Fig. 4.** Phylogenetic tree of PanK from *E. histolytica* and other species. Optimal ML tree inferred by RAxML program with LG +G4 model was shown. Unambiguously aligned 145 positions from 81 sequences were used for the analysis.

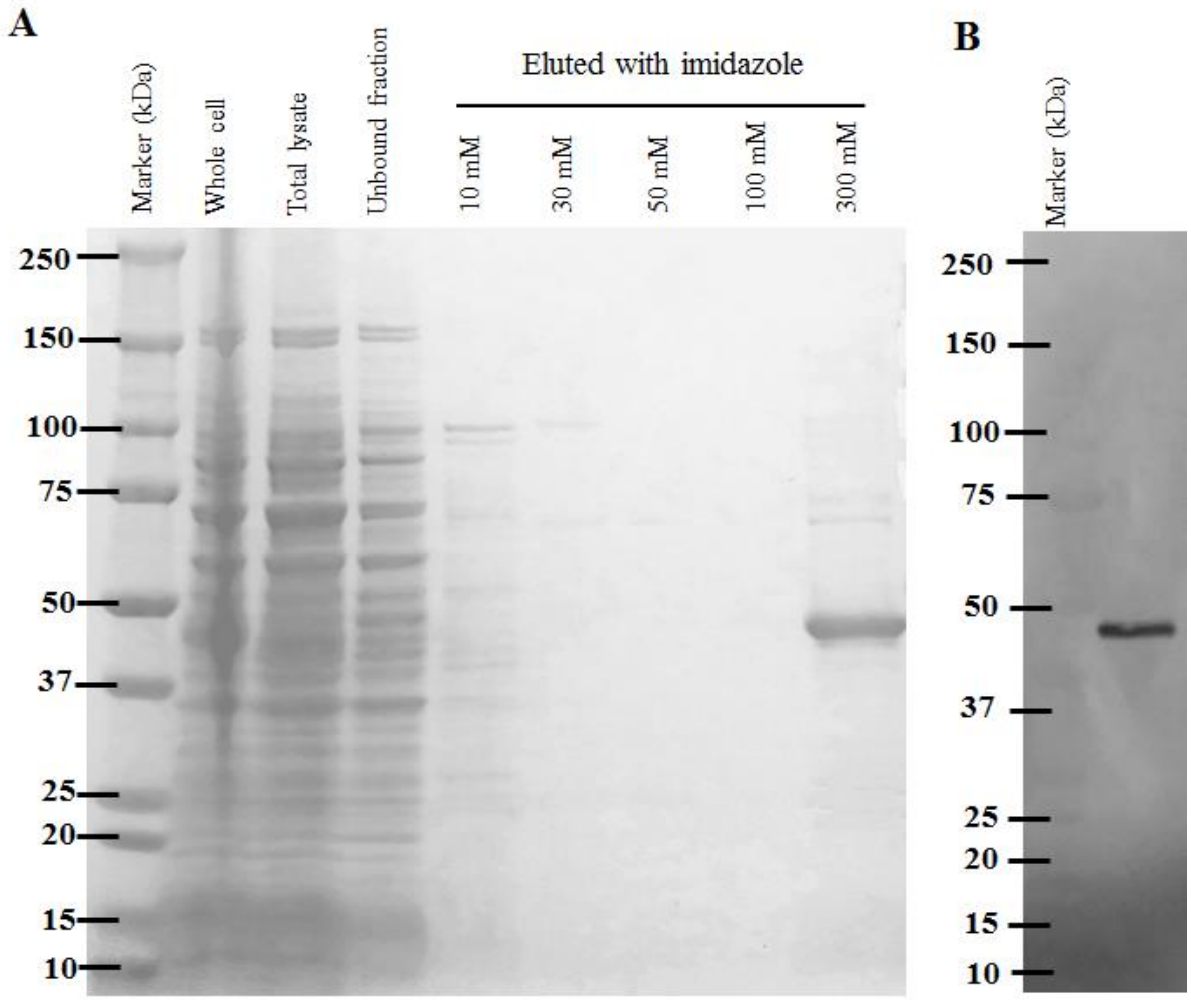


**Fig. 5.** Expression and purification of EhPanK in *E. coli***.** A) Expression and purification of recombinant EhPanK. Protein samples at each step of purification were subjected to 12% SDS-PAGE under reducing conditions, and the gel was stained with Coomassie Brilliant Blue. B) Immunoblot analysis of purified recombinant EhPanK using anti His-Tag antibody.

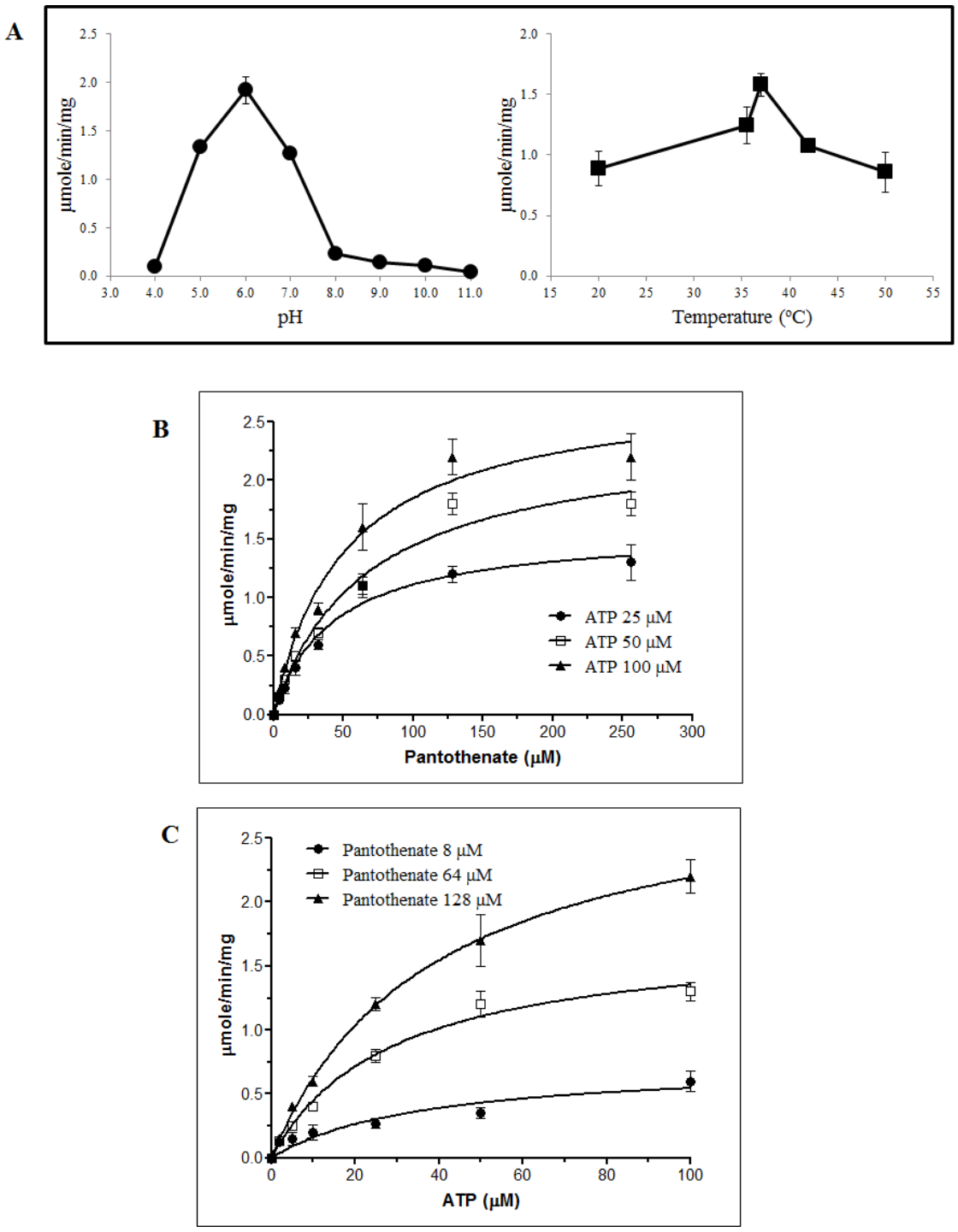


**Fig. 6.** Optimum pH and temperature (A) and initial rate plots (B, C) of EhPanK. A) Enzyme specific activity of recombinant EhPanK was measured at the various pHs and temperatures indicated in the figure. B) The velocity of EhPanK reaction at various pantothenate concentrations in the presence of 25, 50, or 100 µM ATP. C). The velocity of EhPanK reaction at various ATP concentrations in the presence of 8, 64, or 128 µM pantothenate. Assays were performed as described in Materials and methods, with 50 ng of EhPanK recombinant enzyme,

15 mM HEPES, 20 mM NaCl, 10 mM $MgCl_2$, 1 mM EGTA, 0.02% Tween-20, 0.1 mg/mL β−globulins. Assays for panes B and C were conducted at 37ºC at pH 6. Data are shown in mean ± SEM of three replicates.

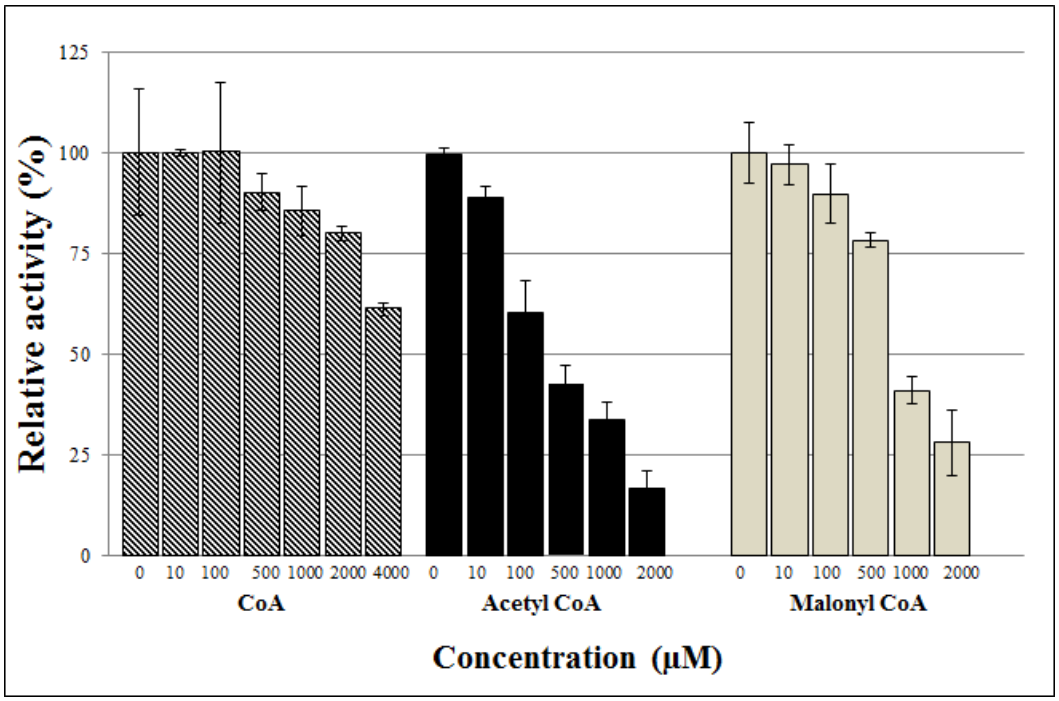


**Fig. 7.** Effect of CoA, acetyl CoA, and malonyl CoA on the pantothenate kinase activities. Relative activities of EhPanK in the presence of various concentrations of inhibitors to those without inhibitors are shown. The assay was performed in 10 mM $MgCl_2$, 15 mM HEPES, 20 mM NaCl, 1 mM EGTA, 0.02% Tween-20, 0.1 mg/mL γ−globulins, 0.2 mM pantothenate, and 100 μM ATP with various concentrations of CoA, acetyl CoA, or malonyl CoA at 37ºC at pH 6. The assays were carried out three times independently, and the results are shown as means ± SEM of triplicates.

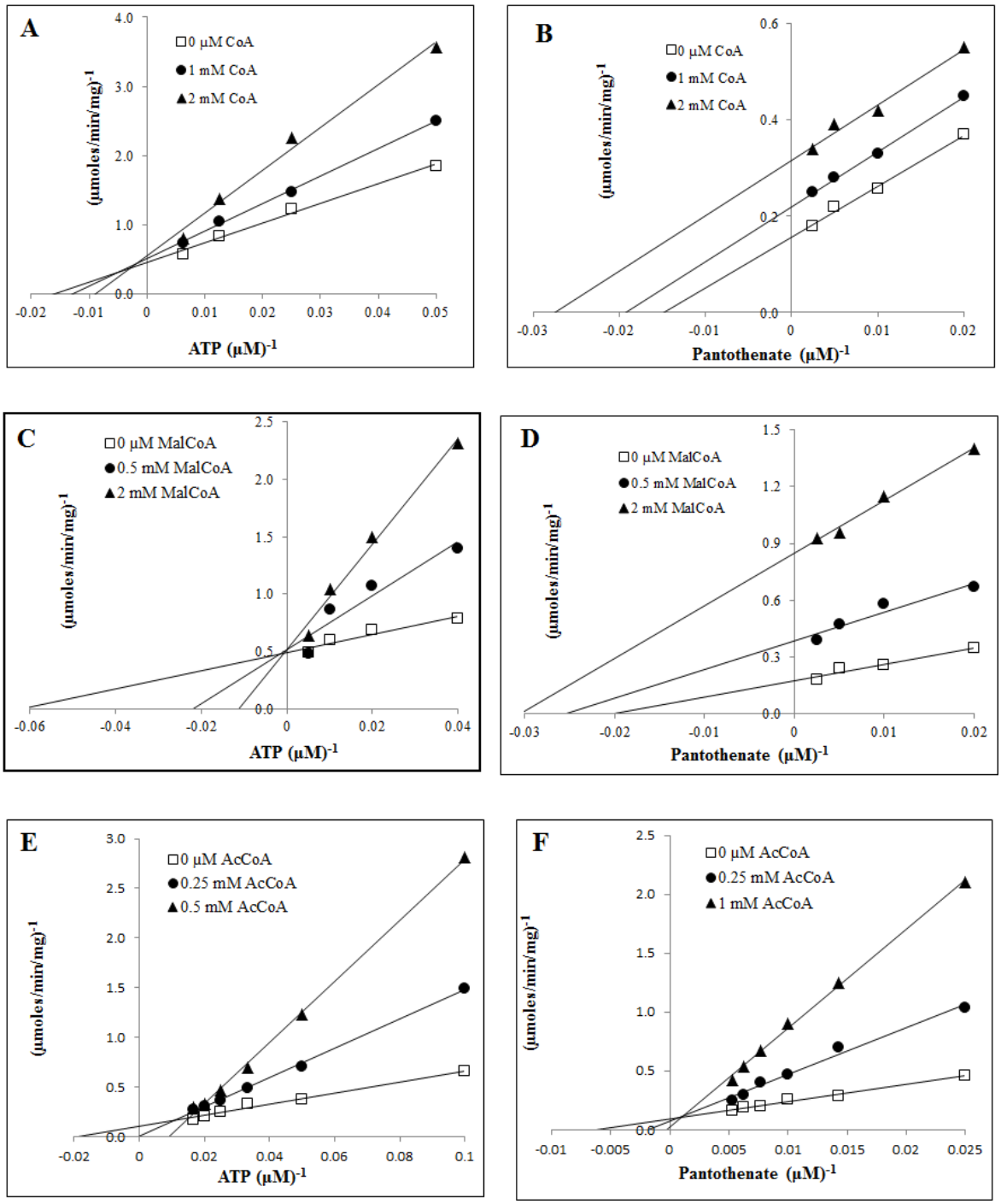


**Fig. 8.** Double-reciprocal plots of the recombinant EhPanK in the presence of CoA (A and B), malonyl CoA (C and D), or acetyl CoA (E and F). The enzymatic activities were determined with various concentrations of ATP and 0.2 mM pantothenate (A, C, and E) or various concentrations of pantothenate and 100 μM ATP (B, D, and F), in the presence of three concentrations of inhibitors (0, 0.5, and 2 mM). Data are shown in means ± SEM of triplicate analyses.

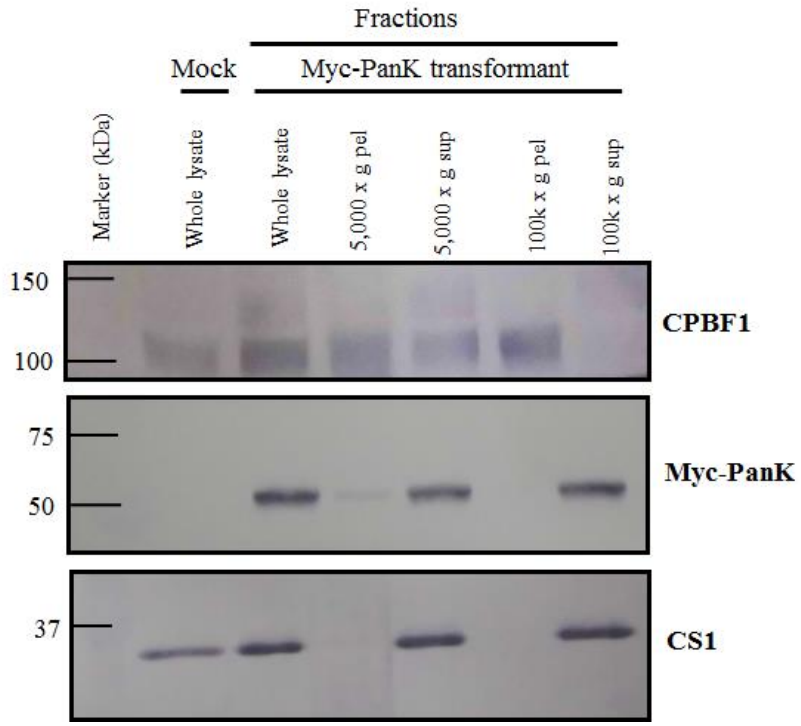


**Fig. 9.** Cellular fractionation and immunoblot analysis of EhPanK. Trophozoites of Myc-EhPanK expressing transformant (Myc-PanK) were fractionated as described in Materials in Methods, and subjected to immunoblot analysis using anti-Myc monoclonal antibody, anti-CPBF1, and anti-CS1 polyclonal antisera. CPBF1 and CS1 serve as control of organelle and cytosolic proteins, respectively. Whole lysate of control strain transformed with empty vector was also subjected to analysis.

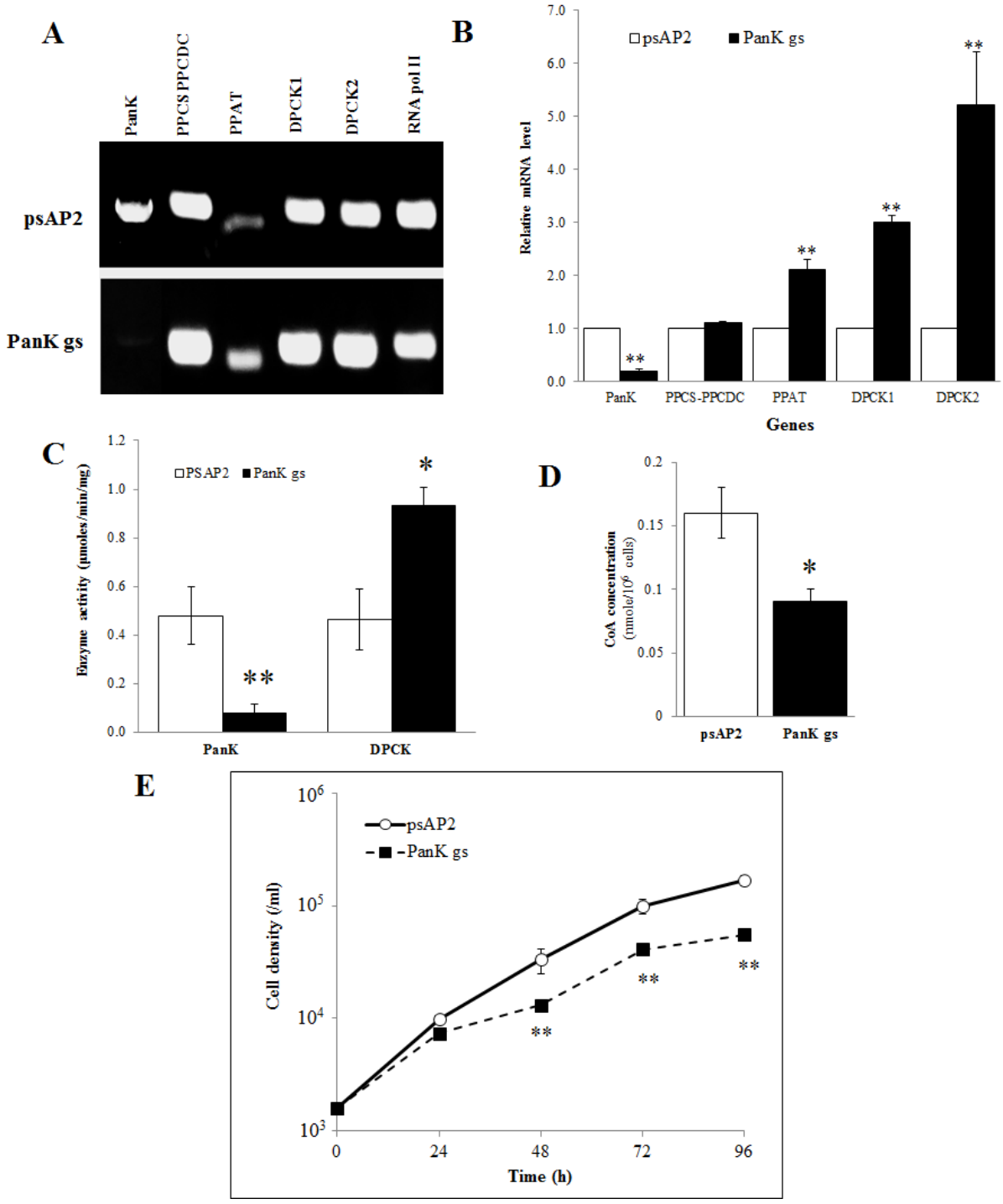


**Fig. 10.** Analyses of *EhPanK* gene silenced strain. A) RT-PCR analysis of *EhPanK* gene transcript from *E. histolytica* transformants. "psAP" indicates control strain transfected with psAP-2-Gunma empty vector, and "PanK gs" indicates *EhPanK* gene silenced strain. B) Relative levels of gene transcripts encoding all four enzymes involved in CoA biosynthesis by qRT-PCR analysis in psAP and Pan Kgs transformants. qRT-PCR data were normalized against RNA polymerase II, and are shown in percentage relative to the transcript level of each gene in psAP

control. C) PanK and DPCK activity in cell lysates of psAP and PanKgs transformants. D) CoA concentration in cell lysates. For B-D, data are shown in mean ± SEM of three biological replicates. Statistical comparison is made by Student's t test (*$P$<0.05, **$P$<0.01). E) Growth kinetic of *E. histolytica* transformants during 96 h incubation in BI-S-33 medium. Data are shown in mean ± SEM of three replicates. Data from one representative experiment of three conducted independently are shown. Statistical comparison is made by Student's t test (*$P$<0.05, **$P$<0.01).

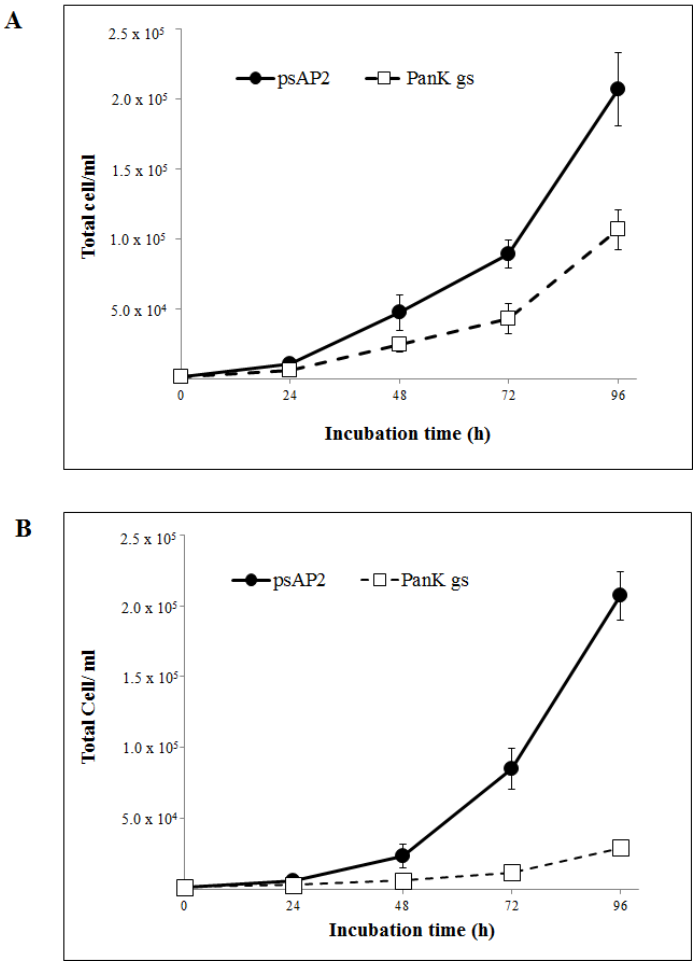


**Fig. 11.** Growth kinetic of *E. histolytica* transformants during 96 h incubation in BI-S-33 medium from two other independent experiments (A and B). Data are shown in mean ± SEM of three replicates.

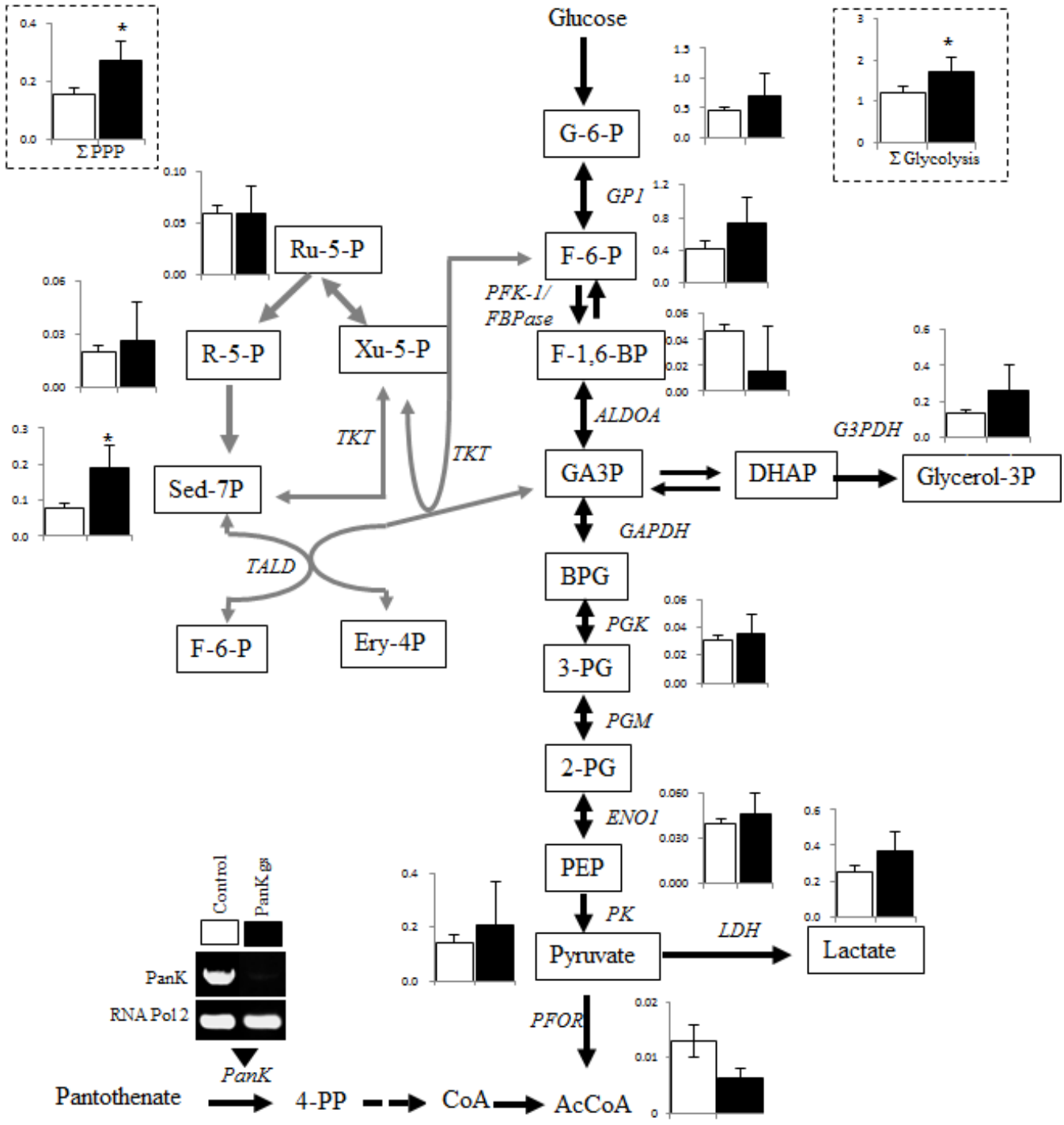


**Fig. 12.** PanK gene silencing promotes the increasing of glycolysis and pentose phosphate metabolites. Data show amounts of some metabolites in glycolysis and PPP. ΣPPP indicates total sum values of R-5-P, Ru-5-P and Sed-7P. Σglycolysis indicates total metabolites in glycolysis pathway from G-1-P to pyruvate. Data are expressed as mean ± s.d. (nmol $10^{-6}$ cells) of three to five separate experiments. *$P$<0.05 versus controls (unpaired Student's t-test). ND; not detected; G-6-P, glucose 6-phosphate; F-6-P, fructose-6-phosphate; F-1,6-BP, fructose 1,6-bisphosphate;

GA3P, glyceraldehyde 3-phosphate; DHAP, dihydroxyacetone phosphate; BPG, bisphosphoglycerate; 3-PG, 3-phosphoglycerate; 2-PG, 2-phosphoglycerate; PEP, phosphoenolpyruvate; AcCoA, Acetyl Co Enzyme A; CoA, Coenzyme A; 4-PP, 4'-Phosphopantothenate; 6-PG, 6-phosphogluconate; Ru-5-P, ribulose-5-phosphate; R-5-P, ribose-5-phosphate; Xu-5-P, xylulose-5-phosphate; Sed-7P, sedoheptulose-7-phosphate; Ery-4P, erythrose-4-phosphate.

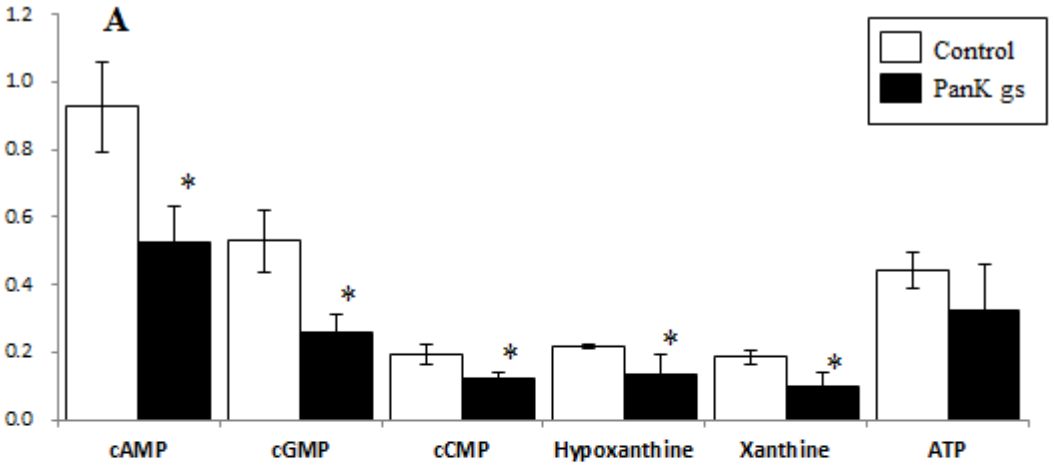
A
Control
PanK gs
1.2
1.0
0.8
0.6
0.4
0.2
0.0
cAMP
cGMP
cCMP
Hypoxanthine
Xanthine
ATP

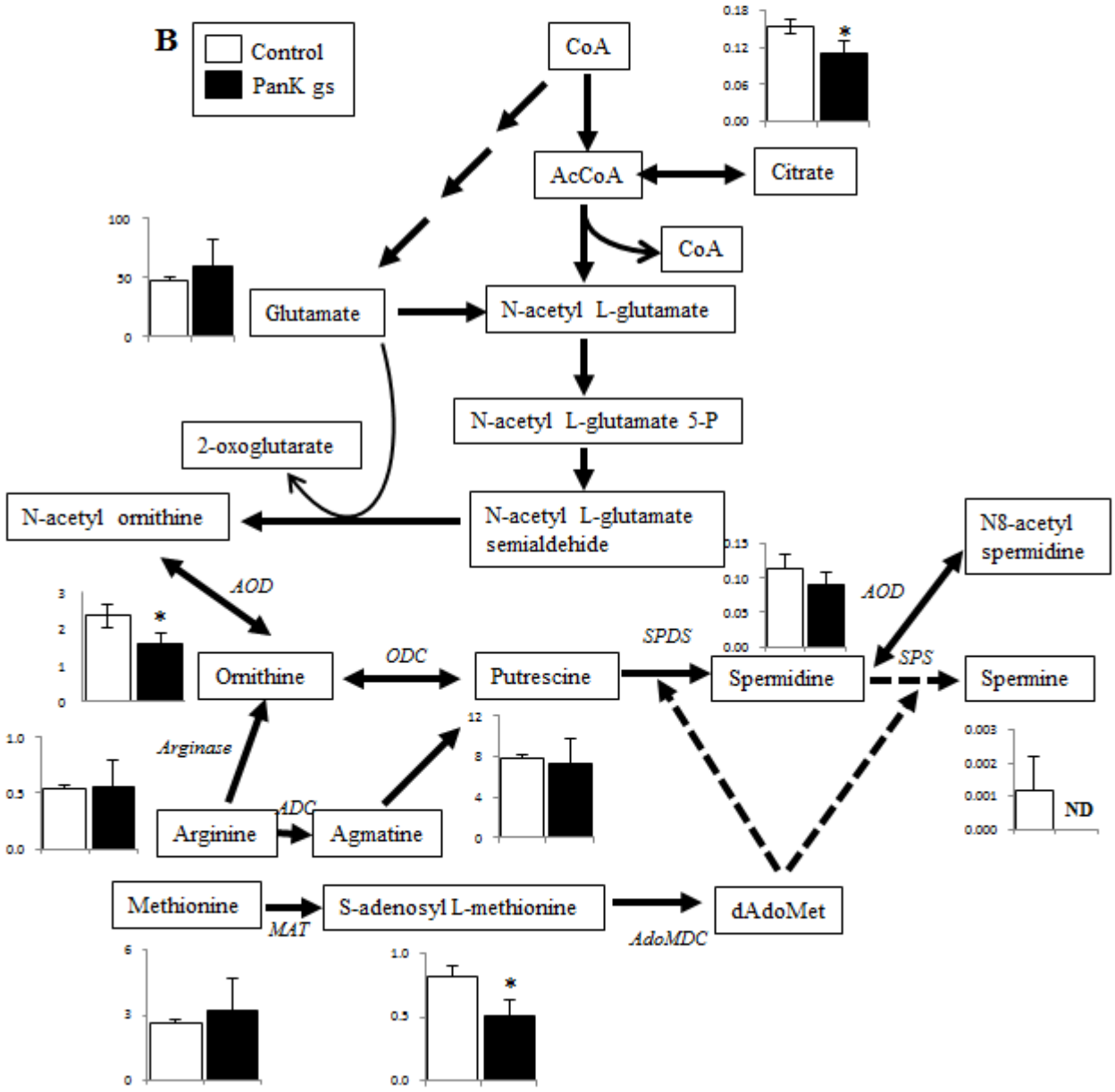
B
Control
PanK gs
CoA
AcCoA
Citrate
CoA
Glutamate
N-acetyl L-glutamate
N-acetyl L-glutamate 5-P
2-oxoglutarate
N-acetyl ornithine
N-acetyl L-glutamate semialdehide
N8-acetyl spermidine
AOD
AOD
SPDS
SPS
Ornithine
ODC
Putrescine
Spermidine
Spermine
Arginase
ADC
Arginine
Agmatine
ND
Methionine
MAT
S-adenosyl L-methionine
AdoMDC
dAdoMet

**Fig. 13.** PanK gene silencing suppresses nucleic acids and polyamines biosynthesis. A, Some nucleic acids were depleted in PanK gene silencing strain. Data are expressed as mean ± S.D. (nmol $10^{-6}$ cells) of three to five separate experiments. **P*<0.05 versus controls (unpaired Student's t-test). B, Depletion of metabolites in ornithine and polyamines biosynthesis. Data show in mean ± s.d. (nmol $10^{-6}$ cells) of three to five separate experiments. Dashes lines indicate genes likely absent in the genome. **P*<0.05 versus controls (unpaired Student's t-test). Abbreviations are: ND, not detected; AdoMet, S-Adenosyl methionine; dAdoMet, Sadenosylmethioninamine; MAO, monoamine oxidase; AdoMDC, S-adenosylmethionine decarboxylase; SPDS, spermidine synthase; SPS, spermine synthase; GAD, glutamate decarboxylase.

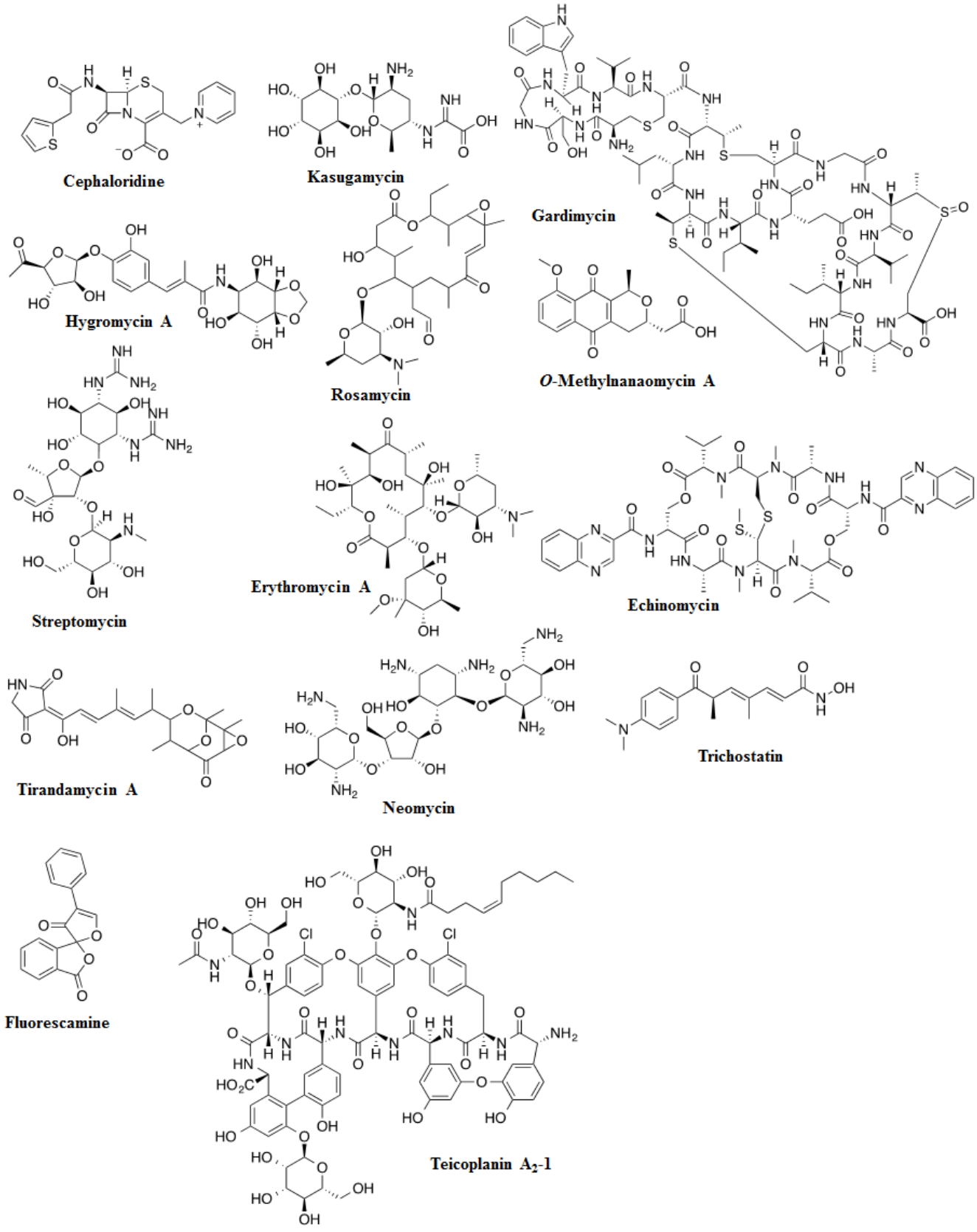


**Fig. 14.** Structures of *EhPanK* inhibitors from compound library identified in this study.

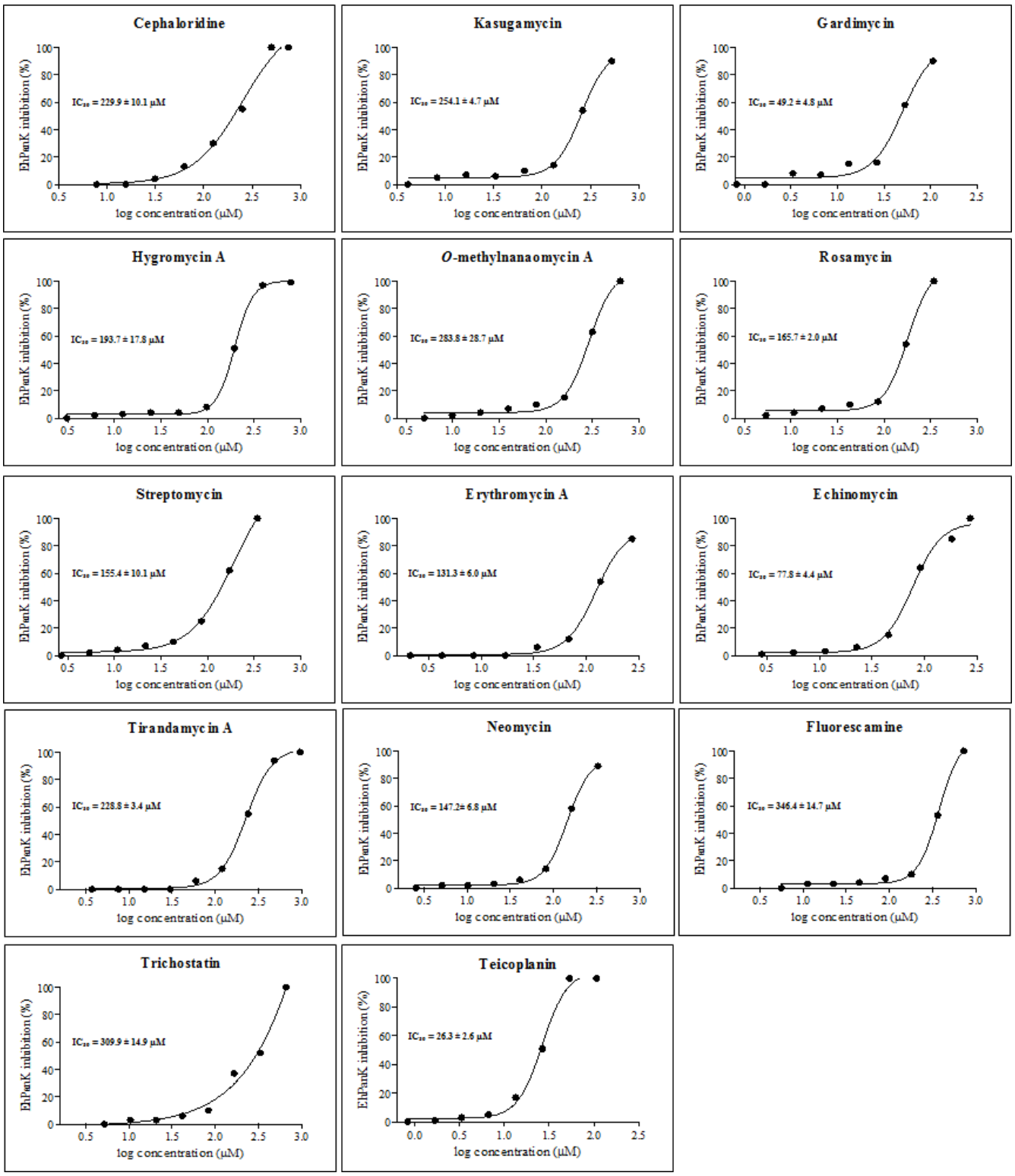


**Fig. 15.** Dose-response data of inhibitors against EhPanK inhibitors. $IC_{50}$ values were determined by dose-response-inhibition using GraphPad Prism (GraphPad Software Inc., San Diego, USA). Data are shown in mean of three replicates.

**Table 1.** Purification of recombinant *E. histolytica* pantothenate kinase. Enzyme activity was measured as described in Materials and methods.

| Sample | Protein concentration (mg/ 500 mL culture) | Total activity (µmole/min) | Specific activity (µmole/min/mg) | Yield (%) | Purification (fold) |
|---|---|---|---|---|---|
| Whole lysate | 4.26 | 1.11 | 0.26 | 100 | - |
| Eluate | 0.25 | 0.39 | 1.59 | 35.2 | 6.1 |

**Table 2.** Kinetic parameters of *E. histolytica* pantothenate kinase

| Substrate | $K_m$ (µM) | $V_{max}$ (µmole/min/mg) | $K_{cat}$ ($min^{-1}$) | $K_{cat}/K_m$ ($min^{-1}µM^{-1}$) |
|---|---|---|---|---|
| Pantothenate | 53.2 ± 7.1 | 2.79 ± 0.1 | 126.8 ± 4.5 | 2.38 ± 0.08 |
| ATP | 41.4 ± 3.9 | 2.84 ± 0.2 | 129.1 ± 9.2 | 3.11 ± 0.22 |

Mean±SEM of three replicates are shown.

**Table 3.** Phosphoryl donor specificity of *E. histolytica* pantothenate kinase

| Phosphoryl donor[a] | Relative activity (%) | Phosphoryl donor[a] | Relative activity (%) |
|---|---|---|---|
| ATP | 100.0 ± 4.1 | CTP | 1.4 ± 0.2 |
| GTP | 78.8 ± 4.9 | Metaphosphate | ND |
| dATP | 19.3 ± 4.3 | Hexametaphosphate | ND |
| Tripolyphosphate | 16.9 ± 0.8 | Trimetaphosphate | ND |
| UTP | 16.6 ± 1.2 | Glucose-6-phosphate | ND |
| Polyphosphate | 16.2 ± 2.5 | Phosphoenolpyruvate | ND |
| TTP | 5.4 ± 1.9 | None | ND |

Assays were performed as described in Materials and methods, in the presence 15 mM HEPES, 20 mM NaCl, 10 mM $MgCl_2$, 1 mM EGTA, 0.02% Tween-20, 0.1 mg/mL β−globulins and 0.2 mM pantothenate. Reactions were conducted at 37ºC at pH 6.

[a] The final concentration used was 100 µM.

The activity is shown in percentage (%) relative to that toward ATP.

ND, not detected.

Mean±SEM of three replicates are shown.

**Table 4.** Effect of metal ions on the activity of *E. histolytica* pantothenate kinase

| Metal[a] | Relative activity (%) |
|---|---|
| $MgCl_2$ | 100.0 ± 0.0 |
| $CuCl_2$ | 84.3 ± 4.7 |
| $MnCl_2$ | 83.2 ± 2.0 |
| $CoCl_2$ | 74.2 ± 6.1 |
| $FeCl_2$ | 72.8 ± 1.7 |
| $LiCl_2$ | 34.5 ± 1.8 |
| $CaCl_2$ | 17.0 ± 3.0 |
| $ZnCl_2$ | 3.9 ± 0.7 |
| $NiCl_2$ | ND |
| NaCl | ND |
| KCl | ND |
| None | ND |

Assays were performed as described in Materials and methods, in the presence of 100 mM ATP, 15 mM HEPES, 20 mM NaCl, 1 mM EGTA, 0.02% Tween-20, 0.1 mg/mL β−globulins and 0.2 mM pantothenate. Reactions were conducted at 37ºC at pH 6.0.
[a] The cation final concentration used was 5 mM.
The activity is shown in percentage (%) relative to that toward $MgCl_2$. ND, not detected.
Mean±SEM of three replicates are shown.

**Table 5.** Inhibitory activities of EhPanK inhibitors from Kitasato Natural Products Library

| Compound | $IC_{50}$ (μM) |
|---|---|
| Cephaloridine | 229.9 ± 10.1 |
| Kasugamycin | 254.1 ± 4.7 |
| Gardimycin | 49.2 ± 4.8 |
| Hygromycin A | 193.7 ± 17.8 |
| *O*-methylnanaomycin A | 283.8 ± 28.7 |
| Rosamycin | 165.7 ± 2.0 |
| Streptomycin | 155.4 ± 10.1 |
| Erythromycin A | 131.3 ± 6.0 |
| Echinomycin | 77.8 ± 4.4 |
| Tirandamycin A | 228.8 ± 3.4 |
| Neomycin | 147.2 ± 6.8 |
| Fluorescamine | 346.4 ± 14.7 |
| Trichostatin | 309.9 ± 14.9 |
| Teicoplanin | 26.3 ± 2.6 |

Mean±SEM of three replicates are shown.

**Table 6.** *In vitro* anti-amebic activity and cytotoxicity against MRC-5 cells of EhPanK inhibitors.

| Compound | $IC_{50}$ (μM) | |
|---|---|---|
| | ***E. histolytica* trophozoite** | **Normal human cell (MRC-5)** |
| Cephaloridine | 245.78 ± 34.92 | 48.20 ± 3.61 |
| Kasugamycin | 66.16 ± 13.68 | 87.10 ± 7.22 |
| Gardimycin | 34.40 ± 3.16 | >52.9 |
| Hygromycin A | 142.22 ± 16.34 | >196 |
| *O*-methylnanaomycin A | 1.68 ± 0.05 | 18.98 ± 0.49 |
| Rosamycin | 56.34 ± 11.72 | 34.40 ± 2.71 |
| Streptomycin | 77.53 ± 1.52 | >172 |
| Erythromycin A | 155.88 ± 20.57 | >136 |
| Echinomycin | 0.26 ± 0.04 | <0.38 |
| Tirandamycin A | 13.71 ± 4.85 | 143.88 ± 3.80 |
| Neomycin | 10.58 ± 1.12 | >163 |
| Fluorescamine | 167.90 ± 20.07 | 287.77 ± 17.84 |
| Trichostatin | 0.29 ± 0.04 | 2.62 ± 0.49 |
| Teicoplanin | 15.08 ± 2.25 | >53.3 |
| Metronidazole | 0.66 ± 0.05 | >100 |

Mean±SEM of three replicates are shown.

**Table 7.** EhPanK inhibitor from compounds library and microbial extracts

| Origin | Number of samples | EhPanK inhibitor* |
|---|---|---|
| Fungi | 1,340 | 66 |
| Actinomycetes | 1,660 | 62 |
| **Total** | **3,000** | **128** |
| | | 4.2% |

*Inhibited >50% EhPanK.

## Chapter 3. Genetic, biochemical, and metabolomic analyses of DPCK involved in coenzyme A biosynthesis in the human enteric parasite *Entamoeba histolytica*

### 3.1. Abstract

Coenzyme A (CoA) is an essential cofactor for numerous cellular reactions in all living organisms. In the protozoan parasite *Entamoeba histolytica*, CoA is synthesized in a pathway consisting of four enzymes with dephospho-CoA kinase (DPCK) catalyzing the last step. However, the metabolic and physiological roles of *E. histolytica* DPCK remain elusive. In this study, I took biochemical, reverse genetic, and metabolomic approaches to elucidate role of DPCK in *E. histolytica.* The *E. histolytica* genome encodes two DPCK isotypes (EhDPCK1 and EhDPCK2). Epigenetic gene silencing of *EhDPCK1* and *EhDPCK2* caused significant reduction of DPCK activity, intracellular CoA concentrations, and also led to growth retardation *in vitro*, suggesting importance of DPCK for CoA synthesis and proliferation. Furthermore, metabolomic analysis showed that suppression of *EhDPCK* gene expression also caused decrease in the level of acetyl-CoA, and metabolites involved in amino acid, glycogen, hexosamine, nucleic acid metabolisms, chitin and polyamine biosynthesis. The kinetic properties of *E. histolytica* and human DPCK showed remarkable differences; e.g., the *K*m values of *E. histolytica* and human DPCK were 58-114 μM and 5.2 μM toward dephospho-CoA and 15-20 μM and 192 μM for ATP, respectively. Phylogenetic analysis also supported the uniqueness of the amebic enzyme compared to the human counterpart. These biochemical, evolutionary features, and physiological importance of EhDPCKs indicate that DPCK represents the rational target for the development of anti-amebic agents.

## 3.2. Introduction

Coenzyme A (CoA) is an essential cofactor as an acyl group carrier and carbonyl activating group (Baddiley et al., 1953) in metabolism that contributes to 9% out of 3,500 cellular activities (www.brenda-enzymes.info/). CoA is synthesized by five to six enzymatic reactions with pantothenic acid (vitamin $B_5$), *L*-cysteine, and purine/pyrimidine nucleotides as substrates (Genschel et al., 1999). Pantothenate is either produced *de novo*, as in bacteria, archaea, mammals, and plants (Begley et al., 2001; Chakauya et al., 2008; Spry et al., 2008), or alternatively, scavenged by uptake (Saliba et al., 1998; Spry et al., 2008). It was shown that the first and last steps, catalyzed by pantothenate kinase (PanK) and dephospho-CoA kinase (DPCK, EC 2.7.1.24) are rate limiting and allosterically regulated (Hart et al., 2017; Leonardi et al., 2005b). Both enzymes utilize ATP as a phosphate donor and are essential in many organisms (Hart et al., 2017).

In *E. histolytica*, it has been previously shown that repression of *PanK* gene causes defect in proliferation, and expression of *DPCK* genes was transcriptionally up-regulated by repression of *PanK* gene expression. This Chapter 2 reinforces the premise that the CoA biosynthetic pathway plays a pivotal role in trophozoite proliferation. While the first rate limiting and regulate enzyme was well characterized, the metabolic and physiological roles of the enzyme that catalyzes the last step of the pathway remain elusive. DPCK utilizes ATP to phosphorylate dephospho-CoA at the 3'-hydroxyl group of the ribose moiety to generate CoA. The *E. histolytica* genome apparently encodes two isotypes of DPCK. In the present study, I conducted biochemical characterization of recombinant enzymes. I also undertook reverse genetic and metabolomic approaches to elucidate the physiological importance of DPCK in this parasitic protist.

### 3.3. Materials and methods

#### 3.3.1. Organisms, cultivation, and chemicals

Trophozoites of the *E. histolytica* clonal strain HM-1: IMSS cl 6 and G3 strains (Bracha et al., 2006) were maintained axenically in Diamond's BI-S-33 medium at 35.5ºC as described previously (Diamond et al., 1978). Trophozoites were continuously maintained in mid-log phase after inoculation of one-thirtieth to one-twelfth of the total culture volume. *Escherichia coli* BL21 (DE3) strain was purchased from Invitrogen (Carlsbad, CA, USA). Lipofectamine and geneticin (G418) were also purchased from Invitrogen. $Ni^{2+}$-NTA agarose was purchased from Novagen (Darmstadt, Germany). All other chemicals of analytical grade were purchased from Sigma-Aldrich (Tokyo, Japan) unless otherwise stated.

#### 3.3.2. Plasmid construction for recombinant EhDPCK1 and EhDPCK2

Plasmids to express recombinant EhDPCK1 and 2 proteins were constructed according to the procedures previously described (Sambrook and Russell, 2001). DNA fragments corresponding to the protein coding region of *EhDPCK1* and *EhDPCK2* gene were amplified from *E. histolytica* cDNA, using oligonucleotide primers:

EhDPCK1 sense (5'- GCCGGGATCCATGAAAAAGATATTTGTTATTGGT -3'), antisense (5'- GCCGGTCGACTTAAAATTTATTTTCATTGAAGTCAA -3') and EhDPCK2 sense (5'- GCCGGGATCCATGGTATTTGTTATTGGTATC -3'), antisense (5'- GCCGGTCGACTTAGTTTAAAGTAATTTTTAATTGTT -3'). Underline letters indicate BamHI and SalI restriction sites. PCR was performed with primeSTAR HS DNA polymerase (Takara) and the following parameters: an initial incubation at 98ºC for 30 sec; followed by the 30 cycles of denaturation at 98ºC for 10 sec; annealing at 55ºC for 30 sec; and elongation at 72ºC for 1 min; and a final extension at 72ºC for 7 min. The PCR fragments were digested with BamHI and SalI, purified with Wizard® SV gel and PCR clean-up system (Promega). The fragments were cloned into BamHI and SalI double digested pCOLD1™ histidine-tag vector

(Takara) to finally produce pCOLD1-EhDPCK1 and pCOLD1-EhDPCK2. The nucleotide sequences of the engineered plasmid were verified by sequencing.

### 3.3.3. Production and purification of recombinant EhDPCK1 and EhDPCK2

pCOLD1-EhDPCK1 and pCOLD1-EhDPCK2 were introduced into *E. coli* BL21(DE3) cells by heat shock at 42ºC for 1 min. *E. coli* BL21 (DE3) harboring pCOLD1-EhDPCK1 and pCOLD1-EhDPCK2 were grown at 37ºC in 100 mL of Luria Bertani medium (Invitrogen) in the presence of 100 μg/mL ampicillin (Nacalai Tesque). The overnight culture was used to inoculate 500 mL of fresh medium, and the culture was further continued at 37ºC with shaking at 180 rpm. When $A_{600}$ reached 0.8, 0.5 mM isopropyl β-D-thio galactopyranoside (IPTG) was added, and cultivation was continued for another 24 h at 15ºC. *E. coli* cells from the induced culture were harvested by centrifugation at 5,000 x g for 20 min at 4ºC. The cell pellet was washed with PBS, pH 7.4, re-suspended in 20 mL of the lysis buffer (50 mM Tris HCl, pH 8.0, 300 mM NaCl, and 10 mM imidazole) containing 0.1% Triton X-100 (v/v), 100 μg/mL lysozyme, and 1 mM PMSF, and incubated at room temperature for 30 min, sonicated on ice and centrifuged at 25,000 x g for 15 min at 4ºC. The supernatant was mixed with 1.2 mL of 50% $Ni^{2+}$-NTA His-bind slurry, incubated for 1 hour at 4ºC with mild shaking. The recombinant enzyme-bound resin in a column was washed three times with buffer A (50 mM Tris-HCl, pH 8.0, 300 mM NaCl, and 0.1% Triton X-100, v/v) containing 10-50 mM of imidazole. Bound protein was eluted with buffer A containing 100-300 mM imidazole. After the integrity and the purity of recombinant protein were confirmed with 12% SDS-PAGE analysis, followed by CBB staining, the sample was dialyzed against a 300-fold volume of 50 mM Tris-HCl, 150 mM NaCl, pH 8.0 containing 10% glycerol (v/v) and the Complete Mini protease inhibitor cocktail (Roche, Mannheim, Germany) for 18 h at 4ºC. Pure enzyme was stored at -80ºC with 20% glycerol in small aliquots until use.

### 3.3.4. Enzymes assay

DPCK activities of recombinant proteins and those in lysates were measured by a coupling assay using ADP Hunter$^{TM}$ Plus Assay kit (DiscoverX, US) according to the manufacturer's instructions. Enzymatic assays were carried out using 50 ng of recombinant EhDPCK1 or EhDPCK2 using 4-256 μM for dephospho-CoA, 5-100 μM ATP. The kinetic parameters were estimated using the non-linear regression function obtained from the GraphPad Prism software (GraphPad Software Inc., San Diego, CA). The experiments were repeated three times in triplicate using protein preparations from three independent extractions, and kinetic values are presented as the means ± S.E.

### 3.3.5. Production of *EhDPCK1* and *EhDPCK2* gene-silenced strains

Small antisense RNA-mediated transcriptomic gene silencing (Bracha et al., 2006; Zhang et al., 2011a) was used to repress gene expression of *EhDPCK1* and *EhDPCK2* genes with some modifications. Briefly, fragments corresponding to a 400 bp long of the open reading frame were amplified by PCR from cDNA using specific of oligonucleotides as follow: EhDPCK1 sense (5'-CAG**AGGCCT**ATGAAAAAGATATTTGTTATTGGTAT-3'), antisense (5'- AAT**GAGCTC**CAATGGCAATTTCAGGTGA-3') and EhDPCK2 sense (5'-CAG**AGGCCT**ATGGTATTTGTTATTGGTATCAC-3'), antisense (5'-AAT**GAGCTC**TTCTAGTTTCCCAGATAACATTTA-3'). These oligonucleotides contained StuI and SacI restriction sites (shown in bold). PCR products were digested with StuI and SacI (New England BioLabs, Massachusetts, USA), and ligated into the StuI and SacI double digested psAP2-Gunma (Husain et al., 2011) to construct gene silencing plasmids. The trophozoites of G3 strain were transformed with the empty vector as a control and silencing plasmids by liposome-mediated transfection as previously described (Nozaki et al., 1999). Transformants were initially selected in the presence of two μg/ml geneticin with gradually increased up to 10 μg/ml.

### 3.3.6. Reverse transcription PCR

Total RNA was extracted from ~$10^6$ trophozoites of *EhDPCK1, EhDPCK2* gene silenced and control transformant strains using TRIzol (Ambion, Life Technologies) reagent as described in the previous study (Chomczynski and Mackey, 1995). DNase treatment was performed using DNase I (Invitrogen) to exclude genomic DNA. RNA quantity was determined by measuring the absorbance at 260 nm with NanoDrop ND-1000 UV-Vis spectrophotometer (NanoDrop Technologies, Wilmington, DE, USA). Approximately one µg total RNA was used for cDNA synthesis using First-Stand cDNA Synthesis (Superscript® III, Invitrogen) with reverse transcriptase and oligo (dT) primers according to manufacturer's instructions. The cDNA product was diluted 10 fold and PCR reactions were carried out in 50 µL, using primer pairs: DPCK1 sense (5'-ATGAAAAAGATATTTGTTATTGGT-3'), antisense (5'-TTAAAATTTATTTTCATTGAAGTCAA-3) and DPCK2 sense (5'-ATGGTATTTGTTATTGGTATC-3), antisense (5'-TTAGTTTAAAGTAATTTTTAATTGTT-3).

The PCR conditions were: 98°C, 10 sec; 55°C, 1 min; and 72°C, 1 min; 20-25 cycles. The PCR products obtained were resolved by agarose gel electrophoresis.

### 3.3.7. Quantitative real-time (qRT) PCR

Relative levels of mRNA of the *EhPanK* (EHI_183060), *EhDPCK1* and *EhDPCK2* (EHI_040840 and EHI_155780, respectively) were measured using qRT-PCR. RNA polymerase II gene (EHI_056690) was used as a reference. Each 20 µL reaction mixture contained 10 µL of 2X Fast SYBR Green Master Mix (Applied Biosystems, Foster City, CA, USA), 0.6 µL each of 10 µM sense and antisense primers, 5 µL 10x diluted cDNA, and nuclease free water. PCR was performed using StepOne Plus Real-Time PCR System (Applied Biosystems, Foster City, CA, USA) with the cycling conditions: enzyme activation at 95°C for 20 sec, followed by 40 cycles of denaturation at 95°C for 3 sec and annealing-extension at 60°C for 30 sec. All reactions were carried out in triplicate, including cDNA-minus controls. The

amount of the steady state mRNA of each target gene was determined by the ΔCt method with RNA polymerase II as a reference gene (Livak and Schmittgen, 2001). The mRNA expression level of each gene in the transformants was expressed relative to that in the control transfected with psAP2.

### 3.3.8. Growth kinetics

Trophozoite cultures were continuously maintained in mid-log phase as described above. Glass tubes (6-ml, Pyrex) containing approximately 0.5 x $10^6$ cells were placed on ice for 5 min to detach cells from the glass surface. Centrifugation at 500 ×g for 5 min at room temperature was conducted to collect cells. After discarding the spent medium, the pellet was re-suspended in 1 mL of BI-S-33 medium. Cell densities were estimated on a hemocytometer. Approximately 10,000 trophozoites were inoculated in 6 mL fresh BI-S-33 medium. Cell density of the cultures were estimated on a hemocytometer every 24 h for 5 days.

### 3.3.9. Enzymes activity and CoA determination from cell lysates

Approximately $10^6$ cells cultivated in 25$cm^2$ flasks (Iwaki, Fukushima, Japan) for 48 h were harvested and the cell number was estimated as described above. The cell pellet was resuspended and homogenized in homogenization buffer (50 mM Tris-HCl, pH 7.5, 250 mM sucrose, 50 mM NaCl) supplemented with 1 mM PMSF and 0.5 mg/ml E-64 (Peptide Institute, Osaka, Japan) by mechanical homogenization with a glass homogenizer. After kept on ice for 30 min, the suspension was centrifuged at 500 x g for 30 min at 4°C to remove unbroken cells. Enzyme activity in the supernatant was used for enzymatic assay.

Concentrations of CoA in cell lysates were measured using the CoA assay kit (BioVision, CA, USA) according to the manufacturer's instructions. CoA at 0.05–1 nmole was used to produce a standard curve to determine the CoA concentrations in lysates. Experiments were conducted in triplicate, and repeated three times on three different days.

### 3.3.10. Intracellular metabolite extraction

Intracellular metabolites from 1 x $10^7$ *E. histolytica DPCK1* and *DPCK2* gene silencing cells were extracted according to the previous protocol (Jeelani et al., 2012). Internal standards, 200 µM of 2-(*N*-morpholino)-ethanesulfonic acid and methionine sulfone, were added to every sample to ensure that experimental artifacts such as ion suppression did not lead to misinterpretation of metabolite levels.

### 3.3.11. Instrumentation of capillary electrophoresis-mass spectrometry (CE-MS)

CE-MS was performed as previously described (Kinoshita et al., 2007; Yamamoto et al., 2014). The instrument used was an Agilent CE Capillary Electrophoresis System equipped with an air pressure pump, an Agilent 1100 series isocratic high-performance liquid chromatography pump and an Agilent 1100 series MSD mass spectrometer. I also used a G1603A Agilent CE-MS adapter kit, and a G1607A Agilent CE-MS sprayer kit (Agilent Technologies). G2201AA Agilent ChemStation software for CE-MSD was used for system control and data acquisition.

### 3.3.12. CE-MS conditions for cationic, anionic compounds, and nucleotides

Cationic nucleotides compounds were carried out on a gas chromatograph capillary, polydimethylsiloxane (DB-1) (50-µm inner diameter x 100-cm total length) (Agilent Technologies). CE separation was using 50 mM ammonium acetate, pH 7.5 as the electrolyte. Samples solution (~3 nL) was injected at 50 mbar for 30 sec, and a positive voltage of 30 kV was applied. All other conditions were the same as in the anionic metabolite analysis. Anionic were coated in SMILE (+) capillary 50-µm inner diameter x 100-cm total length obtained from Nacalai Tesque (Kyoto, Japan). The electrolyte was 50 mM ammonium acetate solution (pH 8.5). Sample solution (~30 nL) was injected at 50 mbar for 30 sec and a negative voltage of 30 kV. The capillary voltage was set at 3.5 kV for ESI-MS in the negative ion mode. Deprotonated [M-H] ions were monitored for anionic metabolites of interest.

### 3.3.13. Statistical analsyisis of metabolomic data and pathway analysis

For each experimental condition, three independent biological replicates were made and for each biological replicate, two technical replicates were made. All data are shown as means ± S.E. or the indicated number of experiments. Statistical comparisons were made by Student's t-test. Pathway analysis was conducted using Kyoto Encyclopedia of Genes and Genomes database (KEGG, https://www.genome.jp/kegg).

### 3.3.14. Phylogenetic analyses of *E. histolytica* DPCK1 and DPCK2

By Basic Local Alignment Search Tool Protein (blastp) searches in public sequence databases, I collected 88 DPCK sequences including two *E. histolytica* sequences from non-redundant protein sequences (nr) database of National Center for Biotechnology Information (NCBI, http://www.ncbi.nlm.nih.gov/) by using *E. histolytica* EhDPCK1 sequence (EHI_040840/ XP_648971) as a query to obtain data from representative taxa. Hit sequences with E-value less than $1 \times 10^{-10}$ were selected. The number of selected sequences in each blastp search for a representative taxon was determined based on the number of listed alignments. Sequences were aligned using Muscle program (Edgar, 2004) in SeaView package version 4.6.1 (Gouy et al., 2010). I selected 112 positions of unambiguously aligned by manual and used for phylogenetic analyses. The data matrices for phylogeny were subjected to IQTREE program (Nguyen et al., 2015) to select appropriate models for amino acid sequence evolution. LG + I + Γ4 and LG + Γ4 models were shown to be the best and the second-best models by using the information criterion. Maximum likelihood (ML) analysis implemented in the RAxML program version 7.2.6 (Stamatakis, 2006) was used to infer ML tree. In the bootstrap analysis, heuristic tree search was performed with a rapid bootstrap algorithm option (-f) for 100 bootstrap replicates. Bootstrap proportion (BP) values greater than 50 were indicated on the corresponding internal branches of the ML tree drawn by the use of FigTree program Version 1.4.2 (http://tree.bio.ed.ac.uk/software/figtree/).

## 3.4. Results

### 3.4.1. Identification and features of two DPCK isotypes

Two genes encoding DPCK were identified from the genome database of *E. histolytica* HM-1:IMSS (HM-1) reference strain (http://amoebadb.org/amoeba/): EHI_040840 and EHI_155780, herein designated as *EhDPCK1* and *EhDPCK2* genes, respectively. The open reading frames of the two genes are 621 and 615 bp in length and encode 206- and 204-amino acid long proteins with the calculated molecular mass of 23.9 and 23.1 kDa, respectively. The two proteins exhibit 38% mutual identity. EhDPCK1 shows 31%, 29%, and 26% percentage identity to orthologs from human, *Arabidopsis thaliana,* and *Escherichia coli*, whereas EhDPCK2 shows 34%, 29% and 28% identity to the orthologs from human, *A. thaliana* and *Escherichia coli*, respectively. Human, *A. thaliana,* and *E. coli* only have one functional copy of DPCK and seem to be slightly closer to EhDPCK2 than to EhDPCK1.

DPCK was reported to consist of five parallel β-strands flanked by α–helices with ATP-binding site and CoA-binding domain (O'Toole et al., 2003; G Obmolova et al., 2001). EhDPCK1 and 2 contain the highly conserved P-loop or Walker A sequence motif (GXXXXGKT/S, where X is any residue) which is reported to be involved in nucleotide binding (Galina Obmolova et al., 2001). When compared to *E. coli* DPCK, almost all key residues implicated for CoA binding are conserved in both EhDPCK1 and 2 (O'Toole et al., 2003). The only exceptions are the substitution of $Val^{473}$ in human ortholog with $Leu^{114}$ and $Leu^{117}$ in EhDPCK1 and EhDPCK2, respectively. $Gly^{56}$ and $Gly^{55}$ in EhDPCK1 and EhDPCK2, respectively, located between helices α3 and α4 are predicted to be important to maintain structural integrity.

### 3.4.2. Kinetic parameters, phosphoryl donor specificities, metal dependence, and inhibition of EhDPCK1 and EhDPCK2

EhDPCK1 and EhDPCK2 recombinant enzymes were successfully produced using *E. coli* expression system and purified for enzymological characterization. As demonstrated by SDS-PAGE analysis under reducing conditions, followed by Coomassie Brilliant Blue (CBB) staining and immunoblot assay, both enzymes were detected in both the soluble and insoluble fractions. Purified proteins were obtained with a relatively low yield: typically around 0.3 mg of protein purified from a 500 ml *E. coli* culture (Table 8). The purity of recombinant EhDPCK1 and 2 was estimated to be 90~95% by densitometric scanning of the CBB stained gels after SDS-PAGE (Fig. 16). Immunoblots also indicate only negligible truncated forms of both EhDPCK1 and 2 were present in the final preparations. The apparent molecular mass of the purified proteins was consistent with the molecular mass of 23.9 and 23.1 kDa for native EhDPCK1 and EhDPCK2, respectively, plus 2.6 kDa corresponding to the histidine tag.

The specific activity of the purified enzymes was estimated as 2.13±0.15 and 2.54±0.26 μmole/min/mg (mean±S.E. of triplicates) for EhDPCK1 and EhDPCK2, respectively. EhDPCK1 and EhDPCK2 showed a broad pH optimum between 7 and 9 with the maximum activity at 8 (Fig. 17). No difference was observed in the pH dependency between EhDPCK1 and EhDPCK2. Kinetic constants for EhDPCK1 and EhDPCK2 were determined by measuring the initial rates obtained with different concentrations of ATP and dephospho-CoA (Table 9). Both ATP and dephospho-CoA exhibited hyperbolic saturation kinetics when assayed over the range of 4-128 μM dephospho-CoA in the presence of 5-100 μM ATP and in the range of 1-100 μM ATP substrates in the presence of 16-128 μM dephospho-CoA (data not shown). EhDPCK1 showed the $K_m$ values of 114±19 μM and 19.6±1.2 μM for dephospho-CoA and ATP, respectively. EhDPCK2 showed lower $K_m$ values with 57.9±6 and 15.0±2.4 μM for dephospho-CoA and ATP, respectively. Neither EhDCPK1 nor 2 utilized pantothenate as a substrate (<0.02 μmole/min/mg).

Recombinant EhDPCK1 and EhDPCK2 could use various nucleoside triphosphates, such as ATP, CTP, GTP, and UTP, as phosphoryl donors (Table 10). GTP could partially replace ATP for both EhDPCK1 and EhDPK2 (24-33% of the activity relative to that with ATP). EhDPCK1 and EhDPCK2 showed slight difference in nucleotide triphosphate preference toward TTP. The effects of metal ions were examined by assaying the activity after the addition of metal salts to the standard reaction mixture (Table 11). The data also suggest that both EhDPCK1 and EhDPCK2 activities are $Mg^{2+}$-dependent. Furthermore, some cations ($Zn^{2+}$ and $Cu^{2+}$) could replace $Mg^{2+}$ with relative activity higher than 50%. No activity was detected when $Na^{+}$ or $K^{+}$ was used instead of $Mg^{2+}$. Both EhDPCK1 and EhDPCK2 showed similar profiles of inhibition by CoA, acetyl-CoA, and malonyl-CoA at relatively high concentrations (Fig. 18).

### 3.4.3. Phenotypes caused by gene silencing of *EhDPCK1* and *EhDPCK2*

To better understand the role of DPCK in *E. histolytica*, I created a transformant strain where *DPCK* gene expression was selectively repressed by small antisense RNA-mediated transcriptional gene silencing. A 400-bp long region of *EhDPCK1* and *EhDPCK2* genes that correnspponds to the amino-terminal portion of the protein was used to design gene silencing constructs. Despite low identity at nucleotide and amino acid levels between the two isotypes, gene silencing of *EhDPCK1* gene also affect *EhDPCK2* gene and vice versa (Figs. 19 and 20, A and B). Gene silencing of *EhDPCK1* gene caused 77±1.2 % and 46±18.9% reduction of *EhDPCK1* and *EhDPCK2* transcripts, respectively, while gene silencing of *EhDPCK2* gene caused 41±14.8% and 88±2.9% reduction of *EhDPCK1* and *EhDPCK2* transcripts, respectively. Interestingly, gene silencing of either *EhDPCK1* or *EhDPCK2* gene caused upreguation of *EhPanK* transcript (Figs. 19B and 20B), which may indicate compensation for *EhDPCK* gene silencing.

*EhDPCK1* and *EhDPCK2* gene silenced (gs) strains showed significant growth defect in normal growth medium (Figs. 19C and 20C). The level of growth inhibition by *EhDPCK2* gene silencing was more severe compared to that by *EhDPCK1* gene silencing; the percentage growth

at 96 h of *EhDPCK1* gs and *EhDPCK2* gs trophozoites was 53.8±9.2% and 23.1±6.2% (mean±S.E. of triplicates) of the control transformant, respectively. Cells lysates from *EhDPCK1* gs strain contained 24.0±2.0% less DPCK activity (Fig. 19E) and an approximately 38.9±7.1% lower level of CoA (Fig. 19D). The effects of *EhDPCK2* gene silencing on the reduction of DPCK activity and CoA concentrations in cell lysates were more severe than those by *EhDPCK1* gene silencing; 44.0±6.2% decrease in DPCK2 activity (Fig. 20E) and 61.1±7.1% decrease in the CoA concentration by *DPCK2* gene silencing (Fig. 20D). Altogether, these results suggest that both EhDPCK isotypes play important roles in cell growth and the role played by EhDPCK2 is more indispensable than that of EhDPCK1.

### 3.4.4. Metabolomic analyses of *EhDPCK1* and *EhDPCK2* gene silenced strains

I performed metabolomics analyses of the *EhDPCK1* and *EhDPCK2* gs strains. The capillary electrophoresis-mass spectrometry (CE-MS) based quantitation systems were used both in cation and anion modes to identify >110 metabolites which include precursors, intermediates, and end products of central carbon metabolism, biosynthetic and catabolic intermediates of amino acids, sugars, nucleic acids, and lipids. All data were presented as normalized by cell number (per 1 x $10^6$ cells), as commonly accepted and used in many studies. The levels of some metabolites were changed in both directions (i.e., increase and decrease) in response to *EhDPCK1* and *EhDPCK2* gene silencing. However, all of the statistically significant changes in the concentrations of metabolites in both *EhDPCK1* and *EhDPCK2* gene silencing were decrease, not increase, relative to the metabolite levels in the control strain.

Besides decrease in the CoA concentration mentioned above, *EhDPCK1* gene silencing caused decrease only in citrate, ornithine, some nucleic acids, and *S*-adenosyl-*L*-methionine (Fig. 21). On the other hand, *EhDPCK2* gene silencing caused decrease in a wider range of metabolites than *EhDPCK1*, such as pantothenate, acetyl-CoA, glutamate, ornithine, putrescine, spermidine, methionine, and *S*-adenosyl-*L*-methionine, which were mapped to metabolites involved in ornithine and polyamine biosynthesis in Kyoto Encyclopedia of Genes and Genomes

Database (KEGG) maps (Fig. 22). *EhDPCK2* gene silencing also caused decrease in metabolites involved in glycogen/glucuronate and chitin metabolism (Fig. 23). Interestingly, most of the intermediate metabolites in purine metabolism were also decreased by *EhDPCK2* gene silencing (Fig. 24). Metabolite changes caused by *EhDPCK1* gene silencing in ornithine and polyamine biosynthesis, glycogen/glucuronate, chitin, and purine metabolisms were presented in supplementary figures (Fig. 25-27).

### 3.4.5. Phylogenetic analysis of DPCK

Eighty eight DPCK sequences from broad taxonomic groups was obtained, aligned, and analyzed. All major groups of Eukaryota possess putative homologs of DPCK. There are only few other eukaryotes that possess more than one copy of DPCK homologs (e.g. trypanosomes). DPCK gene duplication in *E. histolytica* apparently occurred before speciation. However, I did not perform further searches for duplicated homologs in other eukaryotic species. While most of the sequences were well aligned throughout the proteins, three eukaryotic homologs (*Homo sapiens*, *Mus musculus*, and *D. melanogaster*) possess an approximately 350 amino acids long N-terminal extension, which corresponds to phosphopantetheine adenylyltransferase domain of the phosphopantetheine adenylyltransferase / DPCK bifunctional enzyme. As shown in an alignment of the selected DPCK sequences from representative taxa, the amino acid residues involved in the CoA binding (T12, D38, H98, P134, L135, and Q183), and in the ATP binding (G13, G14, I15, G18, K19, R163, and N199) well conserved most of DPCK sequences were perfectly conserved in *Entamoeba* homologs.

Phylogenetic analyses of 88 sequences on the basis of 112 aligned positions inferred an optimal Maximum Likelihood (ML) tree shown in Fig. 28. As a whole, DPCK sequences are highly divergent suggested by long branches. Consequently, no resolution has been inferred for deep branching patterns across all parts of the tree. Neither was inferred the origin of the *Entamoeba* homologs. However, in the genus *Entamoeba,* all DPCK sequences including two isotypic genes for each species (*E. histolytica*, *E. nuttalli*, *E. dispar*, and *E. invadens*) are

monophyletic, although the bootstrap support value was not high (66%). Furthermore, monophyly of copy 1 or copy 2 among the four *Entamoeba* species genes was supported with 87% and 88% BP values, respectively, suggesting that *DPCK* gene duplication likely occurred in the common ancestor of four *Emtamoeba* species, followed by speciation of the four species.

### 3.4.6. Bioactive screening against EhDPC1 and EhDPCK2

Since DPCK1 and DPCK2 indicated indispensable for *E. histolytica* development, I propose these two enzymes to be a drug specific target. I developed assay system for rapid cell free based screening by EhDPCK1 and EhDPCK2 enzyme target. In this condition, one thousand and five hundred microbial extracts were tested against EhDPCK1 and EhDPCK2 and show many inhibitors. Resume of the screening results was presented in Table 12.

## 3.5. Discussion

### 3.5.1. Suggested specific roles of EhDPCK isotypes

My study on *E. histolytica* PanK in Chapter 2, the enzyme that catalyzes the first step of CoA biosynthesis, clearly demonstrated that this enzyme was important for growth of *E. histolytica* trophozoites. In this study, I have shown that both of two DPCKs, EhDPCK1 and EhDPCK2, play an indispensable, likely non-overlapping role in CoA biosynthesis. A line of evidence supports that both enzymes are involved in CoA biosynthesis in *E. histolytica*. First, *E. coli*-produced recombinant enzymes show comparable specific activity and kinetic parameters. Second, *EhDPCK1* and *EhDPCK2* gene silencing caused decrease in DPCK activity and intracellular CoA concentrations, as well as decrease in cell growth.

Most eukaryotic organisms possess a single copy of *DPCK* gene with some exceptions including *Trypanosoma* (TriTrypDB; http:// http://tritrypdb.org/tritrypdb/) and *Entamoeba* (this study). In a rodent *Plasmodium* species, which has only one copy of DPCK, it has recently been reported that DPCK is essential and indispensable for development of blood stage parasites (Hart

et al., 2017). Human infecting *Plasmodium* species (*P. falciparum* and *P. vivax*) also have a single copy of *DPCK* gene.

In this study, I have shown that *Entamoeba,* where two copies of *DPCK* are present, gene silencing of *EhDPCK2* produced more severe effects on both the metabolite profile and growth, compared to that of *EhDPCK1*. The previous microarray analysis of *E. histolytica* trophozoites showed that the *EhDPCK2* transcript level is higher than that of EhDPCK1, approximately 5 fold in HM-1:IMSS cl6 strain (Penuliar et al., 2015, 2012) and 11 fold in G3 strain (Furukawa et al., 2013, 2012; Nakada-Tsukui et al., 2012). Furthermore, based on the previous transcriptomic analysis of encystation (differentiation of the trophozoite into the cyst) of *E. invadens* (De Cádiz et al., 2013), which is the amebic encystation model (Chia et al., 2009; Donaldson et al., 1975; Kojimoto et al., 2001; Stanley, 2003), I found that both of the *E. invadens* genes encoding DPCK1 and DPCK2 were expressed during encystation. *E. invadens DPCK2* gene was expressed at comparable levels throughout encystation. In contrast, *E. invadens DPCK1* transcript was dramatically increased (~30-fold) during encystation. These data suggest that these isoenzymes play specific roles during proliferation and stage conversion. *DPCK1* is likely involved in encystation in *E. invadens*. However, gene silencing of *EhDPCK1* and *EhDPCK2* caused comparable, though slightly more pronounced in *EhDPCK2* gs strain, growth and metabolic defects. My results indicate that EhDPCK2 plays a primary role in the proliferative trophozoite stage and EhDPCK1 may have a specific role during developmental stage transition, which needs to be examined in the future.

### 3.5.2. Uniqueness of Entamoeba DPCK

Two amebic DPCK isotypes, EhDPCK1 and EhDPCK2, showed comparable specific activity and substrate affinity despite only 38% mutual identity. When the $K_m$ values of amebic DPCKs were compared with the human counterpart, phosphopantetheine adenylyltransferase and dephospho-CoA kinase bifunctional enzyme (Aghajanian and Worrall, 2002) from human has an approximately 10-fold higher $K_m$ value toward dephospho-CoA and a 10-fold lower $K_m$

value toward ATP (5.2 μM and 192 μM, respectively). These data indicate significant biochemical and structural differences exist between amebic and human DPCK and also suggest a possibility of discovering or designing parasite-specific DPCK inhibitors. ATP production in *E. histolytica* relies solely on substrate-level phosphorylation during glycolysis because this parasite lacks the enzymes and machineries involved in the Krebs cycle and oxidative phosphorylation and thus is unable to produce ATP as efficiently as aerobic organisms (McLaughlin and Aley, 1985; Reeves, 1985). It is thus plausible that DPCK from *E. histolytica* is able to have higher affinity to ATP than human counterpart. Moreover, my results suggest that both EhDPCK1 and EhDPCK2 activity was regulated biochemically not only by the end products of this pathway, CoA, but also its thioesters, acetyl CoA and malonyl-CoA through feedback inhibition.

### 3.5.3. Domain structures

DPCK have three-domains: the nucleotide binding, the dephospho-CoA binding, and the lid domains (G Obmolova et al., 2001). In *E. coli*, two prolines ($Pro^{90}$ and $Pro^{134}$) are highly conserved and predicted to be essential for the lid flexibility. These residues are located between the nucleotide binding and dephospho-CoA binding domains. However, these residues are only partially conserved in EhDPCK1 ($Pro^{138}$) and EhDPCK2 ($Pro^{90}$), indicating that the lid flexibility of DPCK is different between *E. histolytica* and its bacterial ortholog. A lysine residue in the GXXXGKS motif is also one of the conserved motifs of DPCKs among organisms, and known to be essential for the binding of ATP. $Thr^{10}$ for EhDPCK1 and $Thr^{8}$ for EhDPCK2 are probably involved in dephospho-CoA binding, whereas $Asp^{35}$ in EhDPCK1 and $Asp^{33}$ for EhDPCK2 are involved in activation of the 3'-OH group of the ribose for the attack on the β-phosphate of ATP, as previously reported in bacteria (O'Toole et al., 2003; G Obmolova et al., 2001). $Leu^{85}$ in EhDPCK1 and $Ile^{84}$ in EhDPCK2, both of which are also predicted to be localized to the CoA-binding site, are also conserved. $Asn^{91}$ in EhDPCK1 is replaced with $Pro^{90}$ in EhDPCK2; the corresponding residue $Pro^{90}$ in *E.coli* is located at a hinge and implicated for

the movement of the CoA-binding domain during catalysis, suggesting a potential difference in a catalytic process between EhDPCK1 and 2.

### 3.5.4. Metabolic disturbance caused by *DPCK* gene silencing

Metabolomics analysis has been widely used to complement genomics, transcriptomics, and proteomics analyses (Castro-Santos et al., 2015; Dumas, 2012), and to provide a comprehensive view on the responses to the environmental changes (Fuhrer and Zamboni, 2015), a metabolic-responsive profile (Holmes et al., 2008; Husain et al., 2011), and also to validate target for drug development (Krug and Müller, 2014; Mastrangelo et al., 2014). As expected, *DPCK* gene silencing (particularly gene silencing targeting *EhDPCK2*) caused decrease in the level of CoA and acetyl-CoA levels. Acetyl-CoA occupies a crucial position in metabolisms for all living organisms, and serves as an essential metabolic intermediate, a precursor of many anabolic reactions, also a donor of protein acetylation and allosteric enzymatic regulator (Choudhary et al., 2014). My metabolome data have also shown the disturbance, mostly decrease, in the broad range of related metabolites, in particular those involved in ornithine and polyamine biosynthesis. Ornithine is an important precursor of polyamines and essential for proliferation (Bacchi and Yarlett, 1993; Heby et al., 2003; Müller et al., 2001; Wallace et al., 2003). Polyamine metabolism was targeted to develop drugs against *Trypanosoma* (Begolo et al., 2014) and *Leishmania* (Das et al., 2016). In *P. falciparum*, it has been known that many cellular processes, such as DNA replication, transcription and translation are polyamine dependent and the cellular levels of polyamines reach their peak during the intra-erythrocytic development (Assaraf et al., 1987). My metabolomics analysis has shown that *EhDPCK2* gene silencing significantly reduced the levels of many intermediates in the polyamine pathway, while *DPCK1* gene silencing showed decrease to a lesser extent (not statistically significant). Citrate was significantly decreased by *EhDPCK1* gene silencing, which was not found in *EhDPCK2* gs strain. Citrate is an important intermediate metabolite derived from the condensation of acetyl coenzyme A and oxaloacetate in the Krebs cycle. However,

since Krebs cycle is absent in *E. histolytica*, the role of citrate remains elusive and needs future investigation.

The levels of metabolites in hexose metabolism were also decreased by *EhDPCK2* gene silencing. In particular, metabolites involved in the hexosamine-amino acid amide transfer and chitin biosynthesis, such as glucosamine 6-phosphate and *N*-acetyl-*D*-glucosamine 6-phosphate, significantly decreased compared to control ($p$=0.008). However, it is not well understood how glucosamine 6-phosphate was completely deprived by *EhDPCK2* gene silencing. The decrease in glucosamine 6-phosphates was apparently associated with the decreased level of glutamate in *EhDPCK2* gs strain, via the reaction converting D-fructose-6-phosphate/L-glutamate and D-glucosamine-6-phosophate and L-glutamine. On the other hand, the decrease in *N*-acetyl-D-glucosamine-6-phosphate was likely caused by the decrease in acetyl-CoA as *N*-acetyl-D-glucosamine-6-phosphate is generated from a combination of D-glucosamine-6-phosophate and acetyl-CoA. Glucosamine 6-phosphate and *N*-acetyl-D-glucosamine 6-phosphate are also important intermediates for chitin biosynthesis. Chitin is important and present as the major component of cell wall in cyst and oocyst stages of many protozoan parasites (Chávez-Munguía et al., 2007) including *E. histolytica* (Arroyo-Begovich and Carabez-Trejo, 1982). Chitin biosynthesis was also proposed as a parasite-specific drug target as it is absent in humans (Spindler et al., 1990). Interestingly, reduction in the intermediates in the chitin biosynthetic pathway was observed only in *EhDPCK2* gs strain, but not in *EhDPCK1* gs strain. Although statistically insignificant, several metabolites in the pathway were increased in *EhDPCK1* gs strain: glucose-1-phosphate, glucose-6-phosphate, *N*-acetyl-D-glucosamine-1-phosphate, and *N*-acetyl-D-glucosamine-6-phosphate, suggesting that the roles of EhDPCK1 and 2 in chitin metabolism are different.

Many nucleic acids were also decreased in both *EhDPCK1* and *EhDPCK2* gs strains. This may be explained at least in part by the decrease in polyamine synthesis. Polyamines can interact with macromolecules such as nucleic acids and are required during nucleic acids

packaging (Ruan et al., 1994). Also, the interaction between polyamines and nucleic acids can affect structure and stability of DNA (Gosule and Schellman, 1976; Raspaud et al., 1999; van Dam et al., 2002). Moreover, most of the intermediary metabolites in purine metabolism in *EhDPCK2* gs strain were also reduced. Importantly, these changes were specific to *EhDPCK2* gene silencing. In *EhDPCK1* gs strain, several purines and intermediates including adenine, guanine, IMP, and ADP, were increased compared to control. Purine metabolism is very important for DNA and RNA synthesis, nucleotide-dependent enzyme reactions, as chemical energy sources (e.g. ATP, GTP), intracellular second messengers (e.g. cAMP), and switch signals (e.g. GDP, GTP) for metabolic and gene regulation (Hyde, 2007). However, a majority of parasitic protists including *E. histolytica* (Lo and Wang, 1985) are incapable of *de novo* synthesis of purines and rely on salvage from the host. Hypoxanthine, guanine, xanthine, adenine, and adenosine must be imported from the hosts or media via nucleoside transporters described in *P. falciparum* (Carter et al., 2000), *Toxoplasma gondii* (De Koning et al., 2003), and *T. brucei* (Sanchez et al., 2002). Interestingly, while most of the above-mentioned purines were decreased in *EhDPCK2* gs strain, hypoxanthine was most dramatically decreased. Hypothanthine is regarded as the key precursor of the other purines. For instance, degradation of hypoxanthine by added xanthine oxidase in the culture medium strongly inhibits in vitro growth of *P. falciparum* (Berman et al., 1991). Purine metabolic pathways were proposed as promising targets for novel drug development against infections caused by *P. falciparum* (Cassera et al., 2011), *T. gondii* (De Koning et al., 2003), and *Mycobacterium tuberculosis* (Parker and Long, 2007).

### 3.5.5. Regulation of CoA biosynthesis

*EhDPCK2* gene silencing caused reduction of CoA and also led to decrease in pantothenate, which can be explained by either high consumption of pantothenate or decrease in pantothenate uptake. Most eukaryotes including *E. histolytica* are unable to synthesize pantothenate and rely on uptake of exogenous pantothenate. my qRT-PCR data indicate that the

decreased level of CoA by *EhDPCK1* or *EhDPCK2* gene silencing led to the increase in steady-state mRNA level of *EhPanK* gene encoding the protein that catalyzes conversion of pantothenate to 4'-phosphopantothenate. This was also confirmed by the observation that PanK activity increased in *EhDPCK1* and *EhDPCK2* gs strains. Although none of the intermediates, 4'-phosphopantothenate, 4'-phosphopantothenoyl-L-cysteine, pantetheine 4-phosphate, and dephospho-CoA was measured in my metabolomics analysis, it is conceivable that these metabolites accumulated intracellularly as a consequence of lack of DPCK and upregulation of PanK. These data also reinforce allosteric feedback of EhPanK by the CoA regulatory network of CoA biosynthesis, which was demonstrated in Chapter 2.

### 3.5.6. EhDPCK1 and EhDPCK2 inhibited by microbial extracts

Microbial extracts from Fungi and Actinomycetes could inhibit EhDPCK1 and EhDPCK2, approximately 2-3% from total extracts. I found some microbial broth extracts selectively inhibited one isoenzyme, but most of them inhibited both EhDPCK1 and EhDPCK2. I calculated that only 7 extracts solely inhibited EhDPCK1, while 22 extracts solely inhibited EhDPCK2 and 33 extracts inhibited both EhDPCK1 and EhDPCK3. There showed that more inhibitor obtained from Fungi extract than Actinomycetes. It is suggesting that these enzymes can be proposed as a novel anti-amoebiosis target. However, additional experiments need to be confirmed, against human DPCK or phosphopantetheine adenylyltransferase and dephospho-CoA kinase bifunctional enzyme in particular. Extended experiment of *in vivo* test toward animal model was also required to evident my hypotheses.

Collectively, I have demonstrated that DPCK is the important enzyme involved in CoA biosynthesis, polyamine, hexose, and nucleic acid metabolisms in the proliferation of trophozoite stage of *E. histolytica*. In trophozoites, EhDPCK2 plays a predominant role, while an encystation-specific role is suggested for EhDPCK1. Notable differences in kinetic parameters of DPCK between *Entamoeba* and its host suggest that amebic DPCK is the rational target for the development of anti-amebic agents.

### 3.6. Figures and Tables

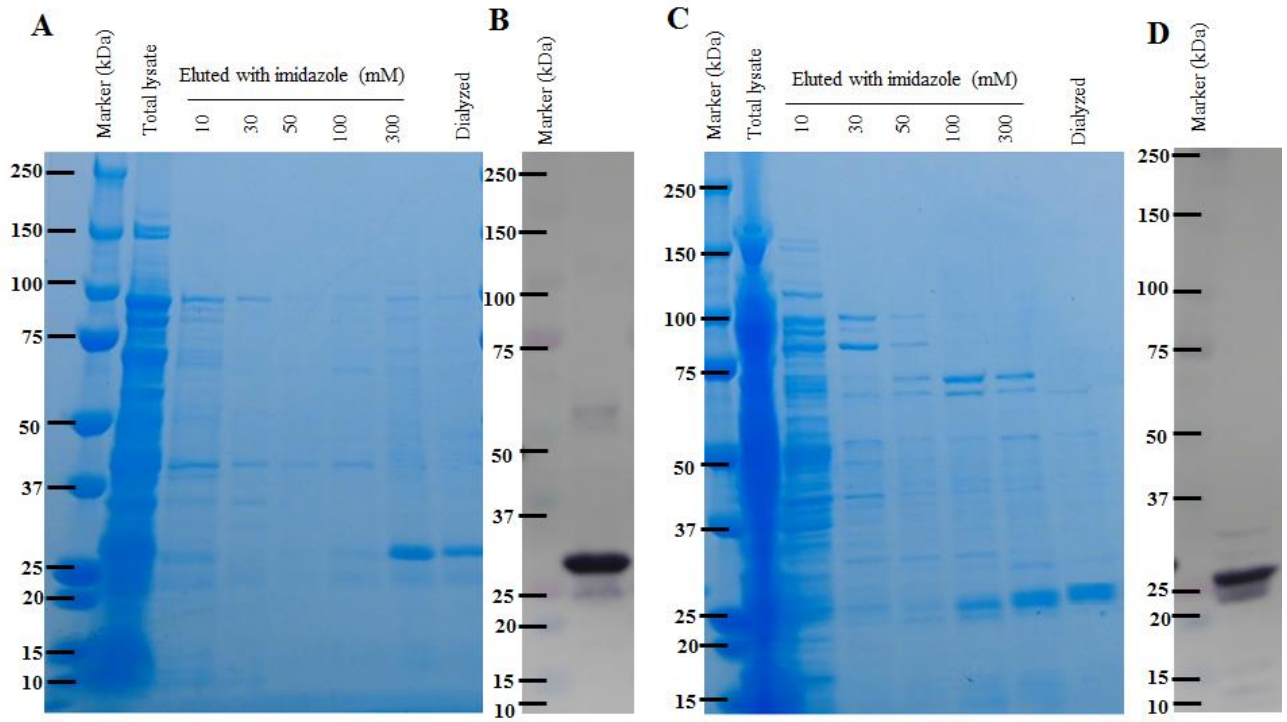


**Figure 16.** Expression and purification of recombinant EhDPCK1 (A and B) and EhDPCK2 (C and D). (A and C) Protein samples of recombinant EhDPCK1 (A) and EhDPCK2 (C) at each step of purification were subjected to 15% SDS-PAGE under reducing conditions and then stained with Coomassie Brilliant Blue R250. (B and D) Immunoblot analysis of purified recombinant EhDPCK1 (B) and EhDPCK2 (D) using anti-His antibody.

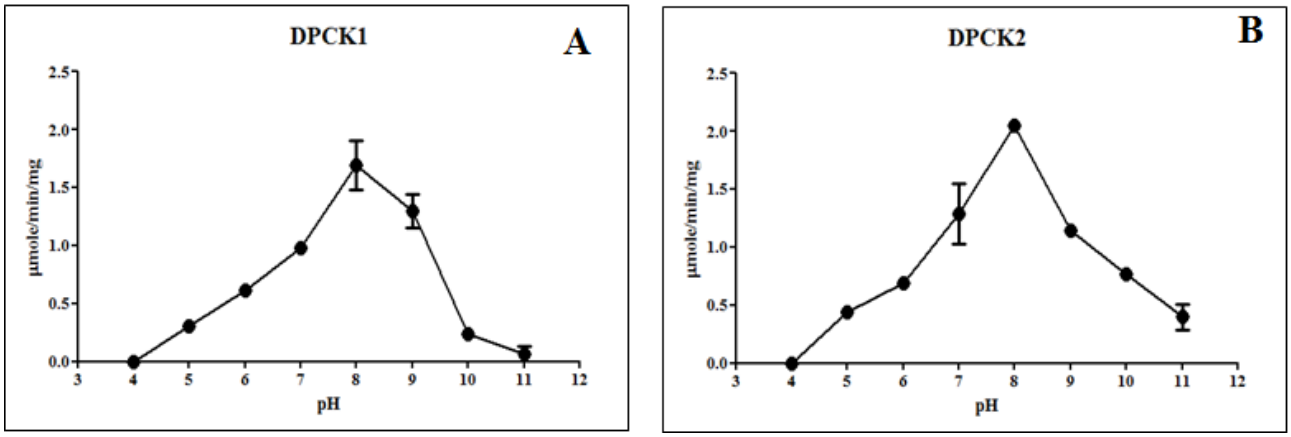

**Figure 17.** Optimum pH of the recombinant EhDPCK1 (A) and EhDPCK2 (B). Enzymes activities were measured at 37°C at the various pHs indicated in the figure. Assays were performed as described in Experimental procedures, with 50 ng of EhDPCK1 or EhDPCK2 recombinant enzyme, 15 mM HEPES, 20 mM NaCl, 10 mM $MgCl_2$, 1 mM EGTA, 0.02% Tween-20, 0.1 mg/mL β−globulins, 100 µM ATP and 200 µM dephospho-CoA at 37ºC. Data are shown in mean ± S.D. of three replicates.

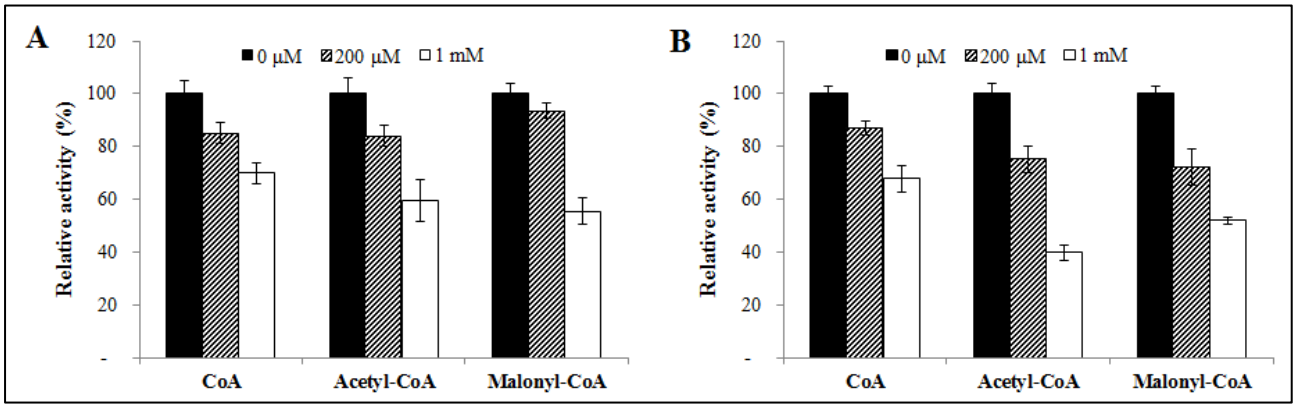


**Figure 18.** Inhibition of on the EhDPCK1 (A) and EhDPCK2 (B) activities by CoA, acetyl-CoA, and malonyl-CoA. The assays were carried out three times independently. Data are shown in mean ± S.D.

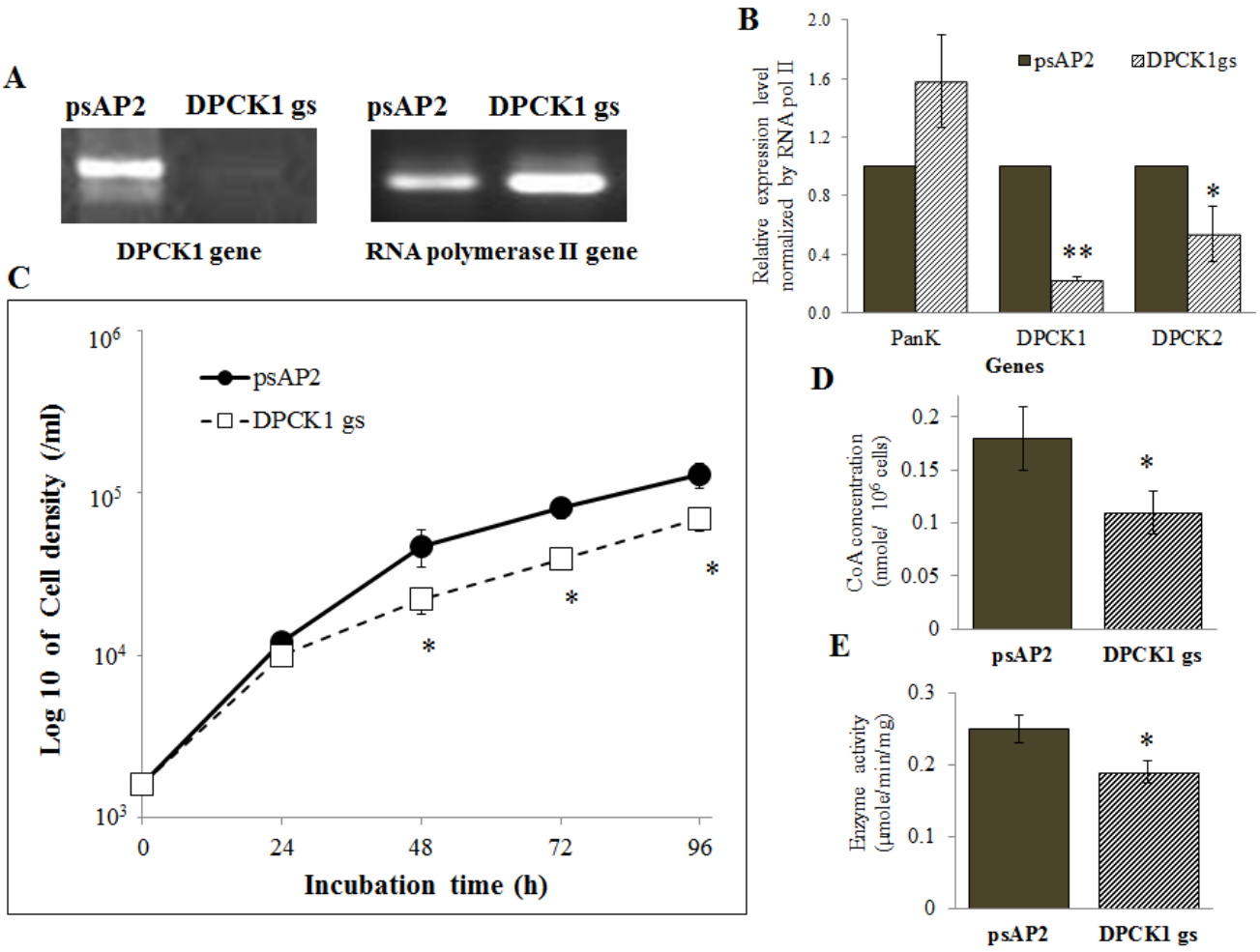


**Figure 19.** DPCK gene expression, cell growth, CoA concentration, and DPCK activity in *EhDPCK1* gene silenced (gs) strain. (A) RT-PCR of *EhDPCK1* gene from cDNA of *E. histolytica* transformants. "psAP2" indicates G3 strain transfected with mock psAP-2-Gunma vector, and "DPCK1 gs" indicates GS strain transfected with *EhDPCK1* gene silencing plasmid. (B) Relative levels of gene transcripts encoding EhPanK, EhDPCK1, and EhDPCK2 involved in CoA biosynthesis, estimated by qRT-PCR analysis in psAP2 and *EhDPCK1* gs transformants. qRT-PCR data were normalized against RNA polymerase II, and are shown in percentage relative to the transcript level of each gene in psAP2 control. (C) Growth kinetics of *E. histolytica* transformants in BI-S-33 medium. (D) CoA concentrations in cell lysates. (E) DPCK activity in cell lysates of psAP2 and *EhDPCK1* gs transformants. Data shown in mean ± S.E. Statistical comparison is made by Student's t-test (**P*<0.05, ***P*<0.01).

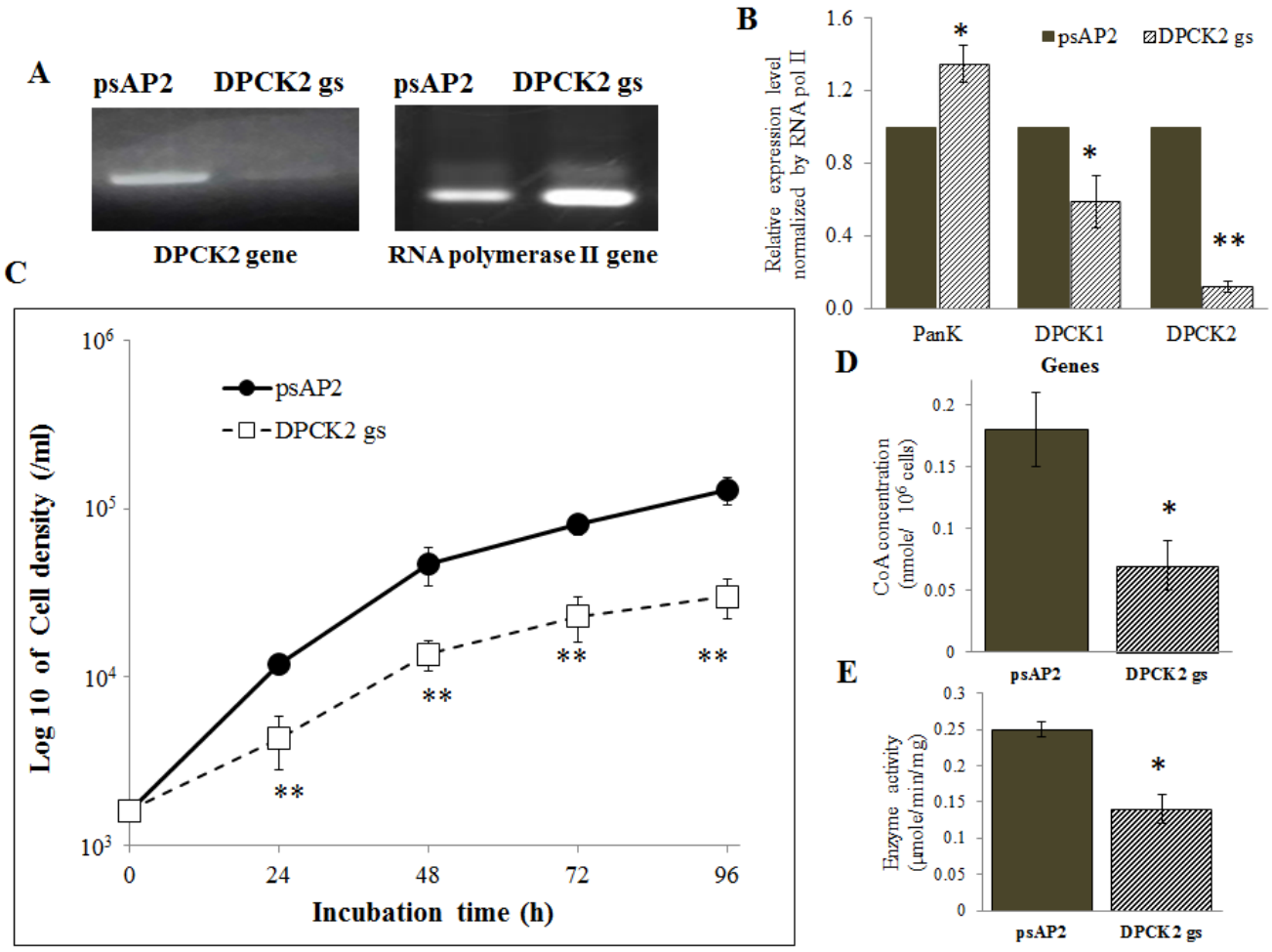


**Figure 20.** DPCK gene expression, cell growth, CoA concentration, and DPCK activity in *EhDPCK2* gene silenced strain. (A) RT-PCR of *EhDPCK1* gene from cDNA of *E. histolytica* transformants. (B) Relative levels of gene transcripts encoding EhPanK, EhDPCK1, and EhDPCK2, estimated by qRT-PCR analysis using RNA from psAP2 and *EhDPCK2* gs transformants. qRT-PCR data were normalized against RNA polymerase II, and are shown in percentage relative to the transcript level of each gene in psAP2 control. (C) Growth kinetic of *E. histolytica* transformants in BI-S-33 medium. (D) CoA concentrations in cell lysates. (E) DPCK activity in cell lysates of psAP2 and *EhDPCK2* gs transformants. Labels and abbreviations are as in Figure 1.

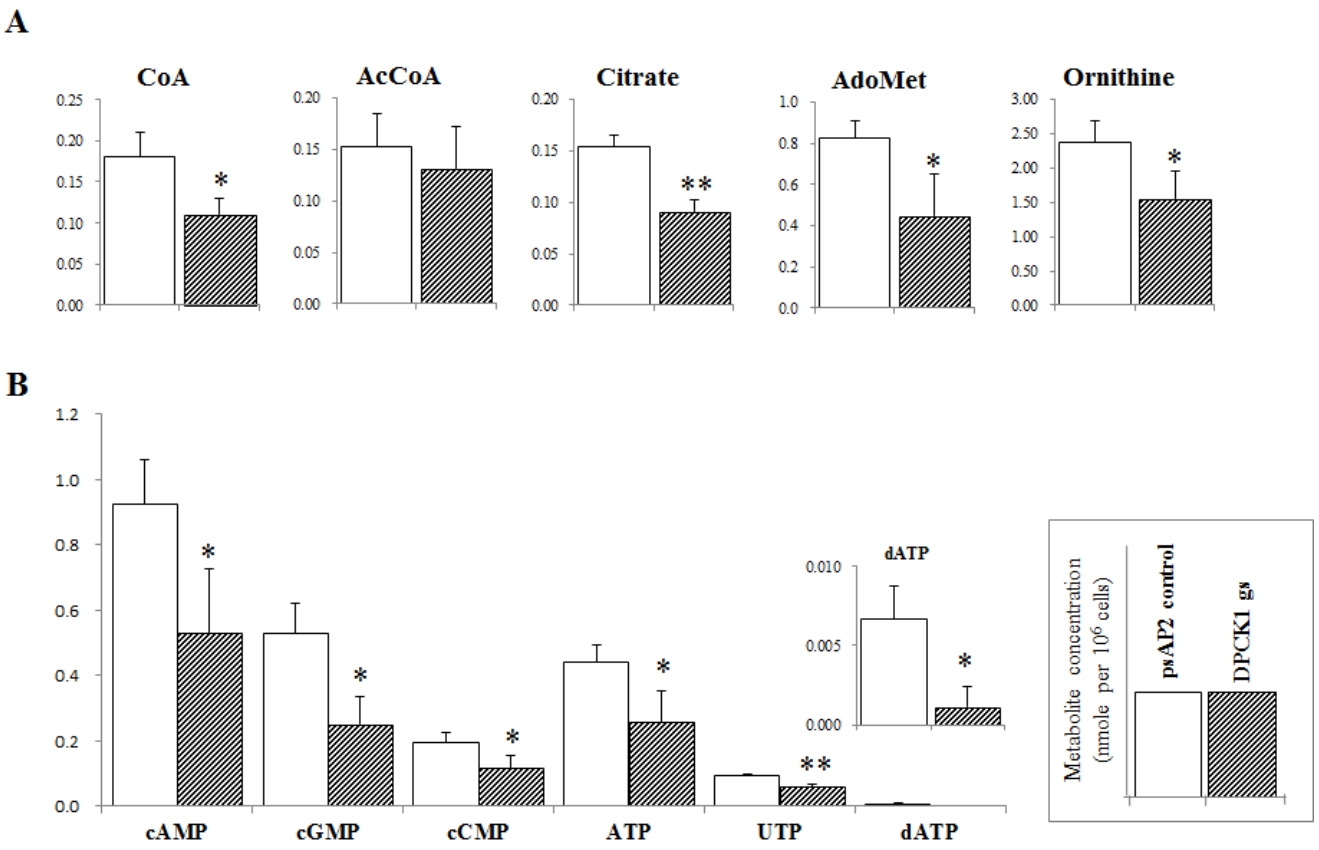


**Figure 21.** The levels of representative intermediary metabolites affected by *EhDPCK1* gene silencing. (A) Note decrese in the concentrations of coenzyme A (CoA), acetyl-CoA (AcCoA), citrate, ornithine, and *S*-adenosyl-L-methionine (AdoMet). (B) Depletion of nucleotides. Data are shown in mean ± S.D. Statistical comparison is made by Student's t-test (**P*<0.05, ***P*<0.01).

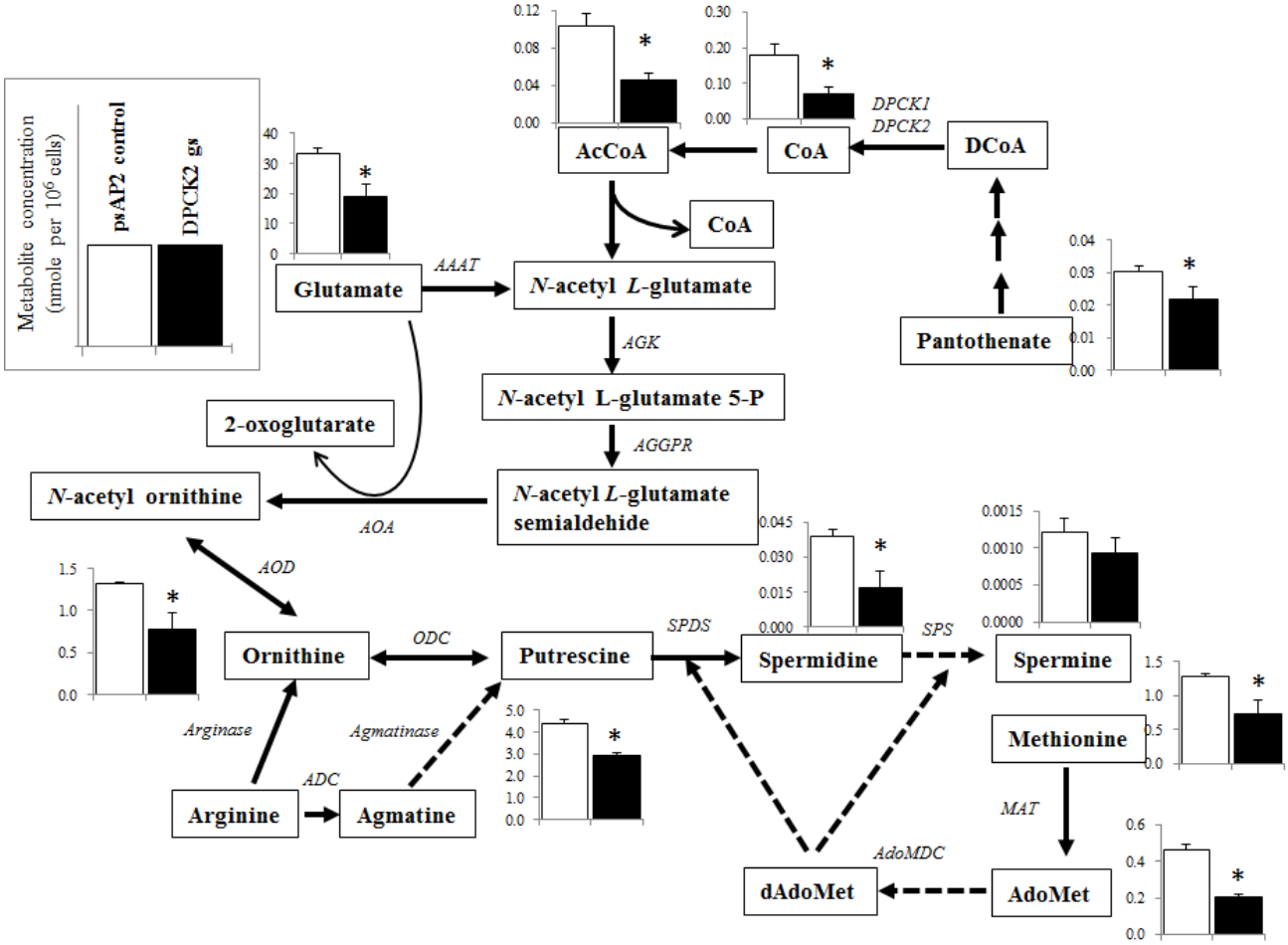


**Figure 22.** Metabolic profiles of amino acids, polyamines, and associated metabolites affected by *EhDPCK2* gene silencing. Broken lines indicate genes whose encoding enzymes known to catalyze the steps are likely absent in the genome. Abbreviations are: ND, not detected; CS, citrate synthase; AAAT, amino-acid N-acetyltransferase; AGK, acetylglutamate kinase; AGGPR, N-acetyl-*L*-glutamyl-phosphate reductase; AOA, acetylornithine aminotransferase; AOD, acetylornithine deacetylase; ODC, ornithine decarboxylase; ADC, arginine decarboxylase; MAT, methionine adenosyltransferase, AdoMet, *S*-adenosyl-L-methionine; dAdoMet, *S*-adenosylmethioninamine; MAO, monoamine oxidase; AdoMDC, S-adenosylmethionine decarboxylase; SPDS, spermidine synthase; SPS, spermine synthase. Data are shown in mean ± S.D. Statistical comparison is made by Student's t-test (**P*<0.05, ***P*<0.01).

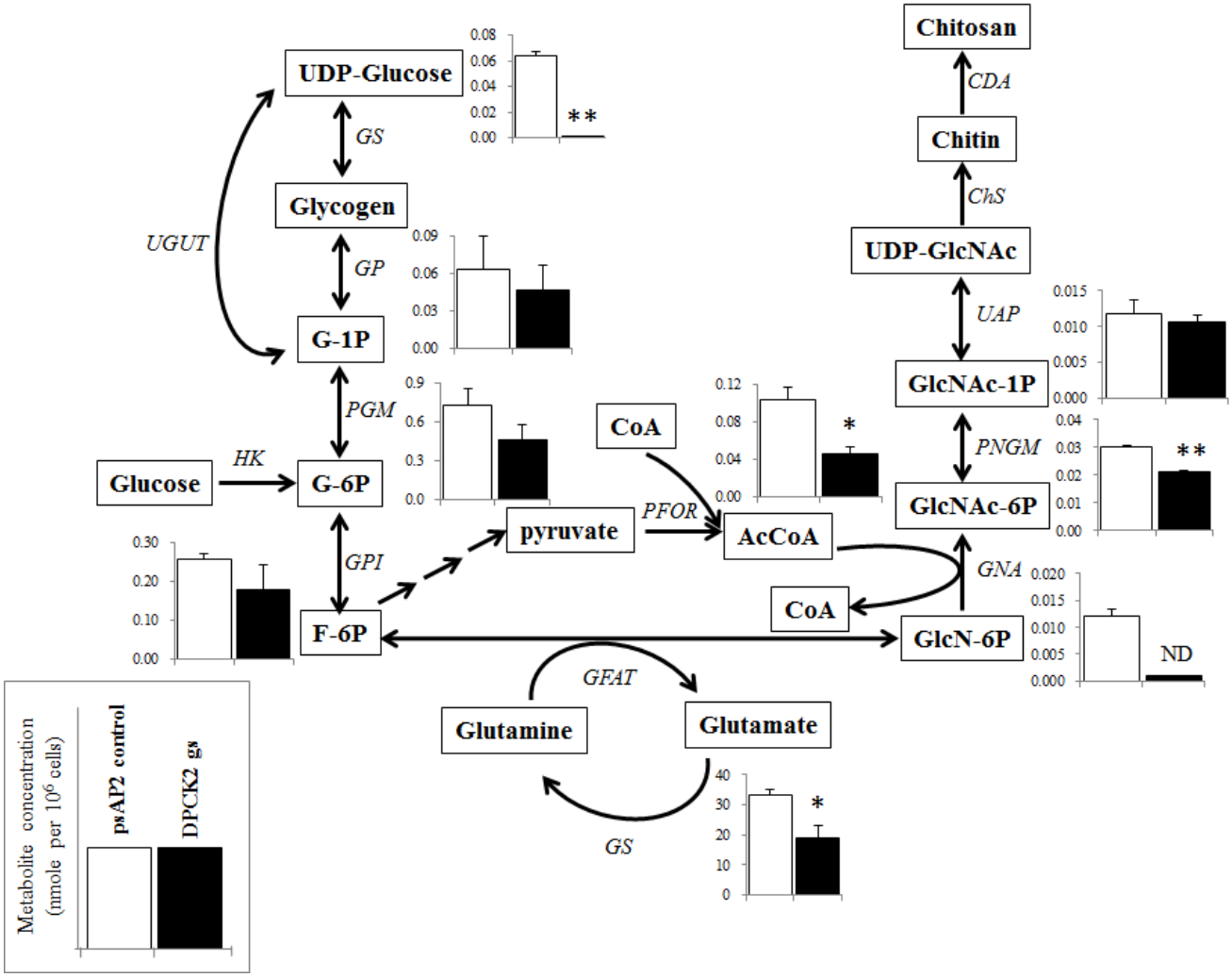


**Figure 23.** Metabolic profiles of hexose phosphates, glycogen metabolism, chitin biosynthesis, and associated metabolism affected by *EhDPCK2* gene silencing. Abbreviation are: G-1P, glucose 1-phosphate; G-6P, glucose 6-phosphate; F-6P, fructose 6-phosphate; GlcN-6P, glucosamine 6-phosphate; GlcNAc-6P, *N*-acetylglucosamine 6-phosphate; GlcNAc-1P, *N*-acetyl glucosamine 1-phosphate; UDP-GlcNAc, UDP-*N*-acetylglucosamine; GS, glycogen synthase; GP, glycogen phosphorylase; UGUT, UTP-glucose-1-phosphate uridyltransferase; PGM, phosphoglucomutase; GPI, glucose-6-phosphate isomerase; HK, hexokinase; GFAT, glutamine:fructose-6-phosphate aminotransferase; GS, glutamine synthetase; PFOR, pyruvate ferredoxin oxidoreductase; GNA, glucosamine-phosphate *N*-acetyltransferase; PNGM, phosphoacetylglucosamine mutase; UAP, UDP-*N*-acetylgalactosamine diphosphorylase; ChS, chitin synthase; CDA, chitin deacetylase. Data are shown in mean ± S.D. Statistical comparison is made by Student's t-test (**P*<0.05, ***P*<0.01).

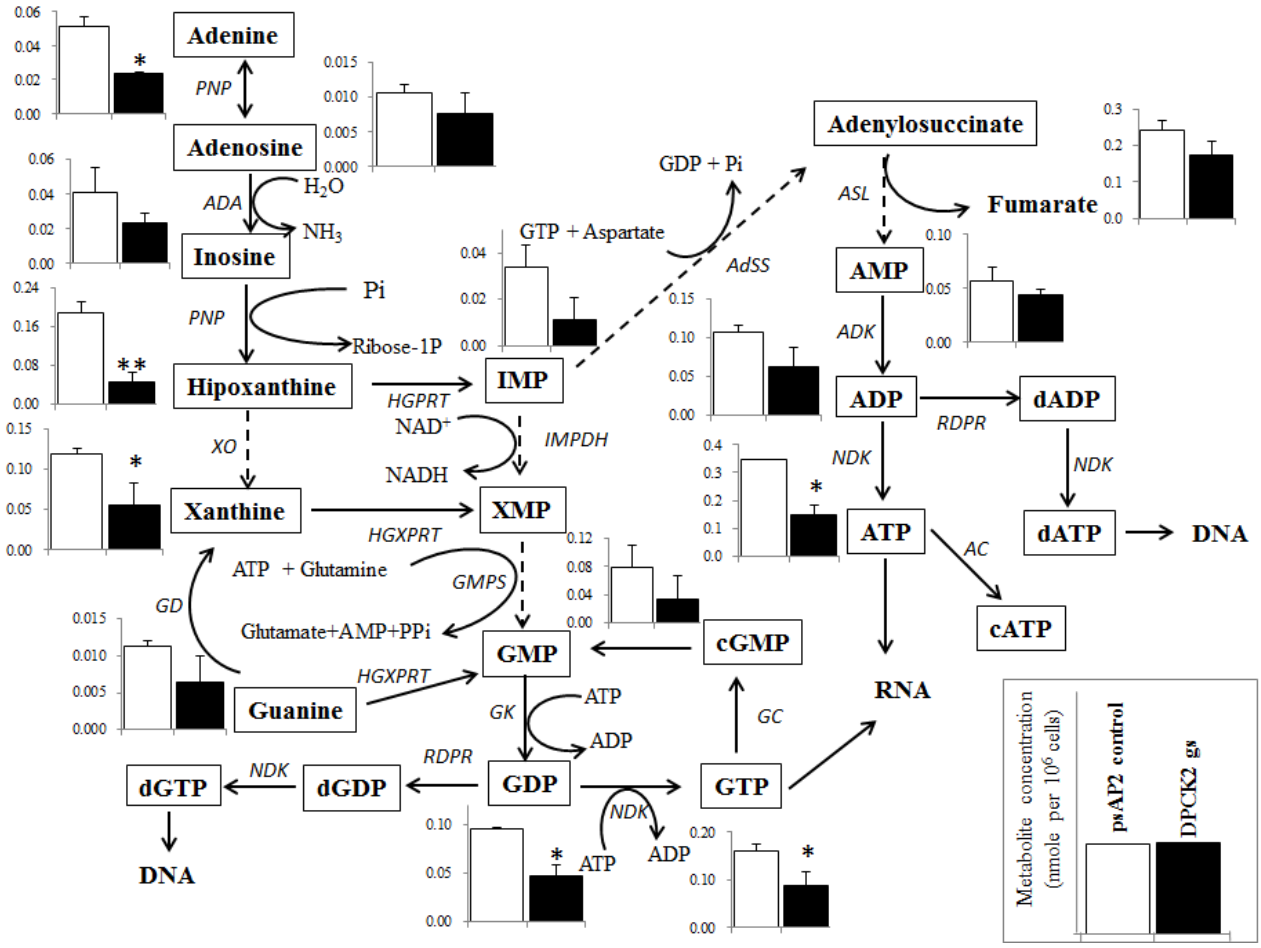


**Figure 24.** Metabolic profiles of purine metabolism affected by *EhDPCK2* gene silencing. Broken lines indicate genes whose encoding enzymes known to catalyze the steps are likely absent in the genome. Abbreviations are: PNP, purine nucleoside phosphorylase ; ADA, adenosine deaminase; XO, xanthine oxidase; HGPRT, hypoxanthine-guanine phosphoribosyltransferase; HGXPRT, hypoxanthine-guanine-xanthine phosphoribosyltransferase; IMPDH, inosine 5′-monophosphate dehydrogenase; GMPS, guanosine monophosphate synthetase; GK, guanylate kinase ; NDK, nucleoside diphosphate kinase; RDPR, ribonucleoside-diphosphate reductase; GC, guanylate cyclase; AdSS, adenylosuccinate Synthetase ; ASL, adenylosuccinate lyase ; ADK, adenylate kinase; AC, adenylate cyclase. Data are shown in mean ± S.D. Statistical comparison is made by Student's t-test (**P*<0.05, ***P*<0.01).

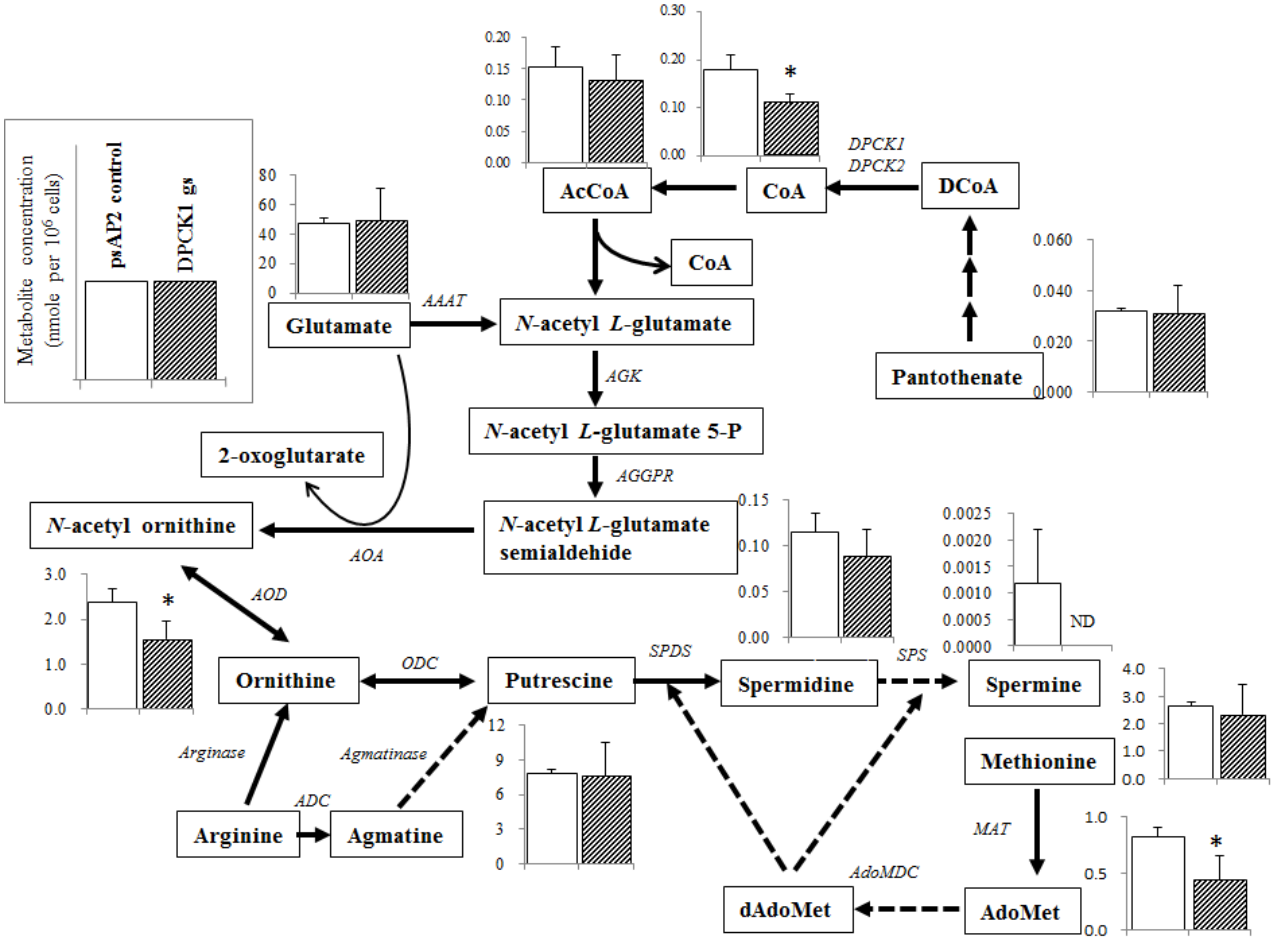


**Figure 25.** Metabolic profiles of amino acids (ornithine, glutamate and methionine), polyamines, and associated metabolites affected by *EhDPCK1* gene silencing. Broken lines indicate genes and their encoded enzymes are likely absent in the genome. Labels and abbreviations are as in Figure 4. Data are shown in mean ± S.D. Statistical comparison is made by Student's t-test (*$P$<0.05).

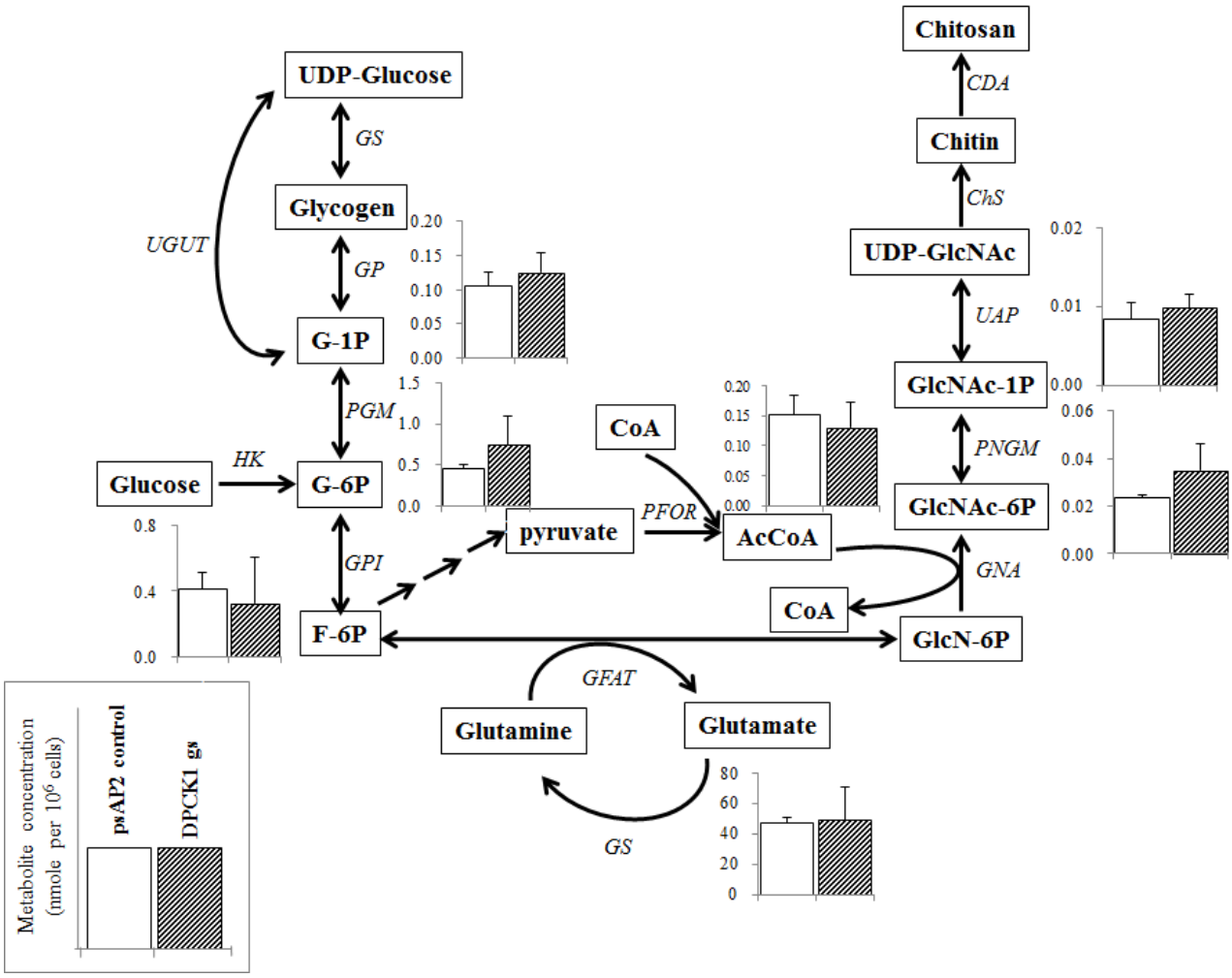


**Figure 26.** Metabolic profiles of hexose phosphates, glycogen metabolism, chitin biosynthesis, and associated metabolism affected by *EhDPCK1* gene silencing. Labels and abbreviations are as in Figure 5. Data are shown in mean ± S.D. Statistical comparison is made by Student's t-test (**P*<0.05).

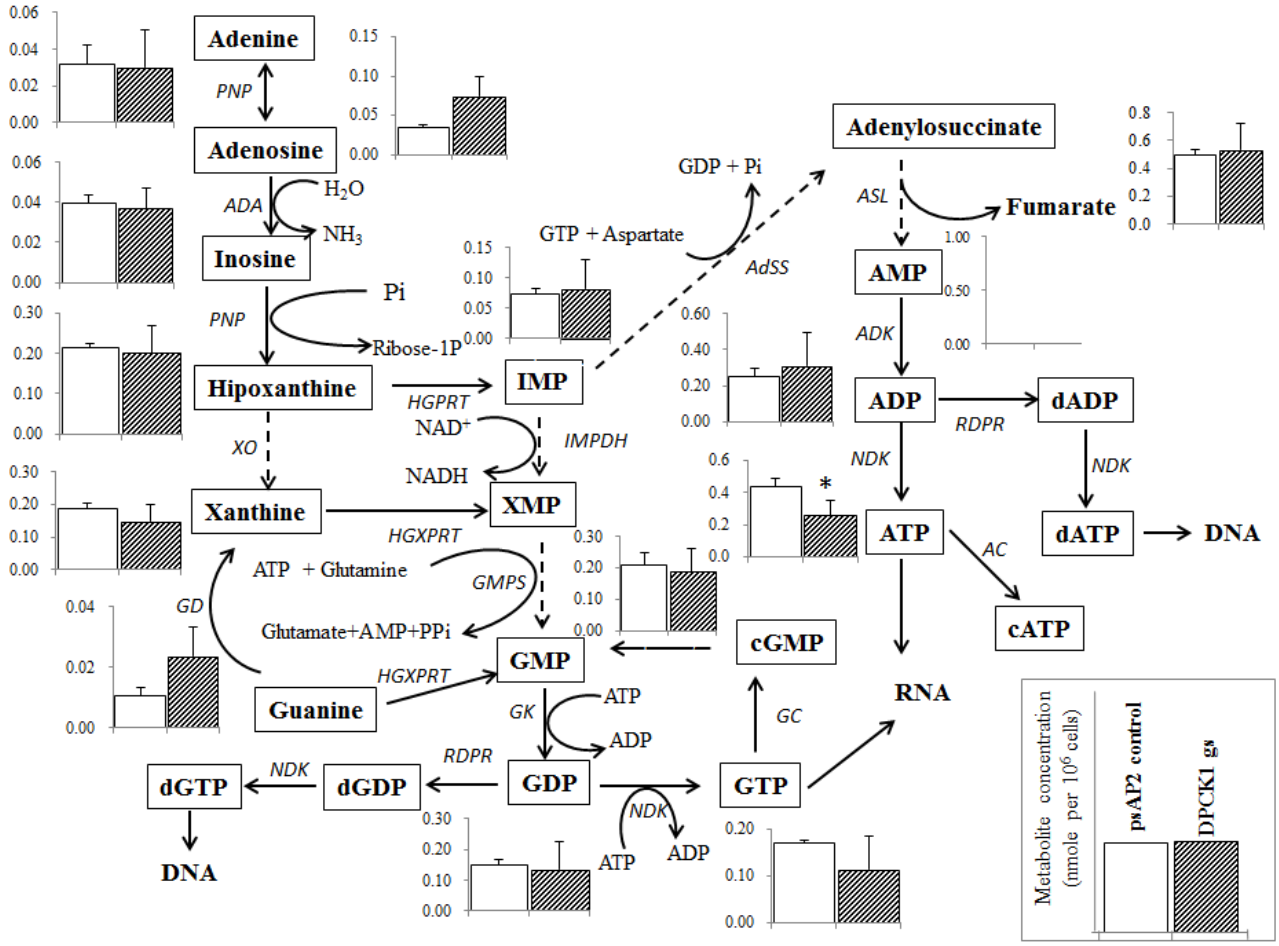


**Figure 27.** Metabolic profiles of purine metabolism affected by *EhDPCK2* gene silencing. Broken lines indicate genes whose encoding enzymes known to catalyze the steps are likely absent in the genome. Labels and abbreviations are as in Figure 5. Data are shown in mean ± S.D. Statistical comparison is made by Student's t-test (**P*<0.05).

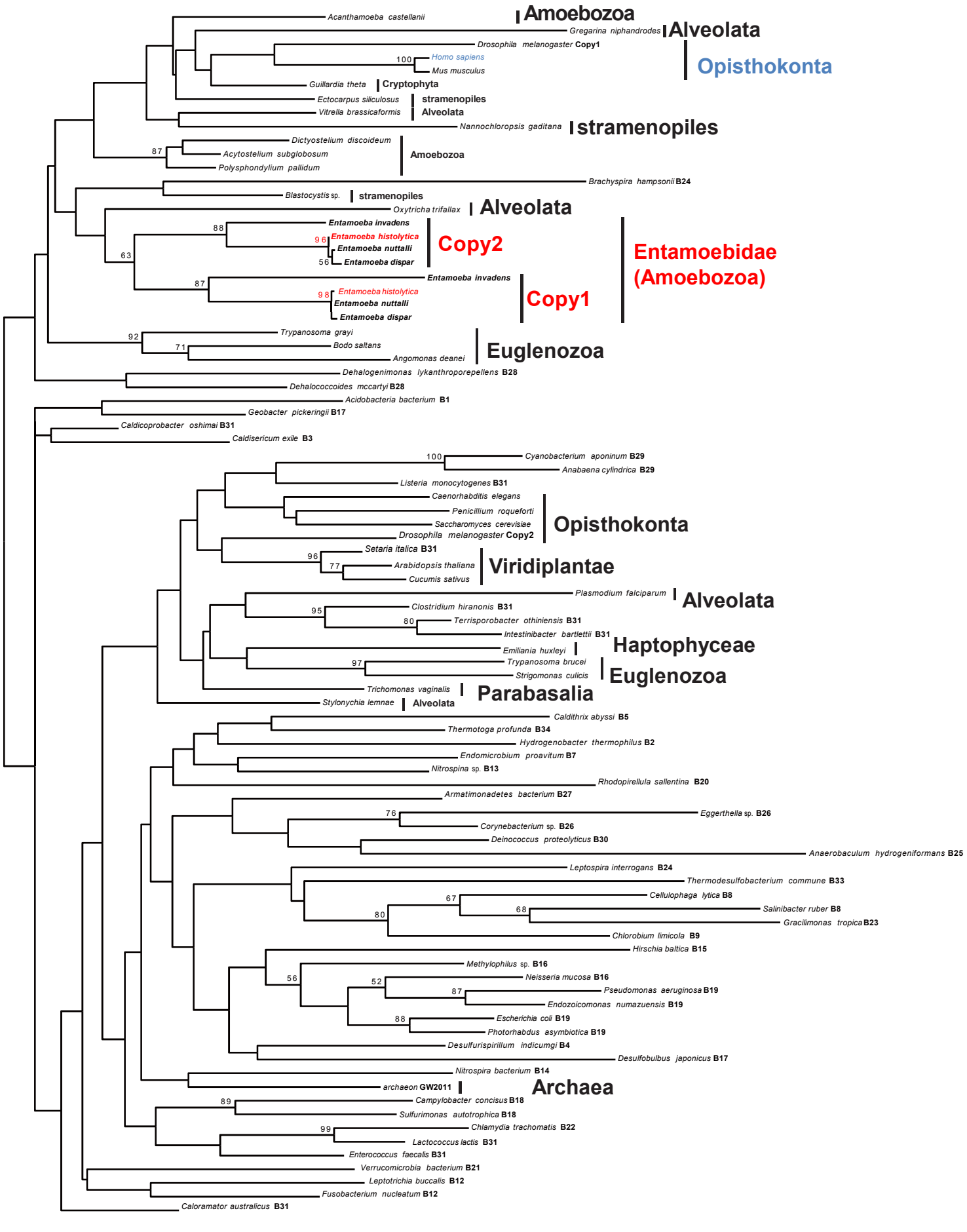


**Fig. 28.** Phylogenetic tree of dephospho-CoA Kinase (DPCK) proteins from *E. histolytica* and other organisms. Optimal ML tree inferred by RAxML program with LG +Γ4 model was shown from 112 DPCK positions were used in this analysis.

**Table 8.** Purification of recombinant *E. histolytica* dephospho-CoA kinase 1 (EhDPCK1) and dephospho-CoA kinase 2 (EhDPCK2).

| **Enzymes** | **Purification step** | **Protein concentration (mg)** | **Activity (µmole/min)** | **Specific activity (µmole/min/mg)** | **Yield (%)** | **Purification (fold)** |
|---|---|---|---|---|---|---|
| EhDPCK1 | Lysate | 2.32 | 2.09 | 0.90 | 100 | - |
| | Eluate | 0.36 | 0.77 | 2.13 | 36.7 | 2.4 |
| EhDPCK2 | Lysate | 4.48 | 3.09 | 0.69 | 100 | - |
| | Eluate | 0.35 | 0.89 | 2.54 | 28.8 | 3.7 |

**Table 9.** Kinetic parameters of *E. histolytica* dephospho CoA kinase 1 (EhDPCK1) and dephospho CoA kinase 2 (EhDPCK2)

| Enzyme | Substrate | $K_m$ (µM) | $V_{max}$ (µmole/min/mg) | $K_{cat}$ ($min^{-1}$) | $K_{cat}/K_m$ ($min^{-1}\mu M^{-1}$) |
|---|---|---|---|---|---|
| EhDPCK1 | Dephospho CoA | 114 ± 19 | 3.71 ± 0.43 | 88.9 ± 10.3 | 0.78 ± 0.04 |
| | ATP | 19.6 ± 1.2 | 3.54 ± 0.09 | 84.8 ± 2.4 | 4.32 ± 0.23 |
| EhDPCK2 | Dephospho CoA | 57.9 ± 6.07 | 2.48 ± 0.15 | 57.5 ± 3.5 | 0.99 ± 0.07 |
| | ATP | 15.0 ± 2.4 | 2.71 ± 0.17 | 62.9 ± 3.7 | 4.25 ± 0.74 |

[a] Assays were performed in the presence 10 mM MgCl2, 15 mM HEPES, 20 mM NaCl, 1 mM EGTA, 0.02% Tween-20, 0.1 mg/ml β−globulins and 4-256 µM dephospho-CoA to determine kinetic parameters toward ATP or 5-100 µM ATP to determine kinetic parameters toward dephospho-CoA. Reactions were conducted at 37°C at pH 8 for 60 min.
Mean±S.E. of three replicates are shown.

**Table 10.** Phosphoryl donor specificity[a] of EhDPCK1 and EhDPCK2

| Phosphoryl donor[b] | Relative activity (%) | |
|---|---|---|
| | EhDPCK1 | EhDPCK2 |
| ATP | 100.0 ± 0.0 | 100.0 ± 0.0 |
| TTP | 24.1 ± 2.2 | 4.9 ± 1.1 |
| GTP | 32.6 ± 2.6 | 33.0 ± 3.8 |
| CTP | 15.4 ± 1.8 | 7.3 ± 1.6 |
| UTP | 2.6 ± 0.1 | 4.5 ± 0.3 |
| None | ND | ND |

[a] Assays were performed in the presence 10 mM MgCl2, 15 mM HEPES, 20 mM NaCl, 1 mM EGTA, 0.02% Tween-20, 0.1 mg/ml β−globulins and 1 mM dephospho-CoA. Reactions were conducted at 37°C in pH 8 for 60 min.
[b] The final concentration used was 0.1 mM.
The activity is shown in percentage (%) relative to that toward ATP. ND, not detected.
Mean±S.E. of three replicates are shown.

**Table 11**. Effect of metal ions[a] on the activity of EhDPCK1 and EhDPCK2.

| Metal[b] | Relative activity (%) | |
|---|---|---|
| | EhDPCK1 | EhDPCK2 |
| $MgCl_2$ | 100.0 ± 0.0 | 100.0 ± 0.0 |
| $FeCl_2$ | 20.9 ± 1.8 | 12.1 ± 2.7 |
| $CaCl_2$ | 10.5 ± 1.7 | 1.0 ± 0.5 |
| $CoCl_2$ | 28.3 ± 6.2 | 40.9 ± 0.2 |
| $MnCl_2$ | 43.8 ± 2.2 | 53.7 ± 3.1 |
| $ZnCl_2$ | 76.9 ± 0.3 | 78.3 ± 0.1 |
| $NiCl_2$ | 45.2 ± 0.3 | 23.0 ± 2.2 |
| $CuCl_2$ | 53.2 ± 5.1 | 61.5 ± 5.1 |
| $LiCl_2$ | 4.9 ± 0.2 | 21.7 ± 1.5 |
| NaCl | ND | ND |
| KCl | ND | ND |
| None | ND | ND |

[a] Assays were performed in the presence 0.1 mM ATP, 15 mM HEPES, 20 mM NaCl, 1 mM EGTA, 0.02% Tween-20, 0.1 mg/ml β−globulins and 1 mM dephospho-CoA. Reactions were conducted at 37ºC in pH 8 for 60 min.
[b] The cation final concentration used was 5 mM.
The activity is shown in percentage (%) relative to that toward $MgCl_2$. ND, not detected.
Mean±S.E. of three replicates are shown.

**Table 12.** EhDPCK1 and EhDPCK2 inhibitor from microbial extracts

| **Origin** | **Number of samples** | **EhDPCK1*** | **EhDPCK2*** | **EhDPCK1 and EhDPCK2*** |
|---|---|---|---|---|
| Fungi | 600 | 31 | 32 | 27 |
| Actinomycetes | 900 | 9 | 23 | 6 |
| **Total** | 1,500 | 40 | 55 | 33 |
| | | 2.6 % | 3.6 % | 2.2 % |

**inhibited >50%*

## Chapter 4. General Discussion

My experiment showed that pantothenate kinase, dephospho-CoA kinase 1 and dephospho-CoA kinase 2 are enzymes involved in CoA biosynthesis pathway in the human parasite *E. histolytica*. Interestingly, these enzymes also showed important or essential to this parasite during trophozoite stage, since gene silencing of PanK, DPCK1, and DPCK2 caused significant retardation in growth, CoA concentration and related enzymes activity (PanK and DPCK enzyme). Metabolomics analyses towards these silencing gene strains also supported the importance of these enzymes by disturbance, mostly decreased, of some key metabolites.

Metabolomics analyses revealed of our understanding regarding the independent role of PanK, DPCK1, and DPCK2 in the cellular mechanism. *PanK* gene silencing caused significant changes in metabolites such as overall increase in the majority of upstream (down to pyruvate) intermediates of glycolysis and the pentose phosphate pathway, and a decrease in acetyl CoA, xanthine, hypoxanthine, ATP, cyclic nucleotides, ornithine, and *S*-adenosyl-L-methionine. *EhDPCK1* gene silencing caused the depletion of ornithine, *S*-adenosyl-L-methionine, some cyclic nucleoside monophosphates, and citrate. On the other hand, suppression of *EhDPCK2* gene affected to the decreasing in the level of acetyl-CoA, and metabolites involved in amino acid, glycogen, hexosamine, nucleic acid metabolisms, chitin and polyamine biosynthesis. In general, EhDPCK2 affected more severe of metabolite changes compared to EhDPCK1 gene silencing. My data indicated both DPCK isotypes play a crucial role in cell cellular reaction, whereas EhDPCK2 is more indispensable.

According to their essentiality, I proposed PanK, DPCK1, and DPCK2 as potential novel drugs target against amebiasis. Therefore, I produced recombinant of EhPanK, EhDPCK1, and EhDPCK2 in *E. coli* expression system and characterized it. Biochemically characterization of these enzymes (e.g. determination of $K_m$, $V_{max}$, phosphoryl donor specificity, effect of various metal ions to the enzyme activity, regulation by the end product, CoA, and its thioester) combined with phylogenetic analyses showed some uniqueness compared to human counterpart

enzymes, suggesting a possibility to discovering or designing entamoeba-specific PanK or DPCK inhibitors. Using these enzymes, cell free-based screening system has been developed. Initially, 244 natural compounds and 3,000 microbial extracts from fungi and actinomycetes were screened against EhPanK and 1,500 microbial extracts were screened against EhDPCK1 and EhDPCK2 recombinant enzyme.

In conclusion, I have shown that pantothenate kinase and dephospho-CoA kinase involved in CoA biosynthesis are physiologically important for this parasite. Some potential EhPanK inhibitors were identified from natural product library. For extracts screening, potential microbial extracts that inhibited EhPanK, specific inhibited EhDPCK1 and EhDPCK2 or inhibited both EhDPCK1 and EhDPCK2 have been found. However, further purification and compound identification from some hit extracts still in progress so that not described in this report. Collectively, my study suggesting that EhPanK, EhDPCK1, and EhDPCK2 are enzymes can be a new target for the development of anti-amebic drugs.

**Acknowledgements**

First, I would like to express my gratitude to my research supervisor and adviser, Prof. Tomoyoshi Nozaki, for accepting me as a Ph.D. student. He also gave very constructive guidance, support, and advice during my research. I also would like to thank Dr. Ghulam Jeelani, Dr. Kumiko Tsukui, Dr. Yumiko Nakano, Dr. Takeshi Annoura, Dr. Herbert. J. Santos, Dr. Koushik Das, Dr. Avik Kumar, Dr. Somlata, Dr. Yoko Chiba, Emi Sato, Yuki Hanadate, Natsuki Watanabe, Konomi Marumo, Tetsuo Kawano, Ratna Wahyuni, and Mihoko Imada from Nozaki's Laboratory (2015-2017) in the Department of Parasitology, National Institute of Infectious Diseases, Tokyo and Dr. Yoh-Ichi Watanabe, Dr. Michio Yamashita, Dr. Shigeo Yoshinari, Penny Dwi Kartikasari, and Russel Miller from the Nozaki's Laboratory in Department of Biomedical Chemistry, Faculty of Medicine, The University of Tokyo (2017-now) for their critical comments and fruitful discussion for the improvement of this research.

Second, I would like to acknowledge all the collaborators who provided a significant contribution to the completion of this study. I thank Prof. Makoto Suematsu, Dr. Takehiro Yamamoto, Takako Hishiki, and Yoshiko Naito from the Department of Biochemistry, School of Medicine, Keio University, Tokyo for their kind contribution on metabolomics analyses. I thank Prof. Kazuro Shiomi and Dr. Mihoko Mori from Kitasato Institute for Life Sciences, Kitasato University, Tokyo for providing compounds to be screened against EhPanK enzyme, discussing and conducting an experiment in the human cell toxicity. I thank Prof. Tetsuo Hashimoto, from Graduate School of Life and Environmental Sciences, the University of Tsukuba, for helping me in the phylogenetic analyses. I also thank Danang Waluyo and all of his team in Biotech Center, BPPT, Indonesia for providing microbial extracts to be screened against EhPanK, EhDPCK1, and EhDPCK2 enzyme.

Third, I would like to acknowledge to the Riset-Pro, The Ministry of Research, Technology and Higher Education (Kemenristek-Dikti), the Republic of Indonesia for providing me the scholarship of my Ph.D. education in Japan. I also thank the financial support providing

of this work, namely grant for Science and Technology Research Partnership for Sustainable Development from Japan Agency for Medical Research and Development (AMED) and Japan International Cooperation Agency (JICA), a grant for Research on Emerging and Re-emerging Infectious Diseases from AMED, Grants-in-Aid for Challenging Research (Exploratory) (17K19416), for Scientific Research (15H04406) and for Scientific Research on Innovative Areas (23117001, 23117005, 23390099) from the Ministry of Education, Culture, Sports, Science and Technology (MEXT).

I thank the professors from the University of Tsukuba: Prof. Tetsuo Hashimoto, Prof. Yuji Inagaki, Prof. Kisaburo Nagamune, and Prof. Shigeharu Moriya for their encouraging support, comment, and advice. I also thank Director and all of my colleagues in the Research Center for Biology, Indonesia Institute of Sciences (LIPI) for their support, before, during, and after completing my Ph.D. course. Finally, I would like to express my deepest gratitude and love to my family. I thank my mother, Rukmini, my wife, Citra Kusuma Asthi, my daughter, Aqila Khairina Nareswari, and my son, Abidzar Khiardana Nirwadipta for their unconditional love and unending support.

## References


Abiko, Y., 1975. Metabolism of Coenzyme A, in: Metabolic Pathways. Academic Press, New York, pp. 1–25.

Acker, M.G., Auld, D.S., 2014. Considerations for the design and reporting of enzyme assays in high-throughput screening applications. Perspect. Sci. 1, 56–73. doi:10.1016/j.pisc.2013.12.001

Aghajanian, S., Worrall, D.M., 2002. Identification and characterization of the gene encoding the human phosphopantetheine adenylyltransferase and dephospho-CoA kinase bifunctional enzyme (CoA synthase). Biochem. J. 365, 13–18. doi:10.1042/BJ20020569

Ali, V., Nozaki, T., 2007. Current therapeutics, their problems, and sulfur-containing-amino-acid metabolism as a novel target against infections by "amitochondriate" protozoan parasites. Clin. Microbiol. Rev. doi:10.1128/CMR.00019-06

Arroyo-Begovich, A., Carabez-Trejo, A., 1982. Location on chitin in the cyst wall of *Entamoeba invadens* with colloidal gold tracers. J Parasitol 68, 253–258.

Assaraf, Y.G., Abu-Elheiga, L., Spira, D.T., Desser, H., Bachrach, U., 1987. Effect of polyamine depletion on macromolecular synthesis of the malarial parasite, *Plasmodium falciparum*, cultured in human erythrocytes. Biochem. J. 242, 221–6.

Awasthy, D., Ambady, A., Bhat, J., Sheikh, G., Ravishankar, S., Subbulakshmi, V., Mukherjee, K., Sambandamurthy, V., Sharma, U., 2010. Essentiality and functional analysis of type I and type III pantothenate kinases of *Mycobacterium tuberculosis*. Microbiology 156, 2691–2701. doi:10.1099/mic.0.040717-0

Bacchi, C.J., McCann, P.P., 1987. Parasitic protozoa and polyamines, in: Inhibition of Polyamine Metabolism: Biological Significance and Basis for New Therapies. Academic Press, New York, pp. 317–344.

Bacchi, C.J., Yarlett, N., 1993. Effects of antagonists of polyamine metabolism on African trypanosomes. Acta Trop. doi:10.1016/0001-706X(93)90095-S

Beavo, J. a, Brunton, L.L., 2002. Cyclic nucleotide research -- still expanding after half a century. Nat. Rev. Mol. Cell Biol. 3, 710–718. doi:10.1038/nrm911

Begley, T.P., Kinsland, C., Strauss, E., 2001. The biosynthesis of coenzyme A in bacteria. Vitam. Horm. 61, 157–171. doi:10.1016/s0083-6729(01)61005-7

Begolo, D., Erben, E., Clayton, C., 2014. Drug target identification using a trypanosome overexpression library. Antimicrob. Agents Chemother. 58, 6260–6264. doi:10.1128/AAC.03338-14

Berman, P.A., Human, L., Freese, J.A., 1991. Xanthine oxidase inhibits growth of *Plasmodium falciparum* in human erythrocytes in vitro. J. Clin. Invest. 88, 1848–1855. doi:10.1172/JCI115506

Bracha, R., Nuchamowitz, Y., Anbar, M., Mirelman, D., 2006. Transcriptional silencing of multiple genes in trophozoites of *Entamoeba histolytica*. PLoS Pathog. 2, 431–441. doi:10.1371/journal.ppat.0020048

Brand, L.A., Strauss, E., 2005. Characterization of a new pantothenate kinase isoform from *Helicobacter pylori*. J. Biol. Chem. 280, 20185–20188. doi:10.1074/jbc.C500044200

Bridges, D., Fraser, M.E., Moorhead, G.B.G., 2005. Cyclic nucleotide binding proteins in the *Arabidopsis thaliana* and *Oryza sativa* genomes. BMC Bioinformatics 6, 6. doi:10.1186/1471-2105-6-6

Bum, S.H., Senisterra, G., Rabeh, W.M., Vedadi, M., Leonardi, R., Zhang, Y.M., Rock, C.O., Jackowski, S., Park, H.W., 2007. Crystal structures of human pantothenate kinases: Insights into allosteric regulation and mutations linked to a neurodegeneration disorder. J. Biol. Chem. 282, 27984–27993. doi:10.1074/jbc.M701915200

Calder, R.B., Williams, R.S.B., Ramaswamy, G., Rock, C.O., Campbell, E., Unkles, S.E., Kinghorn, J.R., Jackowski, S., 1999. Cloning and characterization of a eukaryotic pantothenate kinase gene (PanK) from *Aspergillus nidulans*. J. Biol. Chem. 274, 2014–2020. doi:10.1074/jbc.274.4.2014

Carter, N.S., Ben Mamoun, C., Liu, W., Silva, E.O., Landfear, S.M., Goldberg, D.E., Ullman, B., 2000. Isolation and functional characterization of the PfNT1 nucleoside transporter gene from *Plasmodium falciparum*. J. Biol. Chem. 275, 10683–91.

Cassera, M.B., Zhang, Y., Hazleton, K.Z., Schramm, V.L., 2011. Purine and pyrimidine pathways as targets in *Plasmodium falciparum*. Curr. Top. Med. Chem. 11, 2103–15. doi:BSP/CTMC/E-Pub/-000129-11-16a [pii]

Castro-Santos, P., Laborde, C.M., Díaz-Peña, R., 2015. Genomics, proteomics and metabolomics: their emerging roles in the discovery and validation of rheumatoid arthritis biomarkers. Clin. Exp. Rheumatol.

Chakauya, E., Coxon, K.M., Wei, M., MacDonald, M. V., Barsby, T., Abell, C., Smith, A.G., 2008. Towards engineering increased pantothenate (vitamin B5) levels in plants. Plant Mol. Biol. 68, 493–503. doi:10.1007/s11103-008-9386-5

Chávez-Munguía, B., Omaña-Molina, M., González-Lázaro, M., González-Robles, A., Cedillo-Rivera, R., Bonilla, P., Martínez-Palomo, A., 2007. Ultrastructure of cyst differentiation in parasitic protozoa. Parasitol. Res. doi:10.1007/s00436-006-0447-x

Chia, M.-Y., Jeng, C.-R., Hsiao, S.-H., Lee, A.-H., Chen, C.-Y., Pang, V.F., 2009. *Entamoeba invadens* myositis in a common water monitor lizard (*Varanus salvator*). Vet. Pathol. 46, 673–6. doi:10.1354/vp.08-VP-0224-P-CR

Chiu, J.E., Thekkiniath, J., Choi, J.-Y., Perrin, B.A., Lawres, L., Plummer, M., Virji, A.Z., Abraham, A., Toh, J.Y., Zandt, M. Van, I., A.S.A., Voelker, D.R., Mamoun, C. Ben, 2017. The antimalarial activity of the pantothenamide alfa-PanAm is via inhibition of pantothenate phosphorylation. Sci. Rep. 7, 14234.

Chomczynski, P., Mackey, K., 1995. Modification of the TRI Reagent(TM) procedure for isolation of RNA from polysaccharide- and proteoglycan-rich sources. Biotechniques 19, 942–945. doi:10.2144/000113156

Choudhary, C., Weinert, B.T., Nishida, Y., Verdin, E., Mann, M., 2014. The growing landscape of lysine acetylation links metabolism and cell signalling. Nat. Rev. Mol. Cell Biol. 15, 536–550. doi:10.1038/nrm3841

Das, M., Singh, S., Dubey, V.K., 2016. Novel Inhibitors of Ornithine Decarboxylase of Leishmania Parasite (LdODC): The Parasite Resists LdODC Inhibition by Overexpression of Spermidine Synthase. Chem. Biol. Drug Des. 87, 352–360. doi:10.1111/cbdd.12665

De Cádiz, A.E., Jeelani, G., Nakada-Tsukui, K., Caler, E., Nozaki, T., 2013. Transcriptome Analysis of Encystation in *Entamoeba invadens*. PLoS One 8, e74840. doi:10.1371/journal.pone.0074840

De Koning, H.P., Al-Salabi, M.I., Cohen, A.M., Coombs, G.H., Wastling, J.M., 2003. Identification and characterisation of high affinity nucleoside and nucleobase transporters in *Toxoplasma gondii*. Int. J. Parasitol. 33, 821–831. doi:10.1016/S0020-7519(03)00091-2

Diamond, L.S., Harlow, D.R., Cunnick, C.C., 1978. A new medium for the axenic cultivation of *Entamoeba histolytica* and other Entamoeba. Trans. R. Soc. Trop. Med. Hyg. 72, 431–432.

Donaldson, M., Heyneman, D., Dempster, R., Garcia, L., 1975. Epizootic of fatal amebiasis among exhibited snakes: epidemiologic, pathologic, and chemotherapeutic considerations. Am. J. Vet. Res. 36, 807–817.

Dumas, M.-E., 2012. Metabolome 2.0: quantitative genetics and network biology of metabolic phenotypes. Mol. Biosyst. 8, 2494. doi:10.1039/c2mb25167a

Edgar, R.C., 2004. MUSCLE: Multiple sequence alignment with high accuracy and high throughput. Nucleic Acids Res. 32, 1792–1797. doi:10.1093/nar/gkh340

Espinosa-Cantellano, M., Martínez-Palomo, A., 2000. Pathogenesis of intestinal amebiasis: From molecules to disease. Clin. Microbiol. Rev. doi:10.1128/CMR.13.2.318-331.2000

Fuhrer, T., Zamboni, N., 2015. High-throughput discovery metabolomics. Curr. Opin. Biotechnol. doi:10.1016/j.copbio.2014.08.006

Furukawa, A., Nakada-Tsukui, K., Nozaki, T., 2013. Cysteine protease-binding protein family 6 mediates the trafficking of amylases to phagosomes in the enteric protozoan *Entamoeba histolytica*. Infect. Immun. 81, 1820–1829. doi:10.1128/IAI.00915-12

Furukawa, A., Nakada-Tsukui, K., Nozaki, T., 2012. Novel transmembrane receptor involved in phagosome transport of lysozymes and β-hexosaminidase in the enteric protozoan *Entamoeba histolytica*. PLoS Pathog. 8. doi:10.1371/journal.ppat.1002539

Genschel, U., Powell, C., Abell, C., Smith, A., 1999. The final step of pantothenate biosynthesis in higher plants: cloning and characterization of pantothenate synthetase from *Lotus japonicus* and *Oryza sativum* (rice). Biochem. J 678, 669–678. doi:10.1042/0264-6021:3410669

Gosule, L.C., Schellman, J. a, 1976. Compact form of DNA induced by spermidine. Nature 259, 333–335. doi:10.1038/259333a0

Gouy, M., Guindon, S., Gascuel, O., 2010. SeaView Version 4: A Multiplatform Graphical User Interface for Sequence Alignment and Phylogenetic Tree Building. Mol. Biol. Evol. 27, 221–224. doi:10.1093/molbev/msp259

Griffin, F.M., 1973. Failure of metronidazole to cure hepatic amebic abscess. N. Engl. J. Med. 288, 1397–1397. doi:10.1056/NEJM197306282882610

Hart, R.J., Abraham, A., Aly, A.S.I., 2017. Genetic Characterization of Coenzyme A Biosynthesis Reveals Essential Distinctive Functions during Malaria Parasite Development in Blood and Mosquito. Front. Cell. Infect. Microbiol. 7. doi:Artn 26010.3389/Fcimb.2017.00260

Hart, R.J., Cornillot, E., Abraham, A., Molina, E., Nation, C.S., Ben Mamoun, C., Aly, A.S.I., 2016. Genetic Characterization of Plasmodium Putative Pantothenate Kinase Genes Reveals Their Essential Role in Malaria Parasite Transmission to the Mosquito. Sci. Rep. 6, 33518. doi:10.1038/srep33518

Heby, O., Roberts, S.C., Ullman, B., 2003. Polyamine biosynthetic enzymes as drug targets in parasitic protozoa. Biochem. Soc. Trans. 31, 415–419. doi:10.1042/BST0310415

Holmes, E., Wilson, I.D., Nicholson, J.K., 2008. Metabolic Phenotyping in Health and Disease. Cell. doi:10.1016/j.cell.2008.08.026

Hörtnagel, K., Prokisch, H., Meitinger, T., 2003. An isoform of hPANK2, deficient in pantothenate kinase-associated neurodegeneration, localizes to mitochondria. Hum. Mol. Genet. 12, 321–327. doi:10.1093/hmg/ddg026

Huang, L., Khusnutdinova, A., Nocek, B., Brown, G., Xu, X., Cui, H., Petit, P., Flick, R., Zallot, R., Balmant, K., Ziemak, M.J., Shanklin, J., De Crécy-Lagard, V., Fiehn, O., Gregory, J.F., Joachimiak, A., Savchenko, A., Yakunin, A.F., Hanson, A.D., 2016. A family of metal-dependent phosphatases implicated in metabolite damage-control. Nat. Chem. Biol. 12, 621–627. doi:10.1038/nchembio.2108

Husain, A., Jeelani, G., Sato, D., Nozaki, T., 2011. Global analysis of gene expression in response to L-Cysteine deprivation in the anaerobic protozoan parasite *Entamoeba histolytica*. BMC Genomics 12, 275. doi:10.1186/1471-2164-12-275\r1471-2164-12-275 [pii]

Husain, A., Sato, D., Jeelani, G., Soga, T., Nozaki, T., 2012. Dramatic Increase in Glycerol Biosynthesis upon Oxidative Stress in the Anaerobic Protozoan Parasite *Entamoeba histolytica*. PLoS Negl. Trop. Dis. 6. doi:10.1371/journal.pntd.0001831

Hyde, J.E., 2007. Targeting purine and pyrimidine metabolism in human apicomplexan parasites. Curr. Drug Targets 8, 31–47. doi:10.2174/138945007779315524

J. Baddiley, E.M. Thain, G.D. Novelli, F.L., 1953. Structure of coenzyme A. Nature. doi:10.1038/171076a0

Jackowski, S., 1996. Biosynthesis of pantothenic acid and coenzyme A, in: *Escherichia coli* and *Salmonella typhimurium*: Cellular and Molecular Biology, 2nd Ed., Vol. 1. ASM Press, Washington DC, pp. 687–694.

Jeelani, G., Husain, A., Sato, D., Soga, T., Suematsu, M., Nozaki, T., 2013. Biochemical and functional characterization of novel NADH kinase in the enteric protozoan parasite *Entamoeba histolytica*. Biochimie 95, 309–319. doi:10.1016/j.biochi.2012.09.034

Jeelani, G., Sato, D., Husain, A., Escueta-de Cadiz, A., Sugimoto, M., Soga, T., Suematsu, M., Nozaki, T., 2012. Metabolic profiling of the protozoan parasite *Entamoeba invadens* revealed activation of unpredicted pathway during encystation. PLoS One 7. doi:10.1371/journal.pone.0037740

Johnson, P.J., 1993. Metronidazole and drug resistance. Parasitol. Today. doi:10.1016/0169-4758(93)90143-4

Kimball, E., Rabinowitz, J.D., 2006. Identifying decomposition products in extracts of cellular metabolites. Anal. Biochem. 358, 273–280. doi:10.1016/j.ab.2006.07.038

Kinoshita, A., Tsukada, K., Soga, T., Hishiki, T., Ueno, Y., Nakayama, Y., Tomita, M., Suematsu, M., 2007. Roles of hemoglobin allostery in hypoxia-induced metabolic alterations in erythrocytes: Simulation and its verification by metabolome analysis. J. Biol. Chem. 282, 10731–10741. doi:10.1074/jbc.M610717200

Koch, C.J., Lord, E.M., Shapiro, I.M., Clyman, R.I., Evans, S.M., 1997. Imaging hypoxia and blood flow in normal tissues, in: In Oxygen Transport to Tissue XIX. Springer, US, pp. 585–593.

Kojimoto, a, Uchida, K., Horii, Y., Okumura, S., Yamaguch, R., Tateyama, S., 2001. Amebiasis in four ball pythons, *Python reginus*. J. Vet. Med. Sci. 63, 1365–8. doi:10.1292/jvms.63.1365

Kotzbauer, P.T., Truax, A.C., Trojanowski, J.Q., Lee, V.M.-Y., 2005. Altered neuronal mitochondrial coenzyme A synthesis in neurodegeneration with brain iron accumulation caused by abnormal processing, stability, and catalytic activity of mutant pantothenate kinase 2. J. Neurosci. 25, 689–98. doi:10.1523/JNEUROSCI.4265-04.2005

Krug, D., Müller, R., 2014. Secondary metabolomics: the impact of mass spectrometry-based approaches on the discovery and characterization of microbial natural products. Nat. Prod. Rep. 31, 768. doi:10.1039/c3np70127a

Leonardi, R., Chohnan, S., Zhang, Y.M., Virga, K.G., Lee, R.E., Rock, C.O., Jackowski, S., 2005a. A pantothenate kinase from *Staphylococcus aureus* refractory to feedback regulation by coenzyme A. J. Biol. Chem. 280, 3314–3322. doi:10.1074/jbc.M411608200

Leonardi, R., Zhang, Y.M., Rock, C.O., Jackowski, S., 2005b. Coenzyme A: Back in action. Prog. Lipid Res. doi:10.1016/j.plipres.2005.04.001

Livak, K.J., Schmittgen, T.D., 2001. Analysis of Relative Gene Expression Data Using Real-Time Quantitative PCR and the 2(-Delta Delta C(T)) Method. METHODS 25, 402–408. doi:10.1006

Lo, H.S., Wang, C.C., 1985. Purine salvage in *Entamoeba histolytica*. J. Parasitol. 71, 662–9. doi:10.2307/3281440

Loftus, B., Anderson, I., Davies, R., Alsmark, U.C.M., Samuelson, J., Amedeo, P., Roncaglia, P., Berriman, M., Hirt, R.P., Mann, B.J., Nozaki, T., Suh, B., Pop, M., Duchene, M., Ackers, J., Tannich, E., Leippe, M., Hofer, M., Bruchhaus, I., Willhoeft, U., Bhattacharya, A., Chillingworth, T., Churcher, C., Hance, Z., Harris, B., Harris, D., Jagels, K., Moule, S., Mungall, K., Ormond, D., Squares, R., Whitehead, S., Quail, M.A., Rabbinowitsch, E., Norbertczak, H., Price, C., Wang, Z., Guillén, N., Gilchrist, C., Stroup, S.E., Bhattacharya, S., Lohia, A., Foster, P.G., Sicheritz-Ponten, T., Weber, C., Singh, U., Mukherjee, C., El-Sayed, N.M., Petri, W.A., Clark, C.G., Embley, T.M., Barrell, B., Fraser, C.M., Hall, N., 2005. The genome of the protist parasite *Entamoeba histolytica*. Nature 433, 865–868. doi:10.1038/nature03291

Macuamule, C.J., Tjhin, E.T., Jana, C.E., Barnard, L., Koekemoer, L., De Villiers, M., Saliba, K.J., Strauss, E., 2015. A pantetheinase-resistant pantothenamide with potent, on-target, and selective antiplasmodial activity. Antimicrob. Agents Chemother. 59, 3666–3668. doi:10.1128/AAC.04970-14

Mastrangelo, A., Armitage, E.G., García, A., Barbas, C., 2014. Metabolomics as a tool for drug discovery and personalised medicine. A review. Curr. Top. Med. Chem. 14, 2627–36.

McCann, P.P., Pegg, A.E., 1992. Ornithine decarboxylase as an enzyme target for therapy. Pharmacol. Pharmacol. Ther. 54, 195–215. doi:10.1016/0163-7258(92)90032-U

McCann, P.P., Pegg, A.E., Sjeordsma, A., 1987. Introduction: Polyamine metabolism, in: Inhibition of Polyamine Metabolism: Biological Significance and Basis for New Therapies. Academic Press, New York, pp. 13–16.

McLaughlin, J., Aley, S., 1985. The Biochemistry and Functional Morphology of the Entamoeba. J. Eukaryot. Microbiol. 32, 221–240. doi:10.1111/j.1550-7408.1985.tb03043.x

Mirelman, D., Anbar, M., Bracha, R., 2008. Epigenetic transcriptional gene silencing in *Entamoeba histolytica*. IUBMB Life. doi:10.1002/iub.96

Morf, L., Pearson, R.J., Wang, A.S., Singh, U., 2013. Robust gene silencing mediated by antisense small RNAs in the pathogenic protist *Entamoeba histolytica*. Nucleic Acids Res. 41, 9424–9437. doi:10.1093/nar/gkt717

Mori, M., Jeelani, G., Masuda, Y., Sakai, K., Tsukui, K., Waluyo, D., Tarwadi, Watanabe, Y., Nonaka, K., Matsumoto, A., Omura, S., Nozaki, T., Shiomi, K., 2015. Identification of natural inhibitors of *Entamoeba histolytica* cysteine synthase from microbial secondary metabolites. Front. Microbiol. 6. doi:10.3389/fmicb.2015.00962

Müller, S., Coombs, G.H., Walter, R.D., 2001. Targeting polyamines of parasitic protozoa in chemotherapy. Trends Parasitol. doi:10.1016/S1471-4922(01)01908-0

Nakada-Tsukui, K., Tsuboi, K., Furukawa, A., Yamada, Y., Nozaki, T., 2012. A novel class of cysteine protease receptors that mediate lysosomal transport. Cell. Microbiol. 14, 1299–1317. doi:10.1111/j.1462-5822.2012.01800.x

Newman, D.J., Cragg, G.M., 2012. Natural products as sources of new drugs over the 30 years from 1981 to 2010. J. Nat. Prod. doi:10.1021/np200906s

Nguyen, L.T., Schmidt, H.A., Von Haeseler, A., Minh, B.Q., 2015. IQ-TREE: A fast and effective stochastic algorithm for estimating maximum-likelihood phylogenies. Mol. Biol. Evol. 32, 268–274. doi:10.1093/molbev/msu300

Nozaki, T., Asai, T., Sanchez, L.B., Kobayashi, S., Nakazawa, M., Takeuchi, T., 1999. Characterization of the Gene Encoding Serine Acetyltransferase, a Regulated Enzyme of Cysteine Biosynthesis from the Protist ParasitesEntamoeba histolytica and Entamoeba dispar REGULATION AND POSSIBLE FUNCTION OF THE CYSTEINE BIOSYNTHETIC PATHWAY IN ENTAM. J. Biol. Chem. 274, 32445–32452.

Nozaki, T., Bhattacharya, A., 2015. Amebiasis: Biology and pathogenesis of entamoeba, Amebiasis: Biology and Pathogenesis of Entamoeba. doi:10.1007/978-4-431-55200-0

O'Toole, N., Barbosa, J. a R.G., Li, Y., Hung, L.-W., Matte, A., Cygler, M., 2003. Crystal

structure of a trimeric form of dephosphocoenzyme A kinase from *Escherichia coli*. Protein Sci. 12, 327–336. doi:10.1110/ps.0227803.and

Obmolova, G., Teplyakov, A., Bonander, N., Eisenstein, E., Howard, A.J., Gilliland, G.L., 2001. Crystal structure of dephospho-coenzyme A kinase from *Haemophilus influenzae*. J. Struct. Biol. 136, 119–125. doi:10.1006/jsbi.2001.4428

Parker, W.B., Long, M.C., 2007. Purine metabolism in *Mycobacterium tuberculosis* as a target for drug development. Curr. Pharm. Des. 13, 599–608. doi:10.2174/138161207780162863

Patra, K.C., Hay, N., 2014. The pentose phosphate pathway and cancer. Trends Biochem. Sci. doi:10.1016/j.tibs.2014.06.005

Penuliar, G.M., Furukawa, A., Nakada-Tsukui, K., Husain, A., Sato, D., Nozaki, T., 2012. Transcriptional and functional analysis of trifluoromethionine resistance in *Entamoeba histolytica*. J. Antimicrob. Chemother. 67, 375–386. doi:10.1093/jac/dkr484

Penuliar, G.M., Nakada-Tsukui, K., Nozaki, T., 2015. Phenotypic and transcriptional profiling in *Entamoeba histolytica* reveal costs to fitness and adaptive responses associated with metronidazole resistance. Front. Microbiol. 6. doi:10.3389/fmicb.2015.00354

Pittman, F.E., Pittmann, J.C., 1974. Amebic liver abscess following metronidazole therapy for amebic colitis. Am. J. Trop. Med. Hyg. 23, 146–150.

Przybytkowski, E., Averill-Bates, D.A., 1996. Correlation between glutathione and stimulation of the pentose phosphate cycle in situ in Chinese hamster ovary cells exposed to hydrogen peroxide. Arch. Biochem. Biophys. 325, 91–98. doi:10.1006/abbi.1996.0011

Ralston, K.S., Petri, W., 2011. The ways of a killer: how does *Entamoeba histolytica* elicit host cell death? Essays Biochem. 51, 193–210. doi:10.1042/bse0510193

Raspaud, E., Chaperon, I., Leforestier, A., Livolant, F., 1999. Spermine-induced aggregation of DNA, nucleosome, and chromatin. Biophys. J. 77, 1547–1555. doi:10.1016/S0006-3495(99)77002-5

Reddy, B.K.K., Landge, S., Ravishankar, S., Patil, V., Shinde, V., Tantry, S., Kale, M., Raichurkar, A., Menasinakai, S., Mudugal, N.V., Ambady, A., Ghosh, A., Tunduguru, R., Kaur, P., Singh, R., Kumar, N., Bharath, S., Sundaram, A., Bhat, J., Sambandamurthy, V.K., Björkelid, C., Jones, T.A., Das, K., Bandodkar, B., Malolanarasimhan, K., Mukherjee, K., Ramachandran, V., 2014. Assessment of mycobacterium tuberculosis pantothenate kinase vulnerability through target knockdown and mechanistically diverse inhibitors. Antimicrob. Agents Chemother. 58, 3312–3326. doi:10.1128/AAC.00140-14

Reeves, R.E., 1985. Metabolism of *Entamoeba histolytica* Schaudinn, 1903. Adv. Parasitol. 23, 105–142. doi:10.1016/S0065-308X(08)60286-9

Roberts, S., Paradis, D., Perdeh, J., Harrelson, J., Jan, B., Yates, P., Ullman, B., 2016. The Polyamine Pathway of *Leishmania donovani* as a Potential Therapeutic Target. FASEB J. 30.

Rock, C.O., Karim, M.A., Zhang, Y.M., Jackowski, S., 2002. The murine pantothenate kinase (Pank1) gene encodes two differentially regulated pantothenate kinase isozymes. Gene 291, 35–43. doi:10.1016/S0378-1119(02)00564-4

Ruan, H., Hill, J.R., Fatemie-Nainie, S., Morris, D.R., 1994. Cell-specific translational regulation of S-adenosylmethionine decarboxylase mRNA: Influence of the structure of the 5' transcript leader on regulation by the upstream open reading frame. J. Biol. Chem. 269, 17905–17910.

Saliba, K.J., Horner, H. a, Kirk, K., 1998. Transport and metabolism of the essential vitamin pantothenic acid in human erythrocytes infected with the malaria parasite *Plasmodium falciparum.* J. Biol. Chem. 273, 10190–10195. doi:10.1074/jbc.273.17.10190

Sambrook, J., Russell, D.W., 2001. Molecular Cloning: A Laboratory Manual. Cold Spring Harb. Lab. Press. Cold Spring Harb. NY 999.

Sanchez, M., Tryon, R., Green, J., Boor, I., Landfear, S., 2002. Six Related Nucleoside/Nucleobase Transporters from *Trypanosoma brucei* Exhibit Distinct Biochemical Functions. J. Biol. Chem. 277, 21499–21504.

Slocum, R.D., Kaur-Sawhney, R., Galston, A.W., 1984. The physiology and biochemistry of polyamines in plants. Arch. Biochem. Biophys. 235, 283–303. doi:10.1016/0003-9861(84)90201-7

Soga, T., Ueno, Y., Naraoka, H., Ohashi, Y., Tomita, M., Nishioka, T., 2002. Simultaneous determination of anionic intermediates for Bacillus subtilis metabolic pathways by capillary electrophoresis electrospray ionization mass spectrometry. Anal. Chem. 74, 2233–2239. doi:10.1021/ac020064n

Song, W.J., Jackowski, S., 1993. Cloning, sequencing, and expression of the pantothenate kinase (coaA) gene of *Escherichia coli*. [Erratum to document cited in CA119(7):64394q]. J. Bacteriol. 175, 2792.

Spindler, K.D., Spindler-Barth, M., Londershausen, M., 1990. Chitin metabolism: a target for drugs against parasites. Parasitol. Res. doi:10.1007/BF00928180

Spry, C., Kirk, K., Saliba, K.J., 2008. Coenzyme A biosynthesis: An antimicrobial drug target. FEMS Microbiol. Rev. doi:10.1111/j.1574-6976.2007.00093.x

Srinivasan, B., Baratashvili, M., van der Zwaag, M., Kanon, B., Colombelli, C., Lambrechts, R.A., Schaap, O., Nollen, E.A., Podgoršek, A., Kosec, G., Petković, H., Hayflick, S., Tiranti, V., Reijngoud, D.-J., Grzeschik, N.A., Sibon, O.C.M., 2015. Extracellular 4′-phosphopantetheine is a source for intracellular coenzyme A synthesis. Nat. Chem. Biol. 11, 784–792. doi:10.1038/nchembio.1906

Srivastava, A., Philip, N., Hughes, K.R., Georgiou, K., MacRae, J.I., Barrett, M.P., Creek, D.J., McConville, M.J., Waters, A.P., 2016. Stage-Specific Changes in Plasmodium Metabolism Required for Differentiation and Adaptation to Different Host and Vector Environments. PLoS Pathog. 12. doi:10.1371/journal.ppat.1006094

Stamatakis, A., 2006. RAxML-VI-HPC: Maximum likelihood-based phylogenetic analyses with thousands of taxa and mixed models. Bioinformatics 22, 2688–2690. doi:10.1093/bioinformatics/btl446

Stanley, S.L., 2003. Amoebiasis. Lancet 361, 1025–1034. doi:10.1016/S0140-6736(03)12830-9

Strauss, E., 2010. Coenzyme A Biosynthesis and Enzymology, in: Comprehensive Natural Products II Chemistry and Biology. pp. 351–410. doi:10.1016/B978-008045382-8.00141-6

Susskind, B.M., Warren, L.G., Reeves, R.E., 1982. A pathway for the interconversion of hexose and pentose in the parasitic amoeba Entamoeba histolytica. Biochem J 204, 191–196. doi:10.1042/bj2040191

Tabor, C.W., Tabor, H., 1985. Polyamines in microorganisms. Microbiol. Rev. 49, 81–99.

Takagi, M., Tamaki, H., Miyamoto, Y., Leonardi, R., Hanada, S., Jackowski, S., Chohnan, S., 2010. Pantothenate kinase from the thermoacidophilic archaeon *Picrophilus torridus.* J. Bacteriol. 192, 233–241. doi:10.1128/JB.01021-09

Taylor, M.C., Kaur, H., Blessington, B., Kelly, J.M., Wilkinson, S.R., 2008. Validation of spermidine synthase as a drug target in African trypanosomes. Biochem. J. 409, 563–569. doi:10.1042/BJ20071185

Tilton, G.B., Wedemeyer, W.J., Browse, J., Ohlrogge, J., 2006. Plant coenzyme A biosynthesis: Characterization of two pantothenate kinases from Arabidopsis. Plant Mol. Biol. 61, 629–642. doi:10.1007/s11103-006-0037-4

Tsouko, E., Khan, A.S., White, M.A., Han, J.J., Shi, Y., Merchant, F.A., Sharpe, M.A., Xin, L., Frigo, D.E., 2014. Regulation of the pentose phosphate pathway by an androgen receptor–mTOR-mediated mechanism and its role in prostate cancer cell growth. Oncogenesis 3, e103. doi:10.1038/oncsis.2014.18

Vallari, D.S., Jackowski, S., Rock, C.O., 1987. Regulation of pantothenate kinase by coenzyme A and its thioesters. J. Biol. Chem. 262, 2468–2471.

van Dam, L., Korolev, N., Nordenskiöld, L., 2002. Polyamine-nucleic acid interactions and the effects on structure in oriented DNA fibers. Nucleic Acids Res. 30, 419–428. doi:10.1093/nar/30.2.419

Wallace, H.M., Fraser, A. V, Hughes, A., 2003. A perspective of polyamine metabolism. Biochem. J. 376, 1–14. doi:10.1042/BJ20031327

Williams, K.P., Scott, J.E., 2009. Enzyme assay design for high-throughput screening. Methods Mol. Biol. 565, 107–126. doi:10.1007/978-1-60327-258-2_5

World Health Organization, 1997. Weekly Epidemiological Records 72, 97–100.

Yamamoto, T., Takano, N., Ishiwata, K., Ohmura, M., Nagahata, Y., Matsuura, T., Kamata, A., Sakamoto, K., Nakanishi, T., Kubo, A., Hishiki, T., Suematsu, M., 2014. Reduced methylation of PFKFB3 in cancer cells shunts glucose towards the pentose phosphate pathway. Nat. Commun. 5. doi:10.1038/ncomms4480

Yang, K., Eyobo, Y., Brand, L.A., Martynowski, D., Tomchick, D., Strauss, E., Zhang, H., 2006. Crystal structure of a type III pantothenate kinase: Insight into the mechanism of an essential coenzyme A biosynthetic enzyme universally distributed in bacteria. J. Bacteriol. 188, 5532–5540. doi:10.1128/JB.00469-06

Yousuf, M.A., Mi-Ichi, F., Nakada-Tsukui, K., Nozaki, T., 2010. Localization and targeting of an unusual pyridine nucleotide transhydrogenase in *Entamoeba histolytica*. Eukaryot. Cell 9, 926–933. doi:10.1128/EC.00011-10

Zhang, A., Sun, H., Wang, P., Han, Y., Wang, X., 2012. Modern analytical techniques in metabolomics analysis. Analyst 137, 293–300. doi:10.1039/C1AN15605E

Zhang, H., Alramini, H., Tran, V., Singh, U., 2011a. Nucleus-localized antisense small RNAs with 5'-polyphosphate termini regulate long term transcriptional gene silencing in *Entamoeba histolytica* G3 strain. J. Biol. Chem. 286, 44467–44479. doi:10.1074/jbc.M111.278184

Zhang, H., Pompey, J.M., Singh, U., 2011b. RNA interference in *Entamoeba histolytica*: implications for parasite biology and gene silencing. Future Microbiol. 6, 103–117. doi:10.2217/fmb.10.154

Zhang, Y.M., Rock, C.O., Jackowski, S., 2005. Feedback regulation of murine pantothenate kinase 3 by coenzyme A and coenzyme A thioesters, in: Journal of Biological Chemistry. pp. 32594–32601. doi:10.1074/jbc.M506275200